

**AN INVESTIGATION OF ELECTROCHEMICAL
STABILITY OF ZINC ELECTRODES FOR
BATTERY APPLICATIONS**

**A Thesis Submitted to
The Graduate School of Engineering and Sciences of
Izmir Institute of Technology
In Partial Fulfillment of the Requirements for the Degree of**

MASTER OF SCIENCE

in Chemical Engineering

**by
Gizem PAYER**

**July 2014
İZMİR**

We approve the thesis of **Gizem PAYER**

Examining Committee Members:

Assist. Prof. Dr. Özgeç EBİL

Department of Chemical Engineering, Izmir Institute of Technology

Prof. Dr. Muhsin ÇİFTÇİOĞLU

Department of Chemical Engineering, Izmir Institute of Technology

Dr. Ogan OCALI

Ocalı Bilişim Teknolojileri, Yazılım, Donanım San. ve Tic. A.Ş.

Prof. Dr. M. Mustafa DEMİR

Department of Material Science and Engineering, Izmir Institute of Technology

Assist. Prof. Dr. Ayben TOP

Department of Chemical Engineering, Izmir Institute of Technology

4 July 2014

Assist. Prof. Dr. Özgeç EBİL

Supervisor, Department of Chemical Engineering, Izmir Institute of Technology

Prof. Dr. Muhsin ÇİFTÇİOĞLU

Co-Supervisor, Chemical Engineering, Izmir Institute of Technology

Prof. Dr. Fehime Seher ÖZKAN

Head of the Department of Chemical Engineering

Prof. Dr. R. Tuğrul SENGER

Dean of the Graduate School of Engineering and Sciences

ACKNOWLEDGEMENTS

I am heartily thankful to my supervisor, Assist. Prof. Dr. Özgenç EBİL whose knowledge, encouragement, valuable advice and sincerity have broaden my mind and supported me to complete my M.Sc. thesis. I am also grateful to my co-advisor, Prof. Dr. Muhsin ÇİFTÇİOĞLU for his crucial contributions, valuable advice throughout my study.

I would like to express my appreciation for Dr. Ogan OCALI for his great help, valuable suggestions, and knowledge. I am also grateful for his financial support.

I ought to thank Prof. Dr. Devrim BALKÖSE for providing some of the chemicals used in this work. Additionally, I would like to thank Assist. Prof. Dr. Ayben TOP for letting me use some of the equipment in her laboratory.

I would like to thank H. Arda YURTSEVER for his help in laboratory work. I would like to thank Dr. Filiz ÖZMIHÇI ÖMÜRLÜ, Dr. Özlem ÇAĞLAR DUVARCI and Dr. Nesrin TATLIDİL for their help in characterization. I wish to thank the whole staff of Department of Chemical Engineering for their help and technical assistance, especially Belgin TUNÇER KIRKAR. I would like to thank the Center for Materials Research staff at Izmir Institute of Technology (İYTE-MAM) for their help with SEM, XRD and XRF analyses.

I would also like to thank all my friends the Department of Chemical Engineering; Selcan ATEŞ, Sezen Duygu ALICI, Emre DEMİRKAYA, and especially Derya BİLGİNPERK for their help and friendship.

This journey would not have been possible without the support of my family. First, I would like to express my gratitude to my parents, for their devotion, understanding, and support throughout my life. My special thanks to Aydın CİHANOĞLU for his endless devotion, understanding, friendship and support at the beginning and during my master thesis. They always encouraged me in my graduate endeavor.

ABSTRACT

AN INVESTIGATION OF ELECTROCHEMICAL STABILITY OF ZINC ELECTRODES FOR BATTERY APPLICATIONS

Energy is the most important and inevitable requirement for humankind. The increasing energy demand has been connected with technological advances and the population growth. One of the most serious problems of the world is to provide sustainable energy. New alternative energy sources and renewable energy technologies have become notable research subjects due to wide availability of renewable energy sources in the world. However, most renewable energy sources do not provide uninterrupted energy to consumers. An economic, efficient and reliable energy storage technology is desperately needed. Therefore, academic research has focused on improving the capacity of electrochemical energy storage technologies.

The main goal of this study is the preparation and characterization of zinc electrodes for battery applications using different zinc oxide powders with various morphologies and additives. Zinc oxide powders were synthesized with chemical precipitation method under different conditions (precursors, temperatures and aging times) in order to investigate their effects on ZnO morphology and on the performance of nickel-zinc battery. It was found out that the initial morphology of ZnO powder was not crucial for the electrochemical performance. Nickel-Zinc batteries with zinc electrodes prepared from commercial ZnO powder had discharge capacities around 247 mAhg^{-1} and showed slightly better performance compared to nickel-zinc batteries with zinc electrodes prepared from ZnO powders synthesized via chemical precipitation method. It was also determined that zinc electrode morphology was greatly affected by battery additives (PVA and PEG) and charging current density. The effects of some selected electrode additives (Ca(OH)_2 , PbO and PEG) on battery performance were also investigated. Zinc electrode with all additives showed improved electrochemical properties, such as higher discharge capacity (322 mAhg^{-1}) and utilization ratio (48.86 %.).

ÖZET

BATARYA UYGULAMALARI İÇİN ÇİNKO ELEKTROTLARIN ELEKTROKİMYASAL KARARLILIĞININ İNCELENMESİ

Enerji insanlığın en önemli ve vazgeçilmez bir ihtiyacıdır. Artan enerji talebi teknolojik gelişmeler ve artan nüfus ile ilişkilidir. Dünyanın en ciddi sorunlarından biri, sürdürülebilir enerjiyi sağlamaktır. Dünyadaki yenilenebilir enerji kaynaklarının yaygın bulunabilirliğinden dolayı, yeni alternatif enerji kaynakları ve/veya yenilenebilir enerji teknolojileri önemli araştırma konuları haline gelmiştir. Ancak, çoğu yenilenebilir enerji kaynakları tüketicilere kesintisiz enerji sağlayamamaktadır. Ekonomik, verimli ve güvenilir bir enerji depolama teknolojisine son derece ihtiyaç duyulmaktadır. Bu nedenle, akademik çalışmalar elektrokimyasal enerji depolama teknolojilerinin kapasite gelişimine odaklanmıştır.

Bu çalışmanın asıl amacı, batarya uygulamaları için çeşitli morfolojilere sahip farklı çinko oksit tozları ve katkı malzemeleri kullanılarak çinko elektrotların hazırlanması ve incelenmesidir. Çinko oksit morfolojisi ve nikel-çinko batarya performansı üzerindeki etkilerini incelemek için farklı koşullar altındaki (öncü madde, sıcaklık ve bekleme süresi) kimyasal çöktürme yoluyla çinko oksit tozları sentezlenmiştir. Çinko oksit tozunun başlangıç morfolojisinin elektrokimyasal performans açısından bir öneminin olmadığı görülmüştür. Ticari çinko oksit tozundan hazırlanan çinko elektrotlarına sahip nikel-çinko bataryaları yaklaşık 247 mAhg^{-1} deşarj kapasitesine sahiptir ve kimyasal çöktürme yoluyla sentezlenen çinko oksit tozlarından hazırlanan çinko elektrotlarına sahip nikel-çinko bataryalarına kıyasla bu elektrot kısmen daha iyi bir performans göstermiştir. Ayrıca, çinko elektrot morfolojisinin batarya katkı malzemeleri (PVA ve PEG) ve şarj akım yoğunluğu tarafından büyük ölçüde etkilendiği tespit edilmiştir. Seçilen bazı elektrot katkı malzemelerinin (Ca(OH)_2 , PbO ve PEG) batarya performansı üzerindeki etkileri de incelenmiştir. Tüm katkı malzemelerine sahip çinko elektrotu daha yüksek deşarj kapasitesi (322 mAhg^{-1}) ve kullanım oranı (48.86 %) gibi gelişmiş elektrokimyasal özellikler göstermiştir.

TABLE OF CONTENTS

LIST OF FIGURES.....	viii
LIST OF TABLES.....	xi
CHAPTER 1. INTRODUCTION.....	1
1.1. Batteries.....	3
CHAPTER 2. ZINC BATTERIES.....	10
2.1. Rechargeable Nickel-Zinc Batteries.....	10
2.1.1. Problems with Rechargeable Nickel-Zinc Batteries.....	12
2.1.1.1. Additives to Electrolyte.....	14
2.1.1.2. Additives to Electrodes.....	16
2.1.1.3. Morphology of Electrodes.....	19
2.2. Rechargeable Zinc-Air Batteries.....	20
2.2.1. Problems with Rechargeable Zinc-Air Batteries.....	22
2.2.1.1. Additives to Electrodes.....	23
2.2.1.2. Additives to Electrolyte.....	24
2.2.1.3. Improvement of Air Electrodes.....	24
CHAPTER 3. EXPERIMENTAL WORK.....	25
3.1. Materials.....	25
3.2. Preparation of Electrodes for Rechargeable NiZn Battery.....	26
3.2.1. Nickel Anode.....	27
3.2.2. Zinc Cathode.....	27
3.3. Zinc Electrodeposition Setup.....	29
3.4. Preparation of Rechargeable NiZn battery.....	30
3.5. Characterization.....	32
3.6. Charge/Discharge Tests.....	33
CHAPTER 4. RESULTS AND DISCUSSION.....	35
4.1. Zinc Electrodes.....	35

4.1.1. Zinc Oxide Powder Synthesized from Zinc Chloride (ZnCl_2).....	35
4.1.2. Zinc Oxide Powder Synthesized from Zinc Nitrate Hexahydrate ($\text{Zn}(\text{NO}_3)_2 \cdot 6\text{H}_2\text{O}$).....	38
4.1.3. Commercial Zinc Oxide Powder.....	41
4.1.4. Effect of Initial Morphology of Zn Electrodes.....	45
4.1.4.1. Zinc Electrodes As Prepared (Before First Charge).....	45
4.1.4.2. Zinc Electrodes (After First Charge and Discharge).....	50
4.2. Morphology of Nickel Electrodes.....	55
4.3. Effect of Binder/Separator Material on Zinc Growth.....	57
4.3.1. Zinc Growth without Binders/Separator Material.....	58
4.3.2. The Effect of PVA on Zinc Growth.....	60
4.3.3. The Effect of PEG on Zinc Growth.....	63
4.4. Effect of Additives in Zn Electrode on Electrochemical Performance of Zinc Electrode.....	65
4.4.1. Electrochemical Performance of Zinc Electrode with PEG, PbO and $\text{Ca}(\text{OH})_2$	66
4.4.2. Electrochemical Performance of Zinc Electrode with PEG and PbO.....	69
4.4.3. Electrochemical Performance of Zinc Electrode with PEG and $\text{Ca}(\text{OH})_2$	71
4.4.4. Electrochemical Performance of Zinc Electrode with PbO and $\text{Ca}(\text{OH})_2$	74
CHAPTER 5. CONCLUSION.....	80
REFERENCES.....	82

LIST OF FIGURES

<u>Figure</u>	<u>Page</u>
Figure 1.1. Energy supply of the world in 2010.....	1
Figure 1.2. World energy consumption between 1990 and 2040 (quadrillion Btu).....	2
Figure 1.3. Volta pile.....	5
Figure 1.4. Effect of the solubility of the reaction products on electrode structure during discharge/charge process.....	8
Figure 2.1. Sealed NiZn cell.....	11
Figure 2.2. Failed commercial battery separator (Zn electrode side).....	12
Figure 2.3. Failed commercial battery separator (Ni electrode side).....	13
Figure 2.4. The formation of dendrite of zinc electrode during zinc deposition.....	13
Figure 2.5. Typical zinc-air battery with key constructional properties.....	22
Figure 3.1. Experimental work diagram.....	25
Figure 3.2. Experimental set-up for ZnO powder synthesized from ZnCl ₂	28
Figure 3.3. Experimental set-up for ZnO synthesized from Zn(NO ₃) ₂ ·6 H ₂ O.....	29
Figure 3.4. Schematic illustration of preparation of rechargeable NiZn battery: (1) preparation of Zn electrode, (2) Ni electrode obtaining from commercial NiZn and NiMH batteries, (3) NiZn battery.....	31
Figure 3.5. Photos illustration of preparation of rechargeable NiZn battery: (1) preparation of Zn electrode, (2) Ni electrode obtaining from commercial NiZn and NiMH batteries, (3) NiZn battery.	32
Figure 3.6. Charge and discharge set-up.....	33
Figure 3.7. Photos of charge/discharge cycle setup.....	34
Figure 4.1. SEM images of ZnO powder synthesized from ZnCl ₂ at 35°C (a) 1µm (b) 500 nm.....	36
Figure 4.2. SEM images of ZnO powder synthesized from ZnCl ₂ at 50°C scale bars (a) 1µm (b) 500 nm	37
Figure 4.3. SEM images of ZnO powder synthesized from Zn(NO ₃) ₂ ·6 H ₂ O during 15 minutes of the aging time scale bars (a) 1µm (b) 5 µm.....	38
Figure 4.4. SEM images of ZnO powder synthesized from Zn(NO ₃) ₂ ·6 H ₂ O during 30 minutes of the aging time scale bars (a) 1µm (b) 4 µm.....	39

Figure 4.5.	Distribution of hydrolysis solution saturated with ZnO.....	41
Figure 4.6.	SEM images of commercial ZnO powder scale bars (a) 1 μm (b) 4 μm	42
Figure 4.7.	XRD spectra of commercial ZnO, ZnO powder (from ZnCl ₂) and ZnO powder (from Zn(NO ₃) ₂ ·6 H ₂ O).....	44
Figure 4.8.	SEM images of the paste of Zn electrode as-prepared by ZnO powder synthesized from ZnCl ₂ scale bars (a) 5 μm (b) 2 μm	46
Figure 4.9.	SEM images of the paste of Zn electrode as-prepared by ZnO powder synthesized from Zn(NO ₃) ₂ ·6 H ₂ O scale bars (a) 5 μm (b) 2 μm	47
Figure 4.10.	SEM images of the paste of Zn electrode as-prepared by commercial ZnO powder scale bars (a) 4 μm (b) 2 μm	48
Figure 4.11.	XRD spectra of the paste Zn electrode as-prepared from commercial ZnO powder, ZnO powder (from ZnCl ₂) and Zn powder from Zn(NO ₃) ₂ ·6 H ₂ O.....	49
Figure 4.12.	The first discharge curves (voltage vs. capacity) for Zn electrodes with all additives.....	52
Figure 4.13.	SEM images of Zn electrode prepared from (a) ZnO synthesized from ZnCl ₂ (b) ZnO synthesized from Zn(NO ₃) ₂ ·6H ₂ O (c) commercial ZnO after first charge.....	53
Figure 4.14.	SEM images of Zn electrode prepared from (a) ZnO synthesized from ZnCl ₂ (b) ZnO synthesized from Zn(NO ₃) ₂ ·6H ₂ O (c) commercial ZnO after first discharge.....	54
Figure 4.15.	XRD test results for both commercial Ni electrodes.....	57
Figure 4.16.	SEM images of Zn electrode without binders/seperator material after deposit at 25 mA/cm ² scale bars (a) 10 μm (b) 10 μm	59
Figure 4.17.	SEM images of Zn electrode without binders/seperator material after deposit at 75 mA/cm ² scale bars (a) 10 μm (b) 10 μm	60
Figure 4.18.	SEM images of Zn electrode with PVA as a binder after deposit at 25 mA/cm ² scale bars (a) 50 μm (b) 10 μm (c) 10 μm	61
Figure 4.19.	SEM images of Zn electrode with PVA as a binder after deposit at 75 mA/cm ² scale bars (a) 10 μm (b) 10 μm (c) 40 μm	62
Figure 4.20.	SEM images of Zn electrode with PEG as a binder after deposit at 25 mA/cm ² scale bars (a) 10 μm (b) 10 μm	63

Figure 4.21.	SEM images of Zn electrode with PEG as a binder after deposit at 75 mA/cm ² scale bars (a) 4 μm (b) 10 μm (c) 40 μm.....	64
Figure 4.22.	The discharge curves (voltage vs. time) for Zn electrode with all additives.....	67
Figure 4.23.	The discharge curves (voltage vs. capacity) for Zn electrode with all additives.....	67
Figure 4.24.	SEM images of Zn electrode with all additives after 3 rd discharge scale bars (a) 5 μm (b) 5 μm at different locations on the substrate.....	68
Figure 4.25.	The discharge curves (voltage vs. time) for Zn electrode without Ca(OH) ₂	70
Figure 4.26.	The discharge curves (voltage vs. capacity) for Zn electrode without Ca(OH) ₂	70
Figure 4.27.	SEM images of Zn electrode without Ca(OH) ₂ after 3 rd discharge scale bars (a) 5 μm (b) 10 μm at different locations on the substrate.....	71
Figure 4.28.	The discharge curves (voltage vs. time) for Zn electrode without PbO.....	72
Figure 4.29.	The discharge curves (voltage vs. capacity) for Zn electrode without PbO.....	73
Figure 4.30.	SEM images of Zn electrode without PbO after 3 rd discharge (a) scale bars (a) 5 μm (b) 10 μm at different locations on the substrate.....	74
Figure 4.31.	The discharge curves (voltage vs. time) for Zn electrode without PEG.....	75
Figure 4.32.	The discharge curves (voltage vs. capacity) for Zn electrode without PEG.....	76
Figure 4.33.	SEM images of Zn electrode without PEG after 3 rd discharge scale bars (a) 5 μm (b) 10 μm at different locations on the substrate.....	77
Figure 4.34.	XRD spectra of Zn electrode with PEG, PbO and Ca(OH) ₂ , Zn electrode with PEG and Ca(OH) ₂ , Zn electrode with PEG and PbO, Zn electrode with PbO and Ca(OH) ₂ after third discharge.....	78

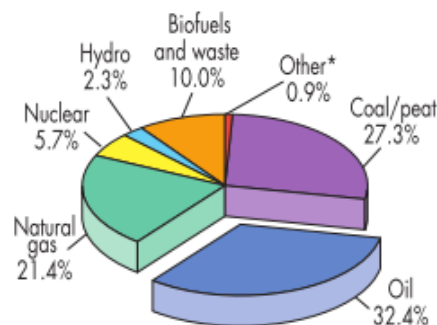
LIST OF TABLES

<u>Table</u>		<u>Page</u>
Table 1.1.	The potential for renewable energy sources.....	3
Table 1.2.	The characteristics and applications of primary and secondary batteries.....	4
Table 1.3.	Characteristics of batteries	7
Table 3.1.	Properties of materials used in this study.....	26
Table 4.1.	XRD test results for ZnO powder in the literature, commercial ZnO powder, ZnO powder (from ZnCl ₂) and ZnO powder (from Zn(NO ₃) ₂ ·6 H ₂ O).....	43
Table 4.2.	The BET surface area, micropore area, total pore volume and average diameter of commercial ZnO powder, ZnO powder (from ZnCl ₂) and ZnO powder (from Zn(NO ₃) ₂ ·6 H ₂ O).....	44
Table 4.3.	XRD test results for the paste of Zn electrodes from commercial ZnO powder, ZnO powder (from ZnCl ₂) and ZnO powder (from Zn(NO ₃) ₂ ·6 H ₂ O).....	50
Table 4.4.	The results of XRF analysis of commercial Ni-1 electrode.....	56
Table 4.5.	The results of XRF analysis of commercial Ni-2 electrode.....	56
Table 4.6.	XRD test results for both commercial Ni electrodes.....	56
Table 4.7.	Zinc electrode additives.....	65
Table 4.8.	XRD test results for Zn electrode with PEG, PbO and Ca(OH) ₂ , Zn electrode with PEG and Ca(OH) ₂ , Zn electrode with PEG and PbO, Zn electrode with PbO and Ca(OH) ₂ after third discharge.....	79

CHAPTER 1

INTRODUCTION

Energy is the most important and inevitable requirement for humankind. The global energy requirement increases with the growth of population. The global energy consumption was 132,000 TWh, in 2008 equivalent to an average energy consumption rate of 15 TW. Energy is produced from various sources, which can be categorized as renewable and non-renewable. Non-renewable energy sources including coal, petroleum, natural gas and radioactive fuel are not only limited and unevenly distributed throughout the globe but also are the main sources of environmental pollution as well as political and military conflicts. Due to political, economic and environmental concerns, renewable energy sources have attracted interest both from industry and academia. Renewable energy sources (solar, wind, ocean, hydropower, biomass, geothermal resources etc.) have the potential to supply ever-increasing global energy demand. Contrary to the nonrenewable sources, they are practically unlimited, clean, economical and nature-friendly (Zeray, 2010; Avci, 2009).



*Others includes geothermal, wind, solar, heat etc.

Figure 1.1. Energy supply of the world in 2010
(Source: IEA, 2012).

The quality of life is closely related to the amount of energy that is being consumed. The energy requirement has been notably increasing with technological advances and population growth. Increasing population in conjunction with demand of materials, transportation, electricity etc. is considered as the main source of the so-called 'energy crisis'. Unevenly distributed primary (non-renewable) energy sources,

exponentially increasing population of developing countries and hence, increasing need for food, transportation, heating result in more energy use from nonrenewable sources leading to political and environmental problems (ozone layer depletion, global warming, climate change, etc.). Therefore, strong economic growth as well as expanding population leads to an increase in global energy use. According to International Energy Agency, world energy consumption will increase approximately 56 % between years 2010 and 2040. As seen in Figure 1.2, energy consumption increases from 524 quadrillion Btu (153,569,240 TWh) in 2010 to 630 quadrillion Btu (184,634,773 TWh) in 2020, and to 820 quadrillion Btu (240,318,276 TWh) in 2040 (Avcı, 2009; Pérez-Lombard et al., 2008; Tester et al., 2005; IEA, 2013).

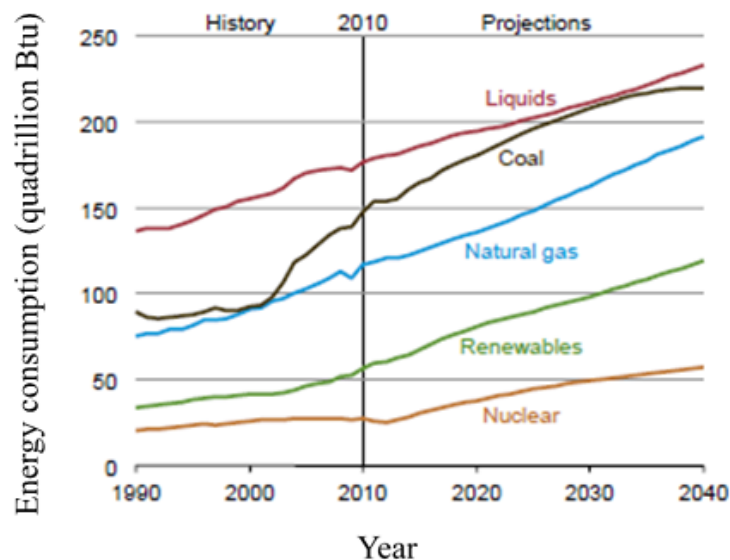


Figure 1.2. World energy consumption between 1990 and 2040 (quadrillion Btu) (Source: IEA, 2013).

As seen in Figure 1.2, liquid fuels consisting of mostly petroleum fuel remain the greatest source of energy. On the other hand, renewable energies and nuclear power are the fastest-growing energy sources. Use of renewable energy and nuclear power will be expanded due to increasing price and environmental impact of petroleum (IEA, 2013).

Table 1.1 lists the potential capacities of selected renewable energy sources. In theory, solar and wind energy have the potential to satisfy the global energy demand. However, sufficient technological advances to increase the efficiencies of these technologies are still needed.

In order for renewable energy sources to be competitive with the conventional primary energy sources, energy needs to be produced at or transported to consumer's

location. This puts a great limit, especially for solar energy since the energy is only available during the day. Therefore, renewable energy technologies have to be complimented with advanced energy storage options so that energy can be transported and will be available at any time. Although there exist various energy storage technologies, none of the existing ones provides a cheap and effective solution. Advanced electrochemical energy storage technologies (batteries) seem to be the only promising pathway for making solar and wind energy solid alternatives to primary energy sources. In recent years, academic and industrial research have focused on improving the capacity while reducing the cost of electrochemical energy storage technologies with the new chemistries (Zito, 2010; Huggins, 2009; Chris et al., 2009; Tahvonen at al., 2001).

Table 1.1. The potential for renewable energy sources.

The renewable energy source	The potential for renewable energy (TWh)
Solar energy	440,000
Wind power	167,000
Geothermal energy	139,000
Biomass	70,000
Hydropower	14,000
Ocean energy	280

1.1. Batteries

Although renewable energy sources (especially solar and wind) have the potential to reduce the economic, environmental and political problems associated with fossil fuels and nuclear energy, unpredictability of these sources in terms of availability has prevented them reaching their full potential. One of the advantages of fossil fuels is the ability to transport fuel or electricity to customer site that might be thousands of kilometers away from the fuel source. In addition to that, power plants that convert fossil fuels into electricity can be operated 24/7 providing uninterrupted energy source for the grid-connected customer. Therefore for any renewable energy technology to be competitive with the conventional energy technologies, the energy from these sources must be converted into other energy forms and stored for transportation or later use. Improvement in energy conversion and storage technologies is a must for advancement of solar energy and wind energy as clean, cheap and economical alternatives to fossil

fuels. So the bottleneck for wide-scale application of renewable energy sources is not these technologies themselves but the lack of efficient and cheap electrochemical energy storage options, namely batteries.

Battery is a device that transforms chemical energy into electricity performing an electrochemical oxidation-reduction reaction. Batteries can be classified into two groups as primary (non-rechargeable) and secondary (rechargeable) batteries. Primary batteries usually have higher energy densities as well as better shelf lives. Secondary batteries are capable of being recharged electrically, making them better suited in applications in which lower life-cycle and cost are needed (Linden & Reddy, 2001; Vincent & Scrosati, 2003; Kiehne, 2003). The characteristics and applications of these batteries are shown in Table 1.2.

Table 1.2. The characteristics and applications of primary and secondary batteries (Source: Linden and Reddy, 2001; web1).

Types of batteries	Characteristics	Applications
Primary battery	Convenient, simple and easy to use, good shelf life, reasonable energy and power density, reliability and acceptable cost	Portable electric and electronic devices, lighting, photographic equipment, PDA's (Personal Digital Assistant), communication equipment, hearing aids, watches, toys, memory backup etc.
Secondary battery	High specific energy, low resistance, and good performance over a wide temperature range	Starting, lighting, and ignition (SLI) automotive applications, industrial trucks, materials handling equipment and emergency and standby power portable devices such as tools, toys, lighting, and photographic, radio, and more significantly, consumer electronic devices (computers, camcorders, cellular phones)

The history of batteries goes back more than 200 years. The first description of a battery as an electrical device was given by Benjamin Franklin, who in 1748 explained multiple Leyden jars by analogy to a battery of cannon. In 1780, the basic electrochemical cell was demonstrated by Luigi Galvani using two different metals (e.g., zinc and copper) in his famous frog leg experiment. The Volta pile was invented in 1800 by Alessandro

Volta, Professor of Natural Philosophy (Physics) at the University of Pavia in Italy. This battery, shown in Figure 1.3, generates electric current from chemical reactions between silver and zinc metal.

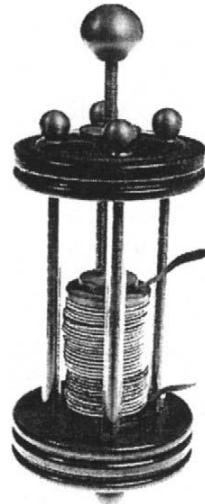


Figure 1.3. Volta pile
(Source: Technical Marketing Staff of Gates Energy Products, 1998).

In 1836 John Frederic Daniell invented Daniell cell consisting of a copper pot and zinc electrode immersed in sulfuric acids saturated with a copper sulfate solution and zinc sulfate, preventing the hydrogen evolution from the cell. After this invention, batteries became more reliable and powerful, and were applied in industry, in particular in telegraph networks. However, Daniell cell had a major problem due to two separate solutions used in the cell.

With the introduction of flashlight at the turn of the century, some 20 years after Edison's invention of the incandescent lamp, the demand for batteries sharply increased.

In 1870s, introduction of dynamos or electromagnetic generators gave rise to the electrical applications in industry worldwide and began slowly replacing other sources; mainly steam power. Since then, electricity has become the undisputed champion for domestic and industrial use.

From 1940s all the way to microelectronics age, the domestic uses of battery were in torches (flash lamps), in toys, in vehicles (for starting, lighting and ignition) and in radios. There were not any significant applications of battery systems in industry. However, with the development of microelectronics-based devices, and their increasing use in domestic and industrial applications, the research and production in battery

technologies have been increasing steadily. Battery technology has become popular due to the main way to meet the demand of portable energy technology (Crompton, 2000; Technical Marketing Staff of Gates Energy Products, 1998; Dell, 2000).

In recent years, due to the economic and environmental factors, research related to battery technologies have increased. Widely established electronic and electrical systems that the world population depends on for their daily life have made the batteries indispensable for portable and stationary applications. With the advent of micro and nanotechnology, batteries have become popular power sources for portable electronic devices. Due to a wide variety of applications that have different power, cost, durability and performance requirements, there are many different types of batteries based on different chemicals.

For instance, lead-acid batteries, one of the commonly used batteries, are cheap, easy to produce and their source materials are widely available. Despite their advantages in many respects, these types of batteries are not convenient to use in portable applications due to their weight (Pavlov, 2011).

Excellent long-term storage and continuous overcharge capability make nickel-cadmium batteries more reliable and commonly used rechargeable battery. However, the major disadvantages of these batteries are mainly related to their high cost; approximately ten times higher than that of lead-acid batteries, and environmental concerns related to the disposal of battery containing cadmium. Nickel-hydrogen battery, which has higher specific energy, was developed in order to meet energy demand in spacecraft applications despite its high cost. Nickel-metal hydrate battery is newer technology of nickel-hydrogen battery in terrestrial application.

Performance of nickel-metal hydrate battery during charge and overcharge process is similar to that of nickel-cadmium battery, while its volumetric energy density is higher than that of nickel-cadmium battery. On the last few decades, the technology of the lithium battery has received interest for use in both primary and secondary battery systems. Among these lithium batteries, lithium-ion battery has widespread applications, in particular portable electronic fields due to its light weight and higher energy density (Linden & Reddy, 2001; Dell, 2000; Shuklaa et al., 2001). The properties of these batteries are summarized in Table 1.3.

Table 1.3. Characteristics of batteries
(Source: Chris et al., 2009; Linden & Reddy, 2001; Pistoia, 2005).

	Lead-Acid, LA	Nickel-Cadmium, Ni-Cd	Nickel-Metal Hydride, Ni-MH	Lithium-ion, LiCoO ₂	Lithium-ion, LiFePO ₄	Lithium-polymer
Voltage, V	2.1	1.2	1.2	3.6	3.25	3.7
Specific energy, Whkg⁻¹	30-40	40-60	30-80	160	80-120	130-200
Energy density, WhL⁻¹	60-75	50-150	140-300	270	1400	300
Power density, Wkg⁻¹	180	150	250-1000	1800	1400	3000
Charge retention at 20°C (shelf life)	6-9 months	3-6 months	12-18 months	9-12 months	9-12 months	24-36 months
Cycle durability, cycles	500-800	2000	500-2000	1000	400-1200	>1000
Operating temperature, °C	-40 to 60	-20 to 45	-20 to 45	-20 to 60	-20 to 60	-20 to 60
Cost, US\$/Wh	0.5	0.25	0.5	0.8	0.8	0.8
Commercial use since	1970	1950	1990	1991	1991	1999

Zinc based batteries such as zinc-air, nickel-zinc (NiZn), zinc-silver and others have attracted attention as power sources due to low cost, low toxicity, safety, abundant resource, low equilibrium potential, high specific energy associated with zinc-metal (Ito et al., 2011; Lee et al., 2006a; Müller et al., 1998; Shivkumar et al., 1995).

The theoretical specific capacities of lead and iron are smaller compared to the capacities of zinc, 825 Ahkg⁻¹, (Vincent & Scrosati, 2003). Furthermore, nickel-zinc battery exhibits high specific energy (55-85 Whkg⁻¹), power density (140-200 Whkg⁻¹), high open circle potential (1.705 V) and a self-discharge rate less than 0.8 % per day (Shuklaa et al., 2001; Cheng et al., 2007; Cheng et al., 2013; Huang et al., 2008; Jindra, 1997). In the NiZn battery system, potassium hydroxide solution with 30-35 % (w/w) is used as an electrolyte to obtain maximum ionic conductivity. The solubility of zinc depends on the concentration of potassium hydroxide, and therefore, the zinc solubility decreases with decreasing concentration of electrolyte. However, there are two problems during recharging in aqueous electrolyte. One of these problems is the dissolution of zinc oxide in aqueous electrolytes due to the increase in the concentration of zincate ions. In other words, the solubility of the reaction products, zincate, is a very important factor for

electrode reactions that occur by dissolution of the reactants. As a consequence, the structure of the zinc electrode will be changed as shown in Figure 1.4. This leads to zinc densification, passivation and dendritic growth of zinc. Therefore, the electrolyte with low potassium concentration is used with both inorganic and organic additives (Linden & Reddy, 2001; Jindra, 1997).







	Initial state		After discharge		After recharge	
Soluble product of reaction				Electrode material to a large extent dissolved		Precipitation causes shape changing
The product of reaction is (nearly) insoluble				Product of reaction widely covers surface		Precipitation of the initial component causes little changes in structure

Figure 1.4. Effect of the solubility of the reaction products on electrode structure during discharge/charge process (Source: Kiehne, 2003).

The other problem is that precipitation of zinc on the electrode does not occur at the same locations during charging. Zincate ions are moved away from the zinc electrode during discharge due to convection and gravity. During charging zinc is deposited to the nearest available electrode surface. This eventually causes a shape change with increasing charge/discharge cycle, and therefore, leads to short lifetime for the electrode (Huggins, 2009; Geng, 2003; Yang et al., 2009; Yuan et al., 2005; Yuan et al., 2006a).

Zinc densification, passivation, dendritic growth of zinc and shape change are important factors for the service-life of zinc based batteries. The passivation of zinc electrode occurs when the dissolution of zinc produces a situation in which the solubility of zincate ($Zn(OH)_2$) in electrolyte is exceeded, and an insulating ZnO barrier layer is formed (Zhang, 1996). One of the crucial problems in zinc electrode is a tendency of dendritic growth of zinc during charging.

Many attempts have been made to eliminate these problems. One approach is to use additives in either electrode (Müller et al., 1998; Huang et al., 2008; Yuan et al., 2006a, Shivkumar et al., 1998; McBreen et al., 1981) or electrolyte (Shivkumar et al.,

1995; Adler et al., 1993; Iwakura et al., 2005). Another one is to make an electrode including different morphology and size of zinc oxide (Yuan et al., 2005; Perez et al., 2006; Yuan et al., 2006b; Yang et al., 2010).

In this study, it was aimed to investigate the electrochemical stability of zinc electrodes for battery applications using different zinc oxide powders with various morphologies and additives. Zinc oxide powders were synthesized under different conditions (precursors, temperatures and aging times) to investigate the effect of initial morphology of zinc oxide on the performance of nickel-zinc battery.

This thesis contains five chapters. In chapter one, general information on batteries, importance of zinc-air and nickel-zinc and their problems, the methods of reduction of their problems are introduced. In chapter two, a literature survey to overcome problems of zinc electrode in both zinc-air and nickel-zinc batteries are presented. In chapter three, the specification of chemicals used in this study and also experimental set-up, material preparation methods, such as synthesis of zinc oxide powders are explained in detail. In chapter four, the structural characterization of synthesized zinc oxide powder, zinc electrodes prepared using these powders and commercial nickel electrodes are presented. Charge/discharge characteristics of pouch cells using these electrodes are also presented and discussed in this chapter. Finally, conclusions and recommendations are given in chapter five.

CHAPTER 2

ZINC BATTERIES

In this chapter, the information related to zinc electrodes in both zinc-air and nickel-zinc batteries are presented. The chapter contains overview of historical development of zinc electrodes, anode and cathode reactions, and a literature survey related to significant problems of zinc electrodes in batteries.

2.1. Rechargeable Nickel-Zinc Batteries

The rechargeable nickel-zinc (NiZn) battery is one of the most popular zinc-based batteries. The history of NiZn batteries dates back to 1901, when Thomas Edison fabricated a rechargeable NiZn battery system and Michaelowski patented a NiZn battery in Russia. Until 1930s, research on NiZn battery was dormant. In late 1930s, Dr. James J. Drumm published his research on NiZn battery in Ireland. The nickel-zinc battery was used in four 2-car Drumm railcar sets between 1932 and 1948 by Dr. Drumm. However, NiZn batteries lagged behind other battery technologies due to the limited charge/discharge cycle. In the 1960s, there were serious efforts for the development of NiZn batteries to replace silver-zinc battery in military applications. The increase of the interest in NiZn battery in electric vehicles continued in the 1970s (Linden & Reddy, 2001; Edison, 1903).

In recent years, nickel-zinc battery systems have found significant applications in rapidly expanding markets, such as in electric bicycles, electric scooters, electric lawn/garden equipment, trolling motors, electric and hybrid vehicles and deep cycle marine applications. Some companies, such as PowerGenix, Pkcell, etc., have stimulated research on NiZn batteries. PowerGenix, San Diego-based company, has focused on NiZn batteries for providing an effective and environmentally friendly recyclable alternative to existing battery technologies. The company produces NiZn battery with various sizes, AAA, AA, Sub-C, D and Prismatic. Other rechargeable NiZn batteries are sold by Pkcell in China. These cells have less capacity, 900 mAh (Size AA) compared with those of the

products of PowerGenix (1500 mAh). These NiZn batteries are generally used in household-electrical devices (web2; web3).

Today, nickel-zinc batteries are employed in the above mentioned applications. Fast recharge capability, sealed maintenance-free design, good specific energy, good cycle life, low environmental effect, abundant raw materials and low cost are the key features associated with NiZn batteries. However, these batteries suffer from higher cost than lead-acid batteries (Linden & Reddy, 2001; Christiansen et al., 2005).

A typical example of a sealed NiZn cell is shown in Figure 2.1.

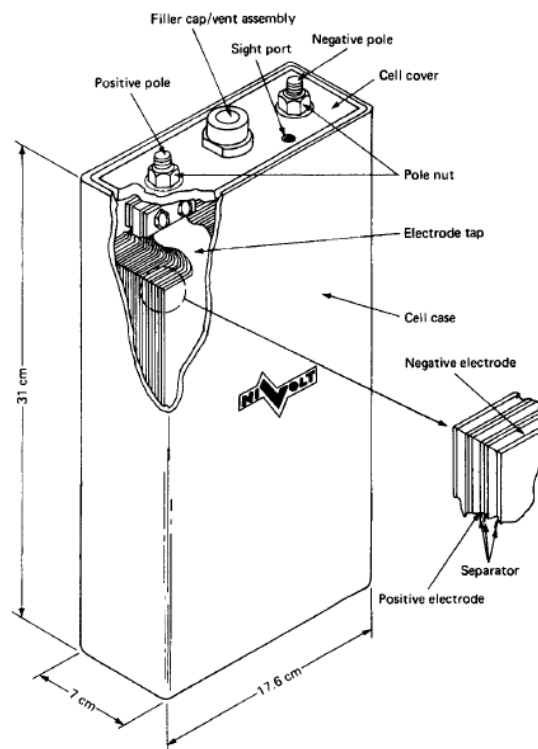
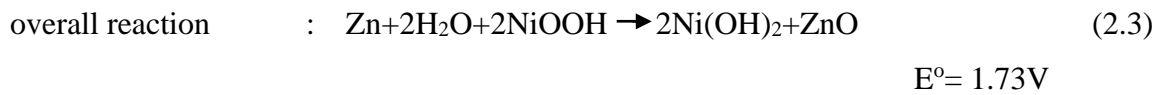
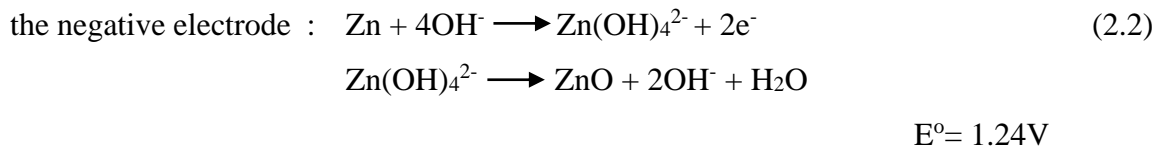
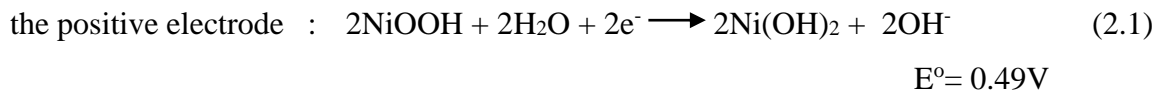


Figure 2.1. Sealed NiZn cell
(Source: Linden & Reddy, 2001)

In NiZn battery system, the nickel/nickel oxide electrode as the positive electrode and the zinc/zinc oxide electrode as the negative electrode are used. Nickel (III) oxyhydroxide is reduced to nickel (II) hydroxide, and at the same time, zinc metal is oxidized to zincate during discharge process, then zinc oxide is formed from zincate ion ($\text{Zn}(\text{OH})_4^{2-}$) in the aqueous electrolyte. The zincate transforms to zinc metal during the charging process. The discharge reaction at the zinc electrode takes place as follows:



2.1.1. Problems with Rechargeable Nickel-Zinc Batteries

The nickel-zinc battery is one of the most significant alkaline energy storage systems. Nickel-zinc batteries have attractive advantages such as being low cost, environmentally friendly and having abundant resources for raw materials. However, these batteries have not reached their full potentials mostly due to limited cycle life of the zinc electrode. The short life time of NiZn batteries is mainly resulted from the shape change of zinc electrode, passivation and dendritic growth of zinc which occur with increasing charge/discharge cycles (Huang et al., 2008; Geng, 2003; Yang et al., 2009; Yuan et al., 2005; Yuan et al., 2006a). Figure 2.2 and Figure 2.3 show both sides of the failed commercial battery separator.

In zinc electrode, the passivation is considered as one of the serious issues for the deterioration of zinc batteries. The phenomena occurs when the dissolution of zinc produces a situation in which the solubility of zincate in electrolyte close to the surface of the zinc electrode is exceeded and then barrier layer is formed (Zhang, 1996).

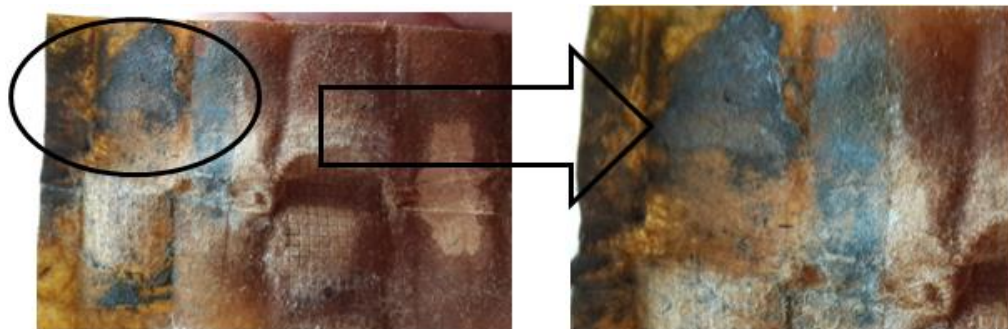


Figure 2.2. Failed commercial battery separator (Zn electrode side).

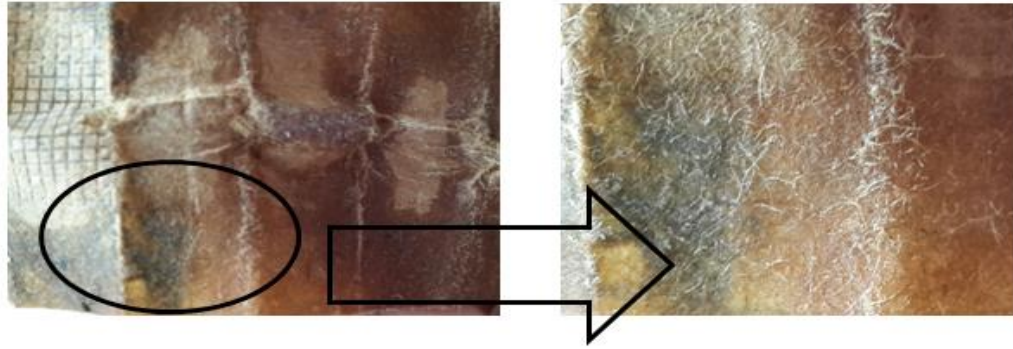


Figure 2.3. Failed commercial battery separator (Ni electrode side).

One of the main negative issues related to the recharge-ability of zinc electrode in aqueous electrolyte is the formation of the dendritic growth of zinc which is mainly resulted from convective forces in aqueous solution. The phenomenon of dendritic growth of zinc takes place due to convective forces, as seen in Figure 2.4. During charging process, the concentration of zincate ions decreases in electrolyte near the surface of zinc electrode, which gives rise to concentration polarization. The diffusion of zincate ions occurs specifically on the protrusion on the surface of zinc electrode, leading to the formation of dendrite (Huggins, 2009; Acton, 2013).

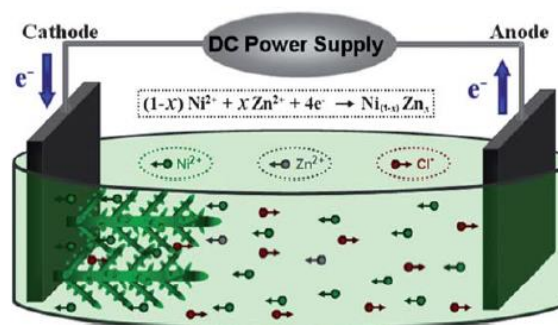


Figure 2.4. The formation of dendrite of zinc electrode during zinc deposition (Source: Wang, J. et al., 2012)

One of the major problems of zinc electrodes is a tendency of zinc electrode shape change during charge/discharge cycling which is mainly due to the solubility of zincate.

In discharge process, zinc is dissolved as zincate in electrolyte before zinc oxide precipitates onto zinc electrode when the solubility limit of zincate is reached. Due to convective forces, this process occurs near the bottom of the zinc electrode, leading to non-uniform electrode thickness (Huggins, 2009; Acton, 2013).

There are hundreds of studies to pinpoint the underlying mechanisms of the issues however, despite all that effort and hundreds of granted patents related to possible solutions such as using additives in either electrode (Huang et al., 2008; Geng, 2003; Yang et al., 2009, Mirmohseni & Solhjo, 2003) or electrolyte (Shivkumar et al., 1995; Adler et al., 1993; Iwakura et al., 2005; Braam et al., 2012) or using different morphologies for electrodes (Ito et al., 2011; Yuan et al., 2005), NiZn batteries are still far behind of competing battery technologies in terms of cycle life and performance/cost arena.

In the following sections, a brief literature review of the use of additives to overcome the problems mentioned above is given.

2.1.1.1. Additives to Electrolyte

The additives in the alkaline electrolyte in NiZn batteries have been the subject of a wide range of investigations. These additives consist of alkaline earth metal hydroxides, halides, sulfates, titanates and polymers which help to reduce zincate concentration and improve electronic conductivity and current distribution (Huang et al., 2008). Most studies involve 5 % to 40 % KOH solution as the traditional electrolyte in NiZn system. Shivkumar et al. examined the influence of the additives such as vanadium pentoxide, zinc oxide, lead oxide and thiourea in the electrolyte on the performance of the battery at various loadings (Shivkumar et al., 1995). The results showed that high concentration of additives (from 10^{-3} to 10^{-2} M) in KOH solution was preferred. V_2O_5 and PbO additives were found to be not suitable because the former causes corrosion and the latter leads to a decrease in the open-circuit voltage. On the other hand, ZnO was suitable to use in electrolyte of NiZn battery since they reduced corrosion and passivation of the zinc electrode, and they improved discharge capability and the cycle life (Shivkumar et al., 1995). In another study the solubility of zinc in KOH solution was investigated by adding KF and K_2CO_3 in NiZn cells (Adler et al., 1993). The solubility of zinc in electrolyte was found to be 20-25 % of the zinc solubility in 30 wt.% alkaline electrolytes. While the capacity-loss rates of 0.07 %/cycle and 0.09 %/cycle were measured in KOHKF and KOHKFK $_2CO_3$ electrolytes, respectively, KOH electrolytes showed 0.4-0.5 %/cycle values in the cell (Adler et al., 1993).

There are also several studies for NiZn batteries involving polymer electrolytes instead of conventional KOH solution. Iwakura and co-workers studied the effect of polymer hydrogel electrolyte on the performance of NiZn battery (Iwakura et al., 2005). The results indicated that the polymer electrolyte containing cross-linked potassium poly(acrylate) and 7.3 M KOH solution had a more positive impact on the charge/discharge characteristics compared to pure KOH solution. In addition, no dendritic growth of zinc was observed (Iwakura et al., 2005).

Fauvarque et al. prepared PEO-based solid polymer electrolytes to fabricate nickel-zinc and nickel-cadmium batteries (Fauvarque et al., 1995). The solid polymer electrolyte containing 60 wt.% PEO, 30 wt.% KOH and 10 wt.% H₂O was shown to have higher conductivities compared to concentrated high KOH (50 wt.%) electrolyte. The effect of temperature was found to be insignificant in terms of ionic conductivity of electrolytes (Fauvarque et al., 1995).

Polyethylene glycol (PEG)

Many organic additives in alkaline solutions are used as zinc corrosion inhibitors. Some of them are either expensive or toxic and not environmentally friendly. One of the few organic materials which is non-toxic and cheap is polyethylene glycol (PEG). Ein-Eli and co-workers investigated the effect of polyethylene glycol with a molecular weight 600 (kg/kmol) and polyoxyethylen alkyl phosphate ester acid on zinc metal electrode (Ein-Eli et al., 2003). The optimum concentration of organic inhibitors including polyethylene glycol and polyoxyethylen alkyl phosphate ester acid form was found to be 2000 ppm. The results indicated that inhibition capability of PEG was more than that of polyoxyethylen alkyl phosphate ester acid form (GAFAC RA600). The electrochemical studies represented PEG in alkaline solution had much more efficient inhibition capability compared to GAFAC RA600 (Ein-Eli et al., 2003). Today, PEG is commonly used in zinc electrodes for corrosion inhibitor and as binding agent in electrode preparation.

Polyvinyl alcohol (PVA)

Usually, alkaline polymers are used as binder to enhance ionic conductivity of electrolyte and electrode. The effect of poly(vinylalcohol) (PVA) and KOH in polymer electrolytes on ionic conductivity of electrolyte was investigated by Mohamad, A.A. et al. (Mohamad et al., 2003). In this study, the zinc electrode consisted of ZnO, lead oxide and graphite and the nickel electrode prepared with Ni(OH)₂ and PVA were used. It was observed that alkaline solid polymer electrolyte with PVA/KOH weight ratio of 60:40 had the highest ionic conductivity ($8.5 \times 10^{-4} \text{ Scm}^{-1}$). In this study, the cell was charged at a constant current of 10 mA for 1 h and at 1.6 V. At the end of 100 cycles, the capacity of the cell was measured as 5.5 mAh (Mohamad et al., 2003).

In another study, polymer gel electrolyte with 60:40 ratio in zinc-carbon cell was discussed by Saleem et al. (Saleem et al., 2009). The current charge/discharge efficiency was found to be 57 %. They claimed that the cell was stable and rechargeable (Saleem et al., 2009).

The PVA-KOH-TiO₂ alkaline polymer solid electrolyte was also examined in NiZn batteries by Wu et al. (Wu et al., 2008). They concluded that the specific capacity of PVA-KOH-TiO₂ polymer electrolyte, 250 mAhg^{-1} , was higher than that of PVA-KOH polymer electrolyte, 190 mAhg^{-1} . Nickel-zinc battery in which PVA-KOH-TiO₂ polymer electrolyte had great electrochemical properties such as ionic conductivity and AC impedance at low charge-discharge rate (Wu et al., 2008).

2.1.1.2. Additives to Electrodes

For NiZn batteries, incorporation of additives into electrode structure is usually achieved by mixing additives in powder form or as solute in alkaline solution with zinc oxide powder (Huang et al., 2008; Zhang, 2008).

Composite ceramic materials are suitable for the nucleation sites for ZnO and help improving efficiency of NiZn batteries. One of the studies based on these materials was performed by Huang et al. (Huang et al., 2008). They investigated the influence of the conductive ceramic having a precise composition of $(\text{ZnO})_{0.92}(\text{Bi}_2\text{O}_3)_{0.054}(\text{Co}_2\text{O}_3)_{0.025}(\text{Nb}_2\text{O}_5)_{0.00075}(\text{Y}_2\text{O}_3)_{0.00025}$ on the electrochemical performance of ZnO. The ZnO/conductive ceramic composite material was prepared with

a homogeneous precipitation method using $\text{Zn}(\text{NO}_3)_2$ and urea. The results indicated that 14 wt.% composite ceramic material revealed better stability, specific capacity and utilization ratio compared to pure nanosized ZnO (Huang et al., 2008). Zhang and co-workers also carried out a similar work (Zhang et al., 2008). The only difference was the investigation of various loadings of conductive-ceramic nanocomposite. Similar to the results of the previous study, 14 wt.% of composite ceramic material was found to improve cycle stability and increase specific capacity and utilization ratio when compared to lower loadings, and especially, pure ZnO. Incorporation of ceramic composite additive also increased the electrical contact between ZnO particles, reaction surface area of ZnO, the growth sites of ZnO deposits and decrease polarization of zinc electrode (Zhang et al., 2008). Average utilization ratios in both studies were found to be same as 99.5 % (Huang et al., 2008; Zhang et al., 2008).

Calcium lignosulfonate as a cathodic corrosion inhibitor and surfactant additive was used in the investigation by Tan and co-workers to explore the effect on electrochemical properties of ZnO electrode (Tan et al., 2012). The results showed that calcium lignosulfonate prevented the increase in the discharge rate and self-corrosion of zinc electrode and enhanced the deposit morphology of zinc electrode (Tan et al., 2012).

$\text{Sn}_6\text{O}_4(\text{OH})_4$, Bi, Ag, TiO_2 , CeO_2 and Ce_2O_3 are used as additives due to their impact on the electrochemical performance of ZnO. Yuan et al. investigated the effect of $\text{Sn}_6\text{O}_4(\text{OH})_4$ on the performance of zinc electrode (Yuan et al., 2007). They prepared modified ZnO containing various loadings of $\text{Sn}_6\text{O}_4(\text{OH})_4$ by hydrolyzation process. The addition of 27 wt.% was found to be effective in increasing electrochemical cycle stability of ZnO and average utilization ratio (98.5 %) of ZnO and decreasing the weight loss of ZnO electrode (Yuan et al., 2007). In another work, Bi based compound film-coated ZnO by hydrolyzation process was compared to Ni film-coated ZnO and Bi-modified ZnO by hydrolyzation process (Yuan et al., 2011). Bi based compound film used in this study consisted of $\text{Bi}(\text{NO}_3)_3(\text{OH})_2\text{O}_6$, BiO and Bi_2O_3 . It was pointed out that the discharge capacity (535 mAhg^{-1}) was better than those of Ni film-coated ZnO and Bi nanocompound-modified ZnO. This electrode was shown to have excellent cycling stability and electrochemical properties (Yuan et al., 2011).

Wu et al. fabricated Ag-modified ZnO by silver mirror process (Wu et al., 2009). The results showed that Ag-modified ZnO had better cycle stability, better midpoint discharge voltage, lower charge voltage and higher discharge voltage in comparison with unmodified ZnO (Wu et al., 2009). Compounds of Ce are also important additives for

ZnO electrode. The difference between CeO₂/ZnO synthesized by hydrothermal method and ZnO physically mixed CeO₂ was examined in detail by Fan et al. (Fan et al., 2013). The result of this study has shown that the CeO₂/ZnO electrode had a better charge/discharge performance. In addition, the Ce₂O₃ layer, which is the product of the reduced form of CeO₂ in charge process, played a key role in zinc electrode due to corrosion protective ability. Thus, it was reported that the layer improved utilization ratio (Fan et al., 2013). In this regard, these additives modified on the electrode are effective solutions to improve the electrochemical properties of zinc electrodes (Yuan et al., 2007; Yuan et al., 2011; Wu et al., 2009; Fan et al., 2013; Lee et al., 2011b).

In addition to additives mentioned above, there are a few other additives that are commonly used in commercially available zinc electrodes available today due to their well-established effects for improving overall performance of zinc electrodes.

Calcium hydroxide

Calcium hydroxide, Ca(OH)₂, as an additive for secondary zinc electrode leads to the formation of calcium zincate, CaZnO₂, as a stable active material. During the charge/discharge process, the material reacts with the Zn discharge product ZnO dissolved in the electrode. Apart from other effective additives such as Bi₂O₃, SnO₂, and In₂O₃ in electrode, calcium hydroxide is thermodynamically stable and prevents zincate concentration from increasing in the electrolyte. Therefore, the life of zinc electrode can be improved (Yuan et al., 2011; Yu et al., 2001; Coates et al., 1997; Luo et al., 2012).

In literature calcium zincate was either prepared by ball-mill method or synthesized by chemical processes (Wang et al., 2014; Yang et al., 2007; Zhu et al., 2003).

The results of a study in which rechargeable Zn electrode with calcium hydroxide showed that calcium zincate material has low solubility in KOH solution (10-30 wt.%), and also, the electrochemical reversibility of the electrode with this composite oxide was better than ZnO-based materials. As a result of this, the zinc electrode containing calcium hydroxide was found to overcome shape change and dendritic zinc formation and has better cycling life (Zhu et al., 2003). Calcium zincate can decrease the zincate solubility and help achieving better electrochemical performance. In order to investigate the properties of calcium zincate, powder microelectrode was developed by Yu et al. (Yu et al., 2001). They compared calcium zincate, ZnO and the mixture of zinc and calcium in the powder microelectrode. Calcium zincate electrode was shown to have better

cycleability than the others. The reason is that calcium zincate is more stable in low concentration of KOH solution. Initial discharge capacity of the electrode with calcium zincate was 230 mAhg^{-1} . As discharge cut-off voltage reached 1.0 V, the discharge capacity of cell did not change throughout 500 cycles (Yu et al., 2001). Wang et al. reported that there is influence of the crystallization and particle size of calcium zincate on the performance of zinc electrodes (Wang et al., 2014). Eth-calcium zincates, iso-calcium zincates and but-calcium zincates were synthesized using ZnO and $\text{Ca}(\text{OH})_2$ powder in ethanol, isopropanol and n-butanol solution, respectively. All of the results showed that eth-calcium zincates and iso-calcium zincates have greater discharge capacity as well as cycle stability in compared to but-calcium zincates. Additionally, as-prepared calcium zincates led to better cycle life and discharge capacity (Wang et al., 2014).

Lead oxide

Lead oxide is an excellent additive to suppress the hydrogen evolution in electrode. In literature, lead oxide was generally used around 2 % ratio in zinc electrode as an additive (Yu et al., 2001; Yang et al., 2007; Zhu et al., 2003; Lee et al., 2006b).

2.1.1.3. Morphology of Electrodes

The initial morphology of ZnO has been suspected to affect the electrochemical performance of Zn electrode. For example, nanorod ZnO, prismatic ZnO and ZnO nanoplates were shown to enhance the lifetime of zinc electrodes (Yuan et al., 2005; Yuan et al., 2006b; Yang et al., 2010). As reported in literature, ZnO in prismatic form and as nanowire in the electrodes have excellent discharge capacity.

ZnO nanowires were synthesized by hydrothermal method without any substrates by Yang et al. (Yang et al., 2010). During fabrication of the zinc electrode, they used acetylene black, carboxymethylcellulose and PTFE as well as ZnO nanowires. They claimed that nanowire ZnO electrode had better cycle stability, higher discharge/lower charge voltage and average discharge capacity reached 609 mAhg^{-1} at the 75th cycle. In addition, it was pointed out that the nanowire structure suppressed the growth of dendrite

because nanowire structures broke and changed into nanorod throughout charging/discharging cycles (Yang et al., 2010).

The prismatic form of ZnO by homogeneous precipitation was carried out by Yuan et al. (Yuan et al., 2006b). Zinc electrode also included Bi₂O₃ and binder additives. The results showed that the midpoint discharge voltage, cycle stability and passivation toleration to be higher than that of commercial ZnO with typical hexagonal prism particles, and also, the discharge capacity measured nearly 600 mAhg⁻¹ at the end of the 250th cycle (Yuan et al., 2006b).

Yuan and co-workers examined the effect of morphology and size of ZnO on the performance of electrode in detail (Yuan et al., 2005). They indicated that the value of the discharge capacity was about 500 mAhg⁻¹ until the 175th cycle. Compared to other morphologies, nanorod of ZnO particles exhibited the best electrochemical cycle stability and charge/discharge performance. The conventional ZnO with hexagonal prism and prismatic ZnO nanoparticles converted into flaky crystals, which decreased performance (Yuan et al., 2005). Plate-like ZnO synthesized by hydrothermal process was investigated by Ma et al. (Ma et al., 2008). Zinc electrode was prepared using PTFE, CMC and PVA as binders and acetylene carbon black. They claimed that this type of morphology displayed a better discharge stability, lower midpoint charge voltage and higher midpoint discharge voltage (Ma et al., 2008). Plate-like ZnO particles remained stable with increasing cycle, and therefore, the shape of zinc electrode did not change.

2.2. Rechargeable Zinc-Air Batteries

Zinc-air batteries are one of the most popular of metal air-batteries which store electrochemical energy by using oxygen from ambient atmosphere.

The first metal-air battery with a MnO₂-carbon cathode electrode was developed by Leclanche' in 1868. First commercial primary zinc-air battery was manufactured by George W. Heise and Erwin A. Schumacher for remote railway signaling and navigation aid systems in 1932. It was reported that the concept of the zinc-air battery attracted less attention between the 1930s and 1960s. In the 1950s, Winckler at al. improved primary air cell consisting of zinc-alkali-carbon, and air-depolarized cathode with suitable electrolyte and a metal anode. The demands for zinc-air batteries increased in late 1960s and early 1970s. In 1996, the rechargeable zinc-air battery was invented by Miro Zoric.

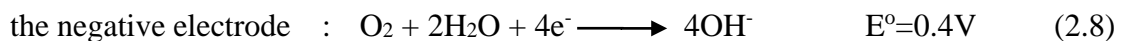
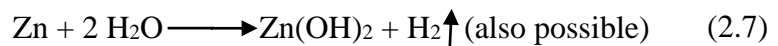
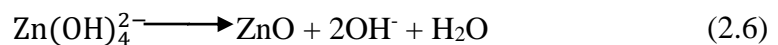
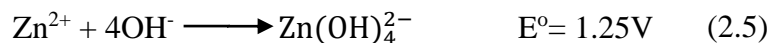
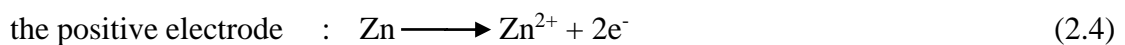
Mr. Zirot assisted to develop rechargeable zinc air batteries for power vehicles using first AC based drive trains (Linden & Reddy, 2001; Vincent & Scrosati, 2003; Crompton, 2000; Winckler, 1953).

In recent years, the commercialization of the zinc-air batteries has been intensified. A few companies are focusing on the development of these batteries to replace traditional secondary batteries such as lithium-ion and nickel-metal hydride. ReVolt, in Staefa, Switzerland, plans to launch small batteries for hearing aids and larger batteries for bigger and brighter color displays, camera and gaming functions and high-speed communication. On the other hand, Duracell as one of the biggest and probably the oldest companies has been manufacturing the rechargeable zinc-air batteries with various size and capacities (web4; web5).

Zinc-air batteries have many advantages over alkaline batteries such as high energy density, low cost, flat discharge voltage, safe and environmentally friendly raw materials and long passive shelf life when sealed.

Although zinc-air batteries are used in hearing aids, pagers, medical devices, some portable electronics, pagers, wireless messaging devices, some bluetooth devices and cellular phones, due their limited power output and activated life, they do not meet the requirements of many applications to be widely used (Linden & Reddy, 2001; Christiansen et al., 2005).

A typical zinc-air battery includes zinc electrode as anode, an air electrode as cathode, gas diffusion layer, a catalytic active layer, and separator as shown in Figure 2.5. The electrochemical reactions of anode and cathode can be written as (Lee et al., 2011a);



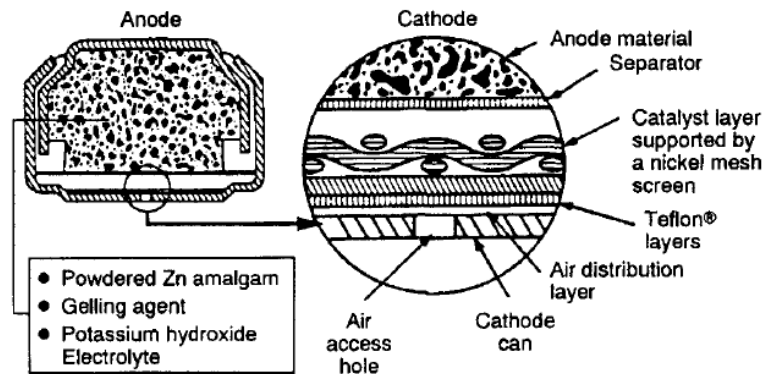


Figure 2.5. Typical zinc-air battery with key constructional properties (Source: Linden, D., 2001).

2.2.1. Problems with Rechargeable Zinc-Air Batteries

Despite the advantages such as low cost, abundance of raw materials having low equilibrium potential, low toxicity, a flat discharge voltage, and a long passive shelf life; zinc-air batteries suffer from serious issues which limit their widespread use (Linden & Reddy, 2001; Lee et al., 2011a).

Similar to NiZn batteries, the issues are due to the shape change of zinc electrode, zinc densification and passivation. The problems related to zinc electrode are explained in detail, in Section 2.1.1. The main problem of rechargeable zinc-air battery is air electrode deactivation limiting power of zinc-air battery. The cycle life of zinc-air battery is related to the air electrode failure including catalysts loss, carbon corrosion, blockage and leakage after hundreds of charge/discharge cycles. The air electrode in zinc-air battery consists of a gas diffusion layer and catalytic layer. The gas diffusion layer must be permeable to air but not to water. To overcome this problem, a smaller hole or lower diffusion membrane can be used in zinc-air battery, for water transfer rates are reduced. Otherwise, water vapor diffusion can cause a degradation in cell power capability and service life (Lee et al., 2011a). Due to these issues, almost all zinc-air batteries that are commercially available today are primary batteries.

Similar to NiZn battery research in literature, most studies on zinc-air batteries have focused on using additives and novel materials for solving issues mentioned above. The lack of widespread use of zinc-air batteries and their limited use in some niche applications are clear signs of the need for more academic and industrial research on the subject.

2.2.1.1. Additives to Electrodes

Similar to NiZn batteries, one of the concerns related to zinc electrode in secondary zinc-air batteries is shape change and dendritic zinc growth during charging. In literature, cellulose, polytetrafluoroethylene (PTFE), lead oxide and some alloys as additives are reported to overcome these difficulties, and also, reduce the hydrogen evolution. For this purpose, the structure of zinc electrode on the zinc-air battery and its wettability were optimized by Müller et al. by using variety of cellulose contents as well as PTFE and traces of PbO (Müller et al., 1998). They improved the porosity and pore size distribution to prevent pore plugging of the electrode. The results showed that the addition of 10 % cellulose to zinc electrode increased the cycle life and the power drain capability of the zinc-air battery. It was also concluded that pore size could be larger with increasing cellulose content (Müller et al., 1998). Lee and co-workers studied the electrochemical performance of three different electrodes prepared by pure zinc powder, zinc oxide powder and the composite material consisted of zinc oxide, lead oxide and PTFE taken by ratios 94, 2, 4 wt.%, respectively (Lee et al., 2006c). The results of both zinc oxide electrode and modified zinc oxide electrode were more promising than that of pure zinc electrode. A reduced level of dendritic growth was observed in zinc oxide electrode and modified zinc oxide electrode with this composite materials. Among the other electrodes, the potential in the hydrogen evolution reaction was the most negative in pure zinc electrode (Lee et al., 2006c).

In addition, the impact of three alloys on the performance of zinc electrode on the zinc-air battery was investigated by Lee et al. (Lee et al., 2006a). They prepared the zinc electrodes containing zinc, nickel and indium with different contents as calcinated at 500°C and 750°C. When their hydrogen overpotentials and the formation of dendrite compared, the electrode which has a composition of zinc 90 %, nickel 5 % and indium 5 % and calcinated at 500°C was more effective. They observed that the more negative values of hydrogen overpotential were, the less the corrosion of zinc electrode was performed (Lee et al., 2006a).

2.2.1.2. Additives to Electrolyte

The research on the effects of additives to electrolyte in zinc-air battery performance has been gaining more attention in recent years. Some of the recent studies have focused on replacing or improving conventional KOH electrolyte with additives. Various types of binders such as PVA, PEG and many kinds of acids (phosphoric acid, tartaric acid, succinic acid, and citric acid) positively affect the electrochemical properties of zinc oxide electrodes (Lee et al., 2006d; Masri et al, 2009; Huang et al., 2013). In a study by Mohamad et al., the electrolyte was prepared by using hydroponics gel with 6 M potassium hydroxide solution (Mohamad, 2006). The results indicated that the concentration of potassium solution was not related to open-circuit of the zinc-air battery as opposed to the findings of Othman et al. (Othman et al, 2001). In the study by Mohamad and co-worker, the surface of air electrode and gelled electrolytes remain stable (Mohamad, 2006). Lee et al. studied effects of additives such as phosphoric acid, tartaric acid, succinic acid and citric acid on the behavior of zinc oxide anode in the rechargeable zinc-air battery (Lee et al., 2006d). They prepared electrolyte by using potassium hydroxide, zinc oxide powder, polyethylene glycol and one of the following additives, phosphoric acid, tartaric acid, succinic acid and citric acid. These additives caused an increase in hydrogen overpotential and the reduction of the dendrite formation. In case of inhibition of hydrogen evolution, the effectiveness of the additives from the most effective to the least was tartaric acid, succinic acid, phosphoric acid, and citric acid, respectively. For the suppression of dendrite formation the order for effectiveness was found to be citric acid, succinic acid, tartaric acid, and phosphoric acid, respectively (Lee et al., 2006d).

2.2.1.3. Improvement of Air Electrodes

The performance of air electrode is considered to be crucial for secondary zinc-air batteries since the cycle life and service life of the secondary zinc-air batteries are mostly limited by air electrode. Catalyst poisoning and carbonate formation still remain as main obstacles for achieving theoretical performance of air electrodes. The details of air electrode morphologies and issues related air electrode performance in zinc-air batteries were reviewed by Pei et al. (Pei et al., 2014).

CHAPTER 3

EXPERIMENTAL WORK

In this chapter, information related to chemicals used in this study, experimental set-up, and material preparation methods such as ZnO powder synthesis, preparation of Zn electrodes are explained in detail. In addition, the material characterization methods such as Scanning Electron Microscopy (SEM), Energy-Dispersive X-ray Spectroscopy (EDX), X-ray Diffraction (XRD), X-ray Fluorescence Spectroscopy (XRF) and the particle size measurement etc. are given. Experimental work is divided into three main parts: preparation of rechargeable NiZn battery including preparations of electrodes and electrolyte, charge/discharge tests, and characterization. A diagram of experimental work is shown in Figure 3.1.

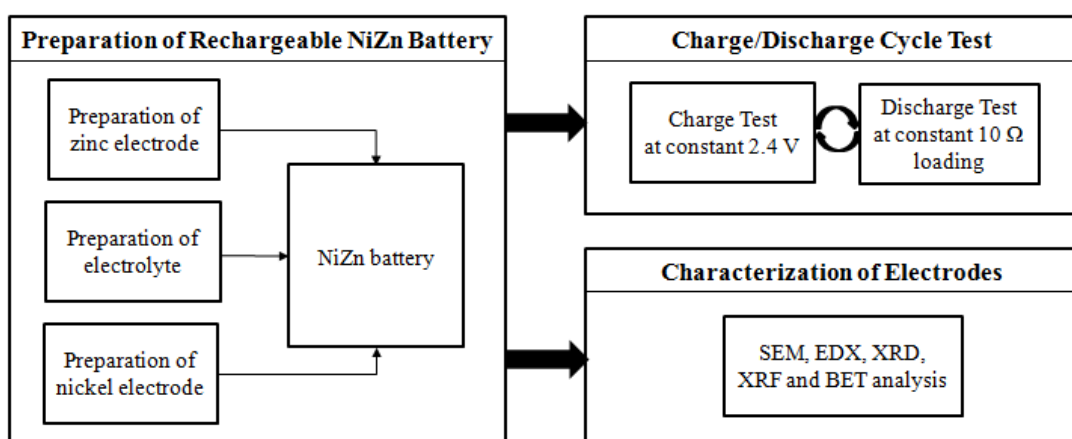


Figure 3.1. Experimental work

3.1. Materials

In this study, ZnO powders with different morphologies were synthesized using ZnCl₂ and Zn(NO₃)₂·6H₂O as starting materials. Analytical grade chemicals, zinc chloride (ZnCl₂, Merck), potassium hydroxide (KOH, Sigma), triethanolamine (TEA, C₆H₁₅NO₃, KIMETSAN), ammonium hydroxide (NH₄OH, Sigma/Aldrich, 28-29 %), zinc nitrate hexahydrate (Zn(NO₃)₂·6H₂O, Scharlau, 98 %), and sodium hydroxide (NaOH, Performans, 98 %) were used for the preparation of ZnO powder throughout the

experimental study. Commercial ZnO powder was supplied by Analitik Kimya Co.. In addition, the effect of organic binders PVA and PEG on zinc deposition during charging were investigated. Electrodeposition of zinc was performed using a zinc metal sheet, a stainless steel (SS 304) counter electrode and KOH electrolyte with various concentration of PEG or PVA. Analytical grade chemicals, potassium hydroxide (KOH, Sigma), zinc oxide powder (ZnO, KİMETSAN), polyethylene glycol (PEG, HO(C₂H₄O)_nH, Merck), polyvinyl alcohol (PVA, (C₂H₄O)_n, Merck) and deionized water (DIW) as solvent were used. For the investigation of the effects of selected electrode additives on the electrochemical performance of the battery analytical grade calcium hydroxide (Ca(OH)₂), lead (II) oxide (PbO), polyvinyl alcohol (PVA), polyethylene glycol (PEG), potassium hydroxide (KOH) were used. Detailed material properties are given in Table 3.1.

Table 3.1. Properties of materials used in this study

Chemicals	Chemical Formula	Molecular Weight (g/mol)	Supplier
Zinc chloride	ZnCl ₂	136.32	Merck
Triethanolamine, TEA	C ₆ H ₁₅ NO ₃	149.2	KİMETSAN
Potassium hydroxide	KOH	56.11	Merck
Ammonium hydroxide, 28-29%	NH ₄ OH	35.04	Sigma/Aldrich
Zinc nitrate hexahydrate, 98 %	Zn(NO ₃) ₂ .6H ₂ O	297.5	Scharlau
Sodium hydroxide 98 %	NaOH	40	Merck
Lead (II) oxide	PbO	223.19	Merck
Calcium hydroxide	Ca(OH) ₂	74.09	Merck
Polyethylene glycol	HO(C ₂ H ₄ O) _n H	4000	Merck
Polyvinyl alcohol	(C ₂ H ₄ O) _n		Merck

3.2. Preparation of Electrodes for Rechargeable NiZn Battery

Preparation of electrodes for rechargeable NiZn batteries involves incorporation of anode, cathode and electrolyte together to form an electrochemical cell, taking place as follows:

3.2.1. Nickel Anode

Since the focus of this study was zinc oxide preparation for the formation of Zn electrode, commercially available nickel anodes were used in NiZn batteries investigated in this work. Nickel electrodes that are used in commercial NiZn and NiMH batteries have been well characterized and do not differ much in terms of chemistry and morphology.

In this study, nickel electrodes with 1500-2050 mAh capacity were used for the preparation of NiZn batteries. No further treatment or process was applied. The crystal structure of nickel electrodes has been characterized by using XRD. Elemental compositions of the electrodes have been studied by XRF.

3.2.2. Zinc Cathode

Zinc cathodes that are employed in NiZn batteries are usually manufactured by mixing zinc oxide powder with various additives to obtain a paste, and then spreading the paste onto a current collector. In this study, various ZnO powders were used to investigate the effect of initial morphology of ZnO powder on the performance of the NiZn battery. Commercial ZnO powder was supplied by Analitik Kimya Co.. The morphology of the ZnO powder was studied by SEM, EDX, XRD and BET.

ZnO powders with different particle sizes and shapes were obtained by using ZnCl_2 and $\text{Zn}(\text{NO}_3)_2 \cdot 6\text{H}_2\text{O}$ as precursors. The processes of precipitation of ZnO from ZnCl_2 at 35°C, ZnO from ZnCl_2 at 50°C (Wei & Chang, 2008), ZnO from $\text{Zn}(\text{NO}_3)_2 \cdot 6\text{H}_2\text{O}$ aged for 15 minutes and ZnO from $\text{Zn}(\text{NO}_3)_2 \cdot 6\text{H}_2\text{O}$ aged for 30 minutes (Musić, 2007) are described in detail below:

ZnO synthesis from ZnCl_2

Synthesis was carried out by a precipitation of aqueous zinc solution and potassium hydroxide according to the reference (Wei & Chang, 2008). 100 ml solution containing 0.2 M KOH and 0.02 M triethanolamine (TEA) as a surfactant was mixed with 100 ml 0.1 M ZnCl_2 solution. Two separate batches were prepared and ultrasonic treatment (WUC-D06H, Wids) was performed at 160 W for 45 minutes at 35°C and at

50°C. The precipitate was separated from the liquid phase by centrifuging (Sigma, 3-16 PK) at 4000 rpm for 2 minutes at room temperature. The solid phase was then washed with 500 mL 0.1 M NH_4OH solution three times. Finally, the solid phase was dried at 50°C for 15 hours, then baked at 180°C for 2 hours in oven (WiseVen, WOV-30). The procedure is shown in Figure 3.2.

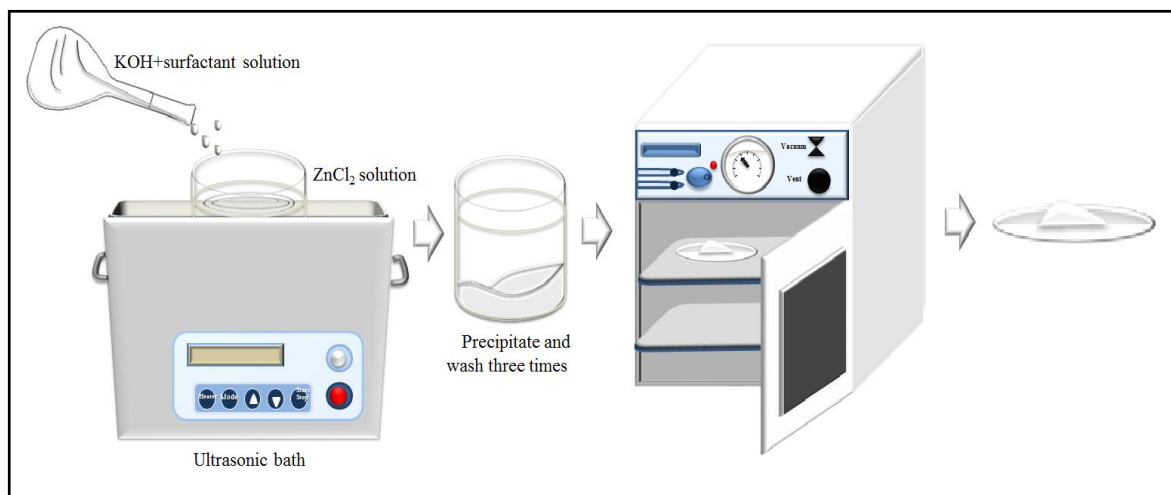


Figure 3.2. Experimental set-up for ZnO powder synthesized from ZnCl_2 .

ZnO synthesis from $\text{Zn}(\text{NO}_3)_2 \cdot 6\text{H}_2\text{O}$

Synthesis was carried out by a precipitation of aqueous zinc solution and sodium hydroxide according to the reference (Musić, 2007). 100 ml of 1 M $\text{Zn}(\text{NO}_3)_2 \cdot 6\text{H}_2\text{O}$ solution, 27.85 ml of 8 M NaOH and 22.15 ml of ultrapure water were mixed to obtain a pH value of 13.05 of the mixture.

NaOH solution and ultrapure water were added into the $\text{Zn}(\text{NO}_3)_2 \cdot 6\text{H}_2\text{O}$ solution while stirring in a magnetic stirrer (at 500 rpm) at 20°C. The precipitation system was aged at 20°C for 15 minutes or 30 minutes. The precipitate was separated from the liquid phase by centrifuging at 4000 rpm for 2 minutes at room temperature. The solid phase was washed with ultrapure water three times. Finally, the solid phase was dried at 50°C for 20 hours, and then baked at 180°C for 2 hours in oven. The procedure is shown in Figure 3.3.

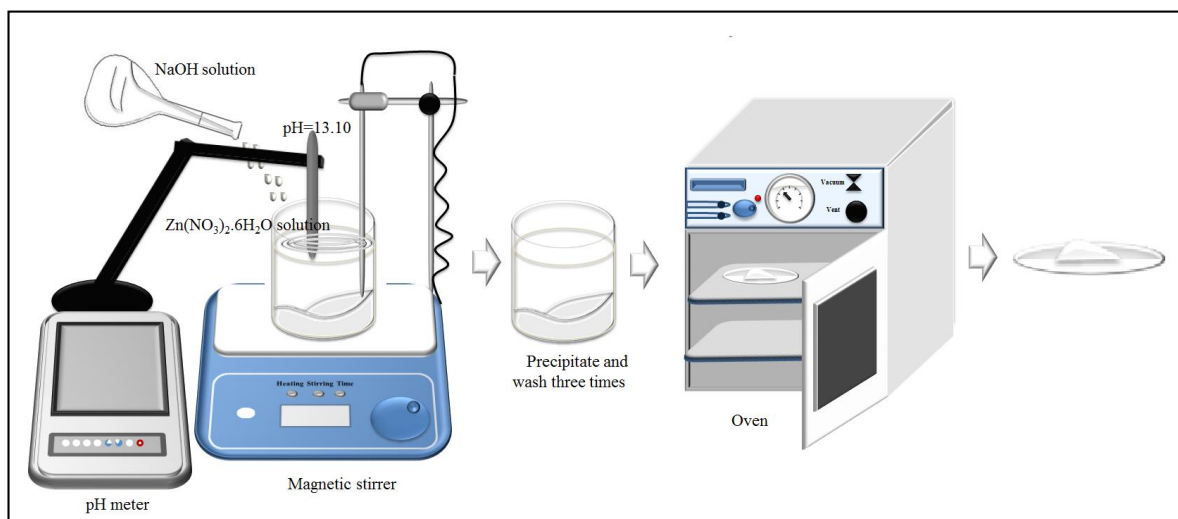


Figure 3.3. Experimental set-up for ZnO synthesized by $\text{Zn}(\text{NO}_3)_2 \cdot 6\text{H}_2\text{O}$.

Zinc Electrode Additives

Calcium hydroxide ($\text{Ca}(\text{OH})_2$), lead (II) oxide (PbO), polyvinyl alcohol (PVA), polyethylene glycol (PEG), potassium hydroxide (KOH) were used as additives. The effects of each additive used in this study are given in Chapter 2.

Deionized water (DIW) as a solvent was used in all steps of the preparation of secondary Zn electrode. As electrolyte, 10 % - 40 % (w/w) (or 1.8 M - 7.1 M) KOH solution was used during electrical characterization (charge/discharge cycle testing).

3.3. Zinc Electrodeposition Setup

A brief experimental study was performed to see if organic binders PVA and PEG have any effect on zinc deposition process during charging of NiZn battery. Electrodeposition of zinc was performed using a zinc metal sheet (0.5 cm x 2.5 cm), a stainless steel (SS 304, 2 cm x 6 cm) counter electrode and 10 % (w/w) (or 1.8 M) KOH electrolyte with 5 % (w/w) of PEG or PVA aqueous solution. 2.5 gram of excess ZnO was added to the solution to simulate battery environment. Zinc deposition was performed at two different current flux, 25 mA/cm^2 and 75 mA/cm^2 .

3.4. Preparation of Rechargeable of NiZn Battery

In order to minimize the time for electrical characterization and materials use, only 1 gram of zinc oxide powder used in Zn electrodes in all experiments. Mixture of powders consisting of 93 % (w/w) ZnO, 3 % (w/w) Ca(OH)₂ and 1 % (w/w) PbO were mixed in a stirrer. The operation was conducted in magnetic stirrer at 700 rpm for 15 minutes then obtained powder was mechanically mixed with 100 μ l of 10 % (w/w) KOH solution and 300 μ l of 3 % (w/w) PEG aqueous solution, respectively.

The paste was then applied onto a 40 μ m thick craft paper to form a uniform layer and a copper wire (7 cm) was placed on top as current collector. The craft paper was then folded twice to obtain a Zn electrode 2 cm x 2 cm in size. To make sure that there is a good contact between current collector and Zn electrode, mechanical pressure was applied either using alligator clips or nylon fishing line.

Zinc electrodes were kept in 15 % (w/w) KOH solutions until their first use. For electrochemical testing, Zn electrodes and nickel electrodes were placed in a beaker filled with a KOH electrolyte at desired concentration. Ni electrode capacity was kept twice the theoretical Ni electrode capacity required for testing by connecting multiple Nickel electrodes in parallel.

Schematic representations of the preparation of NiZn battery system are given in Figure 3.4 and Figure 3.5, respectively.

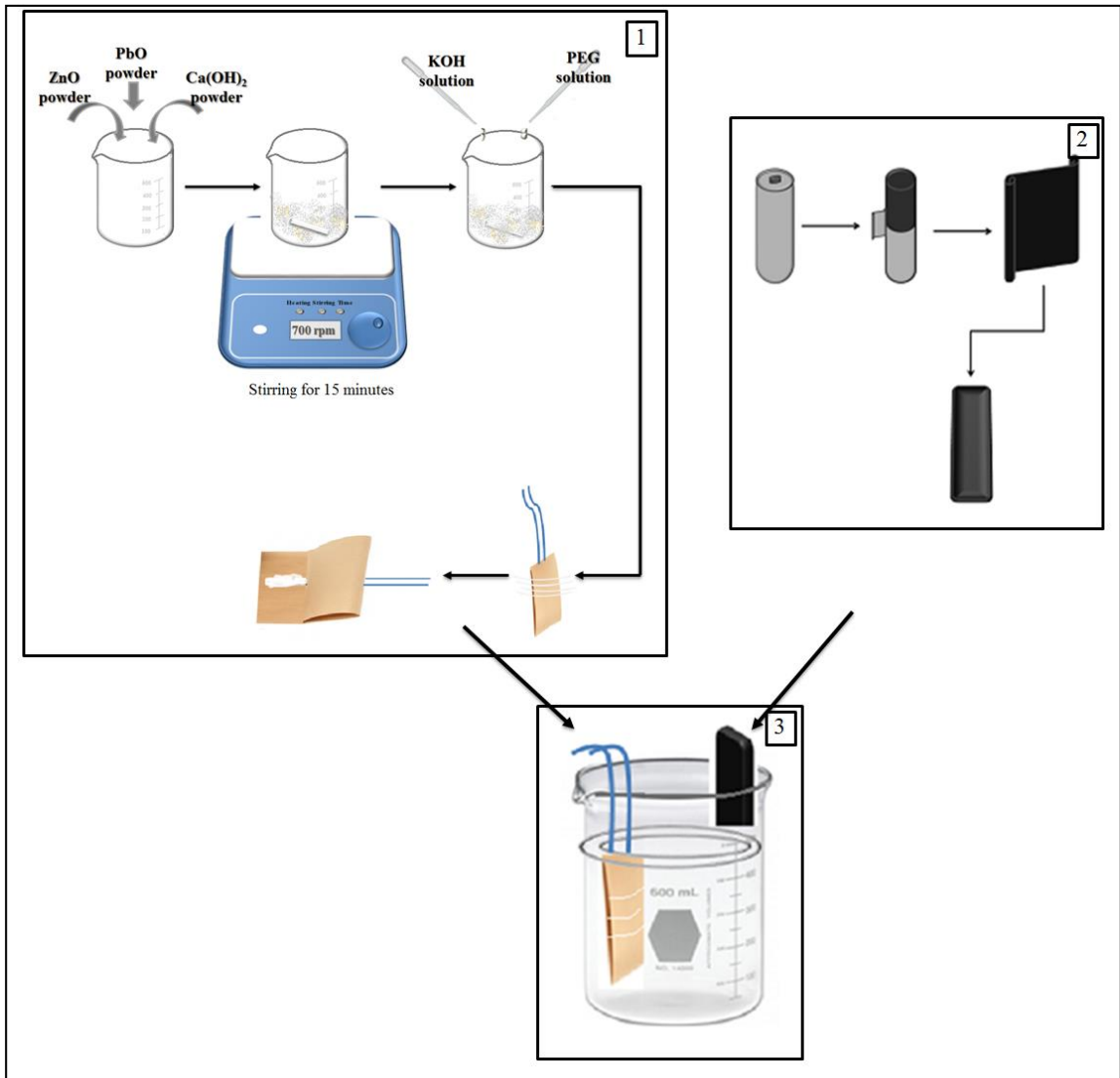


Figure 3.4. Schematic illustration of preparation of rechargeable NiZn battery: (1) preparation of Zn electrode, (2) Ni electrode obtaining from commercial NiZn and NiMH batteries, (3) NiZn battery.

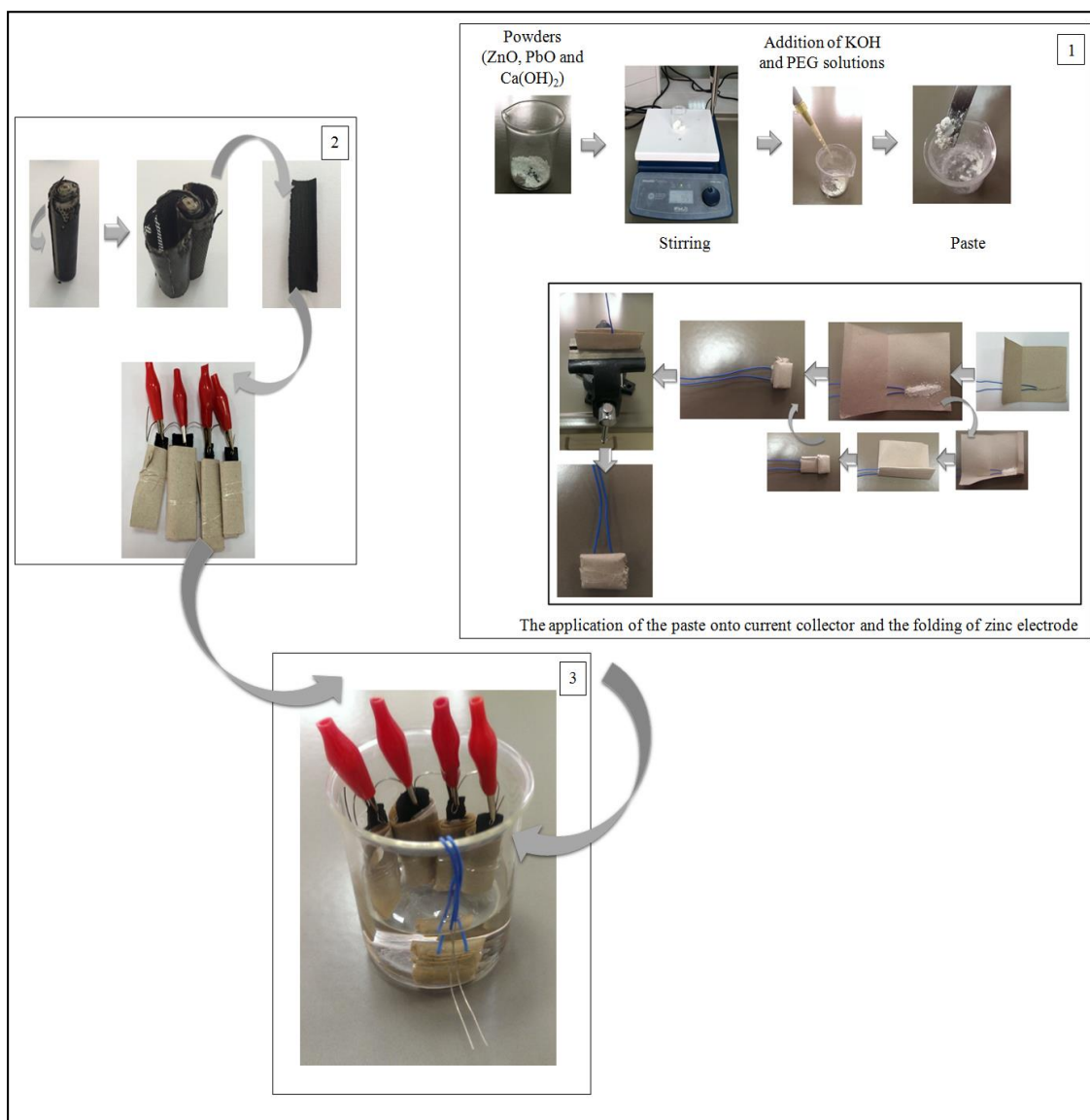


Figure 3.5. Photos illustration of preparation of rechargeable NiZn battery: (1) preparation of Zn electrode, (2) Ni electrode obtaining from commercial NiZn and NiMH batteries, (3) NiZn battery.

3.5. Characterization

Crystal structures of commercial ZnO powder (KIMETSAN), ZnO powder synthesized from ZnCl₂ and ZnO powder synthesized from Zn(NO₃)₂·6H₂O as well as zinc and nickel electrodes before and after charging were characterized by X-Ray diffraction (XRD) analysis using a Phillips™ Xpert diffractometer with Cu Kα as a radiation source. The data were collected in 2θ range of 5-80° with variable speeds from 0.001 to of 0.336θ/sec.

The microstructures of powder and electrodes were investigated with Scanning Electron Microscopy (SEM), FEI Quanta250 with a field emission gun. For powder analysis, 0.1 gram of all ZnO powder were dispersed in 25 ml ethyl alcohol under the ultrasonic treatment for 15 minutes. The solution was dried at 30°C to evaporate ethyl alcohol in suspension. The surface elemental composition was calculated according to the results of energy-dispersive X-ray spectrum (EDX, FEI Quanta250). The elemental analysis of powder and electrodes were performed by X-Ray fluorescence spectroscopy (XRF) using a Spectro IQ II instrument.

The surface area, pore volume and average pore diameters of powders used in this study were determined by BET (Quantochrom Autosorb-1). Degassing was performed at 250°C for 1.5 h.

3.6. Charge/Discharge Tests

The charge/discharge tests were performed using two DC power supplies (RXN 305D) which work either current or voltage limited. All tests were performed at room temperature. Initial charging of the cells was performed at a constant voltage of 2.4 V. Discharge tests were done by attaching a 10-Ω load to cells.

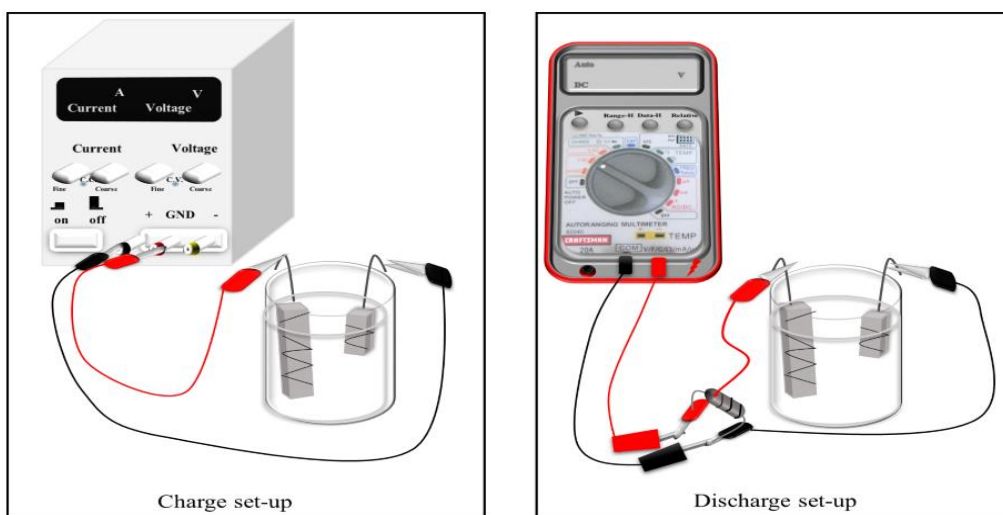


Figure 3.6. Charge and discharge set-up.

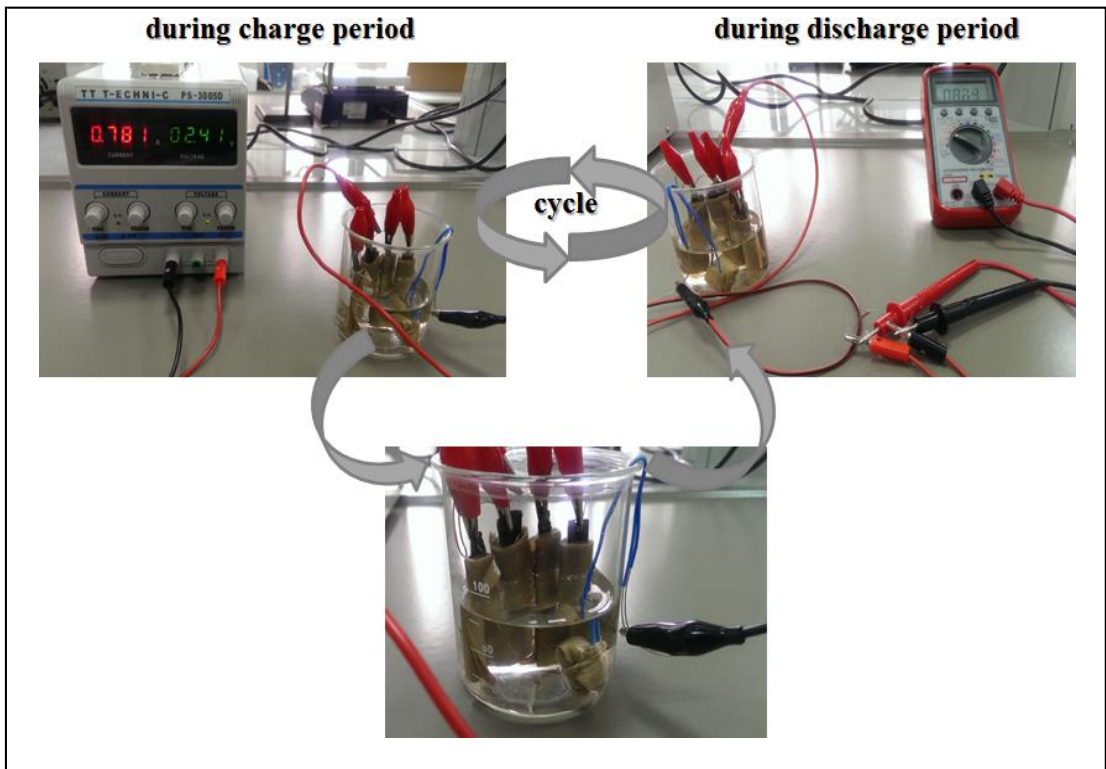


Figure 3.7. Photos of charge/discharge cycle setup.

CHAPTER 4

RESULTS AND DISCUSSION

In this chapter, results related to structural characterization of synthesized zinc oxide powders, zinc electrodes prepared using these powders and commercial nickel electrodes are given. Simple charge/discharge characteristics of pouch cells using zinc and nickel electrodes are also presented.

4.1. Zinc Electrodes

Zinc electrodes that are used in commercial NiZn batteries are usually manufactured by mixing ZnO powder with additives to form a thick paste that can be coated onto the current collector. Before the first use, the battery must be charged, i.e., ZnO in the electrode must be converted to metallic zinc. In order to maximize the capacities, 10-50 % excess ZnO is used in the Zn electrode recipes. In the literature, studies focused on the effect of initial morphology of ZnO powder reported conflicting results (Yuan et al., 2005; Yuan et al., 2006b; Yang et al., 2010; Ma et al., 2008).

In this study, ZnO powders synthesized from ZnCl₂ and Zn(NO₃)₂·6H₂O and commercial ZnO powder were used to prepare Zn electrodes. Powder morphology and its possible effect on the charge/discharge cycle were investigated.

4.1.1. Zinc Oxide Powder Synthesized from Zinc Chloride (ZnCl₂)

The detailed procedure for the synthesis of ZnO powder from zinc chloride is given in Chapter 3. SEM images of ZnO powder synthesized from ZnCl₂ at 35°C and 50°C are shown in Figure 4.1 and Figure 4.2, respectively. SEM image of ZnO powder synthesized at 35°C showed spherical particles with some variation in size as seen in Figure 4.1. No nanowires, nanorods or needle-like particles were observed. Based on SEM image analysis, the particle size was determined to be between 48 and 78 nm. During SEM analysis, EDX measurement were also performed and ZnO powder

synthesized at 35°C was found to contain 54.81 atomic % O and 45.29 atomic % Zn (22.82 wt.% O and 77.18 wt.% Zn).

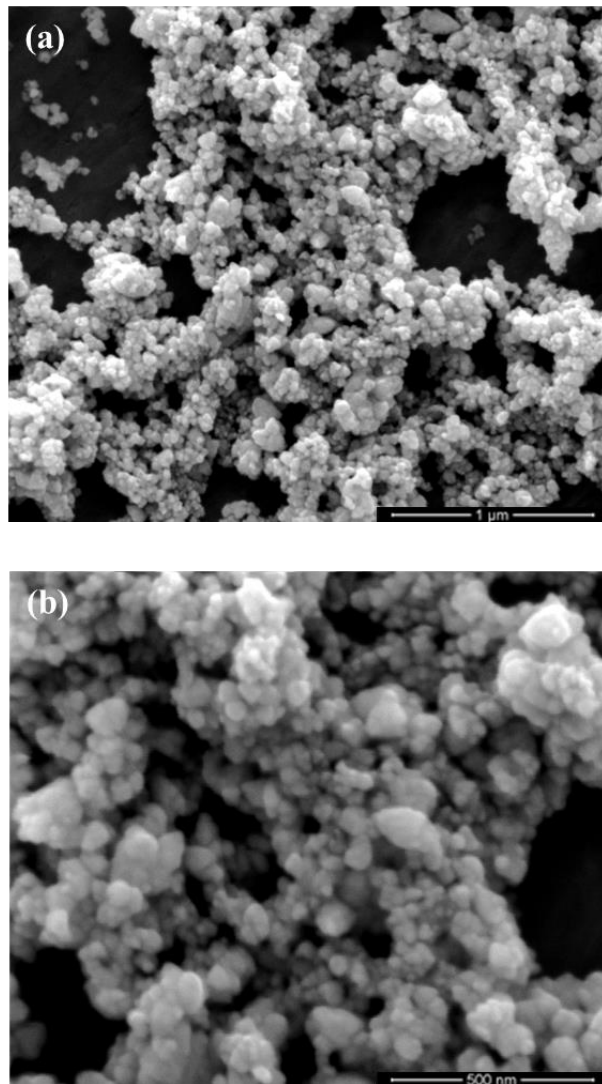


Figure 4.1. SEM images of ZnO powder synthesized from ZnCl₂ at 35°C scale bars (a) 1 µm (b) 500 nm.

SEM images of ZnO powder synthesized from ZnCl₂ at 50°C also show a homogeneous distribution of spherical particles between 20 and 40 nm in diameters as seen on Figure 4.2. This finding is in agreement with previously reported results in literature that as the reaction temperature increases, the average ZnO particle size decreases. The content of ZnO powder synthesized at 50°C was determined to be 51.39 atomic % O and 48.61 atomic % Zn (20.55 wt.% O and 79.45 wt.% Zn) based on EDX analysis. As seen EDX results of synthesized ZnO powder from ZnCl₂, it can be said that

powder synthesized at 35°C was found to be rich in OH⁻ ions and another powder (synthesized at 50°C) was rich in ZnO compound.

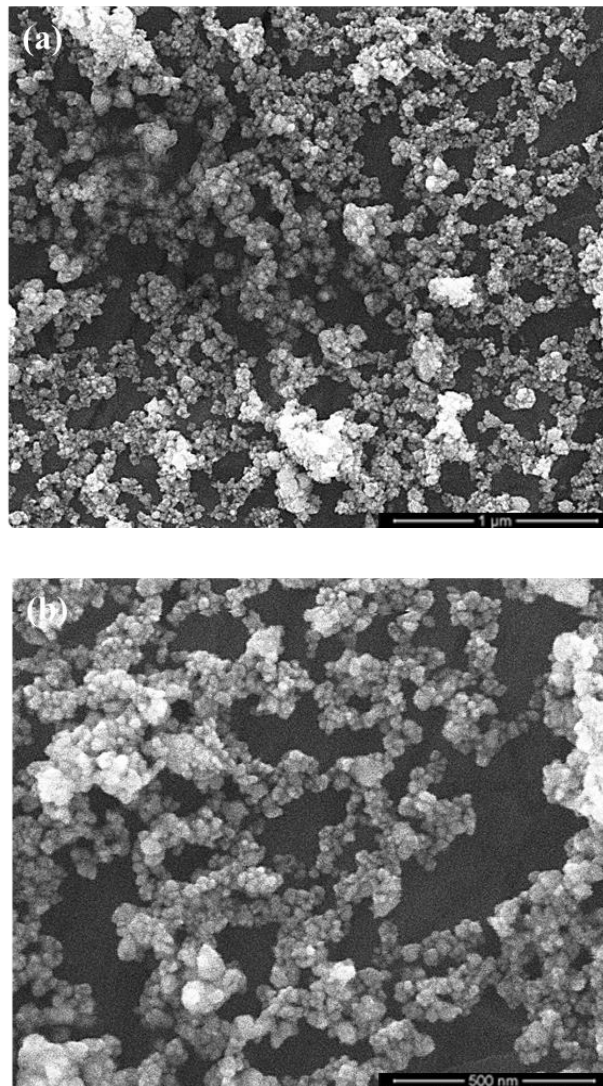


Figure 4.2. SEM images of ZnO powder synthesized from ZnCl₂ at 50°C scale bars (a) 1 µm (b) 500 nm.

In literature, ZnO particles synthesized from ZnCl₂ is usually spherical (Wei and Chang, 2008; Wang et al., 2002). Compared to the particle size of ZnO powder in Figure 4.1 and Figure 4.2, the size of ZnO particles synthesized at 50°C are smaller than that at 35°C since the size can be controlled by reaction temperature.

In precipitation method, ZnO particle size increases with decreasing temperature. The solubility of inorganic materials in water usually increases at elevated temperatures. The formation of crystals can be divided into three steps: (1) the creation of supersaturated solution, (2) crystal nucleation, and (3) crystal growth. In aqueous systems, crystal

nucleation occurs when the solution is saturated. Supersaturation leads to increase in the nucleation rate. The number of nucleation sites increases with the increase in temperature. As a result, the average diameter of crystals will be lower at elevated temperatures (Ömürlü, 2009; Sue et al., 2004; Loh & Chua, 2007; Markov, 1996). This means that the temperature plays key role in this system.

4.1.2. Zinc Oxide Powder Synthesized from Zinc Nitrate Hexahydrate ($\text{Zn}(\text{NO}_3)_2 \cdot 6\text{H}_2\text{O}$)

The detailed description of zinc oxide powder synthesis procedure from $\text{Zn}(\text{NO}_3)_2 \cdot 6\text{H}_2\text{O}$ is given in Chapter 3. Two different aging times (15 and 30 minutes) resulted in slightly different ZnO powder morphologies as seen in Figure 4.3 and Figure 4.4. The sample with 15 minutes aging showed a mixture of different shape and size of ZnO particles. However, most of the particles were plate-like in shape as can be seen in Figure 4.3. Based on the EDX analysis, it was found that sample contained 56.44 atomic % O and 43.56 atomic % Zn (24.08 wt.% O and 75.92 wt.% Zn).

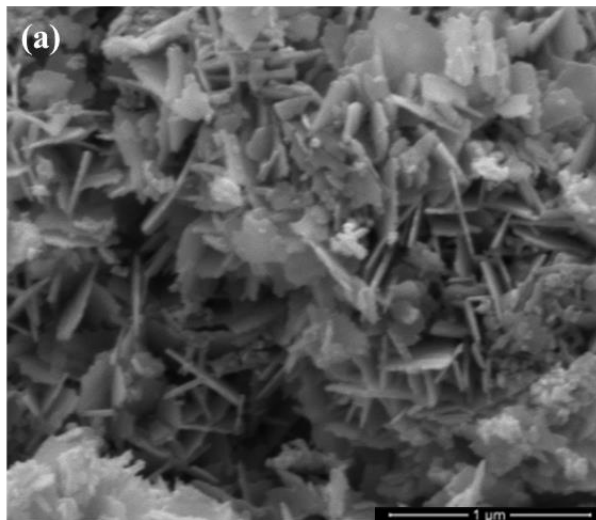


Figure 4.3. SEM images of ZnO powder synthesized from $\text{Zn}(\text{NO}_3)_2 \cdot 6\text{H}_2\text{O}$ during 15 minutes of the aging time scale bars (a) 1 μm (b) 5 μm .

(Cont. on next page)

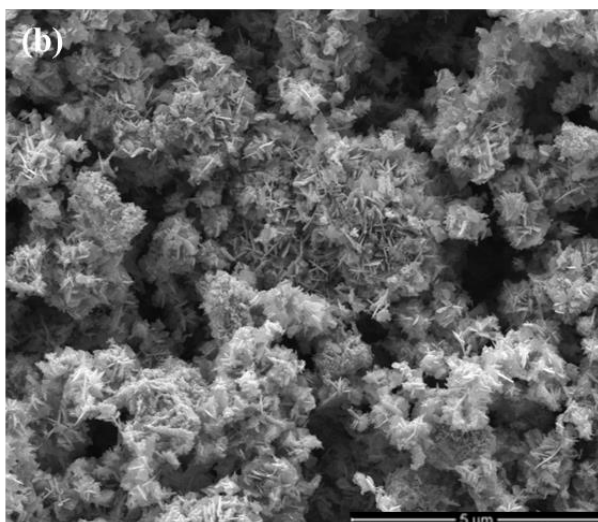


Figure 4.3. (Cont.) SEM images of ZnO powder synthesized from $\text{Zn}(\text{NO}_3)_2 \cdot 6\text{H}_2\text{O}$ during 15 minutes of the aging time scale bars (a) 1 μm (b) 5 μm .

SEM images of ZnO powder synthesized from $\text{Zn}(\text{NO}_3)_2 \cdot 6\text{H}_2\text{O}$ and aged for 30 minutes showed a similar nonuniform particle shape and size distribution. EDX analysis performed on this sample showed that the powder contained 52.37 atomic % O and 47.63 atomic % Zn (21.20 wt.% O and 78.80 wt.% Zn) was obtained.

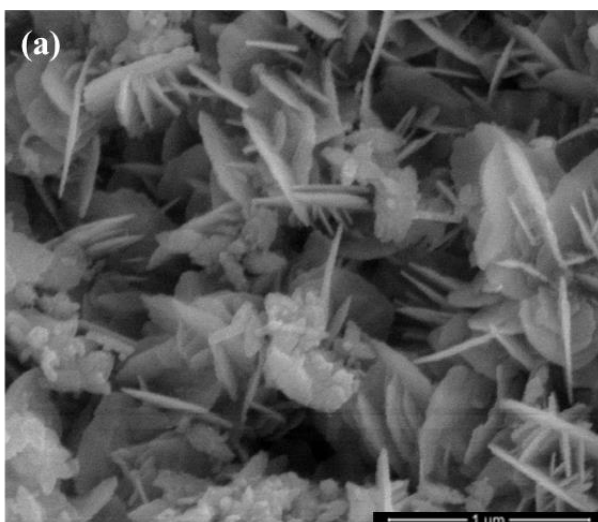


Figure 4.4. SEM images of ZnO powder synthesized from $\text{Zn}(\text{NO}_3)_2 \cdot 6\text{H}_2\text{O}$ during 30 minutes of the aging time scale bars (a) 1 μm (b) 4 μm .

(Cont. on next page)

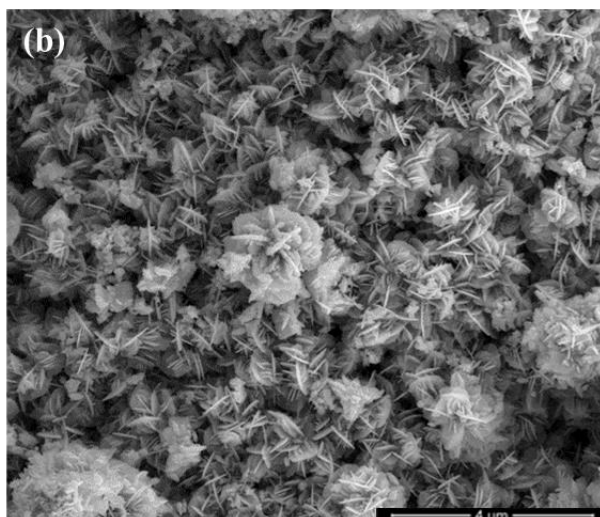


Figure 4.4. (Cont.) SEM images of ZnO powder synthesized from $\text{Zn}(\text{NO}_3)_2 \cdot 6\text{H}_2\text{O}$ during 30 minutes of the aging time scale bars (a) 1 μm (b) 4 μm .

As expected, the morphology of ZnO powder was found to be plate-like or flower-like (Musić et al., 2007; Kazeminezhadn et al., 2013). Compared Figure 4.3 and Figure 4.4, the influence of aging time for this study is not clear since there is not a big observable difference between two samples. However, it is clear that there is a difference between EDX results of ZnO synthesized from $\text{Zn}(\text{NO}_3)_2 \cdot 6\text{H}_2\text{O}$ at different aging times (15 minutes and 30 minutes).

The acidity of the solution plays a significant role for the precipitation of ZnO since the solubility of $\text{Zn}(\text{OH})_2$ or ZnO is a function of pH as seen in Figure 4.5 (Musić et al., 2007; Baes & Mesmer, 1986). During precipitation of ZnO in zinc nitrate hexahydrate solution $\text{Zn}(\text{OH})_4^{2-}$ complex is formed at high pH values (pH 13.05). The zincate ions ($\text{Zn}(\text{OH})_4^{2-}$) diffuse to the surface of ZnO crystals. In the precipitation process without additives, plate-like ZnO particles was formed during different aging times (15 minutes and 30 minutes).

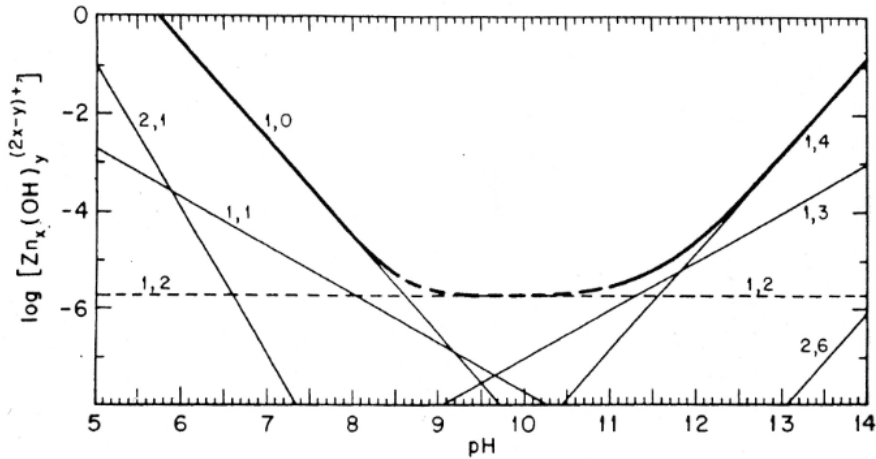


Figure 4.5. Distribution of hydrolysis solutions saturated with ZnO (Source: Baes & Mesmer, 1986).

Surfactants used in the precipitation methods (triethanolamine (TEA), cetyltrimethylammonium bromide (CTAB), etc.) also play key roles providing a low degree of agglomeration and homogeneous size distribution as seen in Figure 4.1 and Figure 4.2.

When synthesized ZnO powders are compared to each other, it can be said that the morphology of the particles depends on precursors and process temperature. In general, size and morphology can be controlled by reaction temperature, concentration of Zn^{2+} ion, pH, additives and the rate of stirring in precipitation method. In the study carried out by Liang et al. (Liang et al., 2014), it was observed that increasing concentration of Zn^{2+} ions changes the particles size and morphology of the zinc oxide powder. Moreover, anions and cations resulting from starting materials have an important effect on the morphology of the particles since they might lead different crystallographic orientations. (Sue et al., 2004; Markov, 1996; Wang et al., 2002; Liang et al., 2014).

4.1.3. Commercial Zinc Oxide Powder

In addition to ZnO powder synthesized using wet chemistries, commercial zinc oxide powder obtained by thermal vaporization method was purchased from KIMETSAN. In thermal vaporization process, zinc and oxygen or oxygen mixture vapor react with each other by using catalyst, forming ZnO nanostructures. Zinc powder is heated up accompanied with oxygen flow. In literature, the morphology of ZnO particles

synthesized by the method of thermal vaporization shows a large variation with regard to ZnO particle shapes and size (Fan & Lu, 2005; Fan et al., 2011; Chang et al., 2004; Shen et al., 2005).

SEM images of the commercial zinc oxide powder are shown in Figure 4.6. As expected due to the production method, commercial ZnO showed a wide range of particle size distribution with most of the particles having needle shape as well as having tripod and nanorod shapes. The morphology was distinctly different than the morphologies of ZnO powder synthesized from ZnCl_2 and $\text{Zn}(\text{NO}_3)_2 \cdot 6\text{H}_2\text{O}$. EDX analysis of commercial powder also showed that the sample contained 19.66 wt.% O and 80.34 wt.% Zn (50 % O and 50 % Zn). It is obvious that the EDX results of synthesized ZnO powder and commercial ZnO powder are seen to be nearly the same with respect to the oxygen and zinc contents.

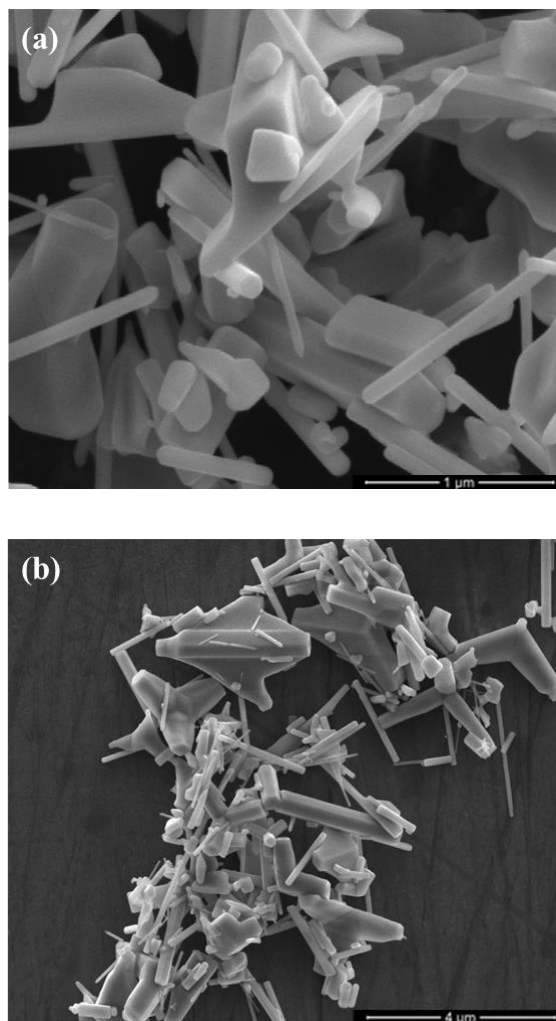


Figure 4.6. SEM images of commercial ZnO powder scale bars (a) 1 μm (b) 4 μm.

In addition to SEM and EDX analysis, XRD analysis was also performed to confirm the crystalline nature of the ZnO particles. In literature, XRD peaks of ZnO powder corresponding to (100), (002), (101), (102), (110), (103), (200), (112) and (201) planes of ZnO (wurtzite structure) are given at 2θ values of 31.77° , 34.42° , 36.25° , 47.54° , 56.59° , 62.85° , 66.37° , 67.94° , and 69.08° , respectively (Kisi & Elcombe, 1989, JCPDS-2 database number 79-2205).

Table 4.1 shows all XRD peak's for ZnO powder in literature, commercial ZnO powder, ZnO powder synthesized from ZnCl₂ at 50°C and ZnO powder synthesized from Zn(NO₃)₂.6H₂O for 30 minutes aging time.

Table 4.1. XRD test results for ZnO powder in literature, commercial ZnO powder, ZnO powder (from ZnCl₂) and ZnO powder (from Zn(NO₃)₂.6H₂O).

Crystal plane	2 Theta values				
	Literature (Kisi & Elcombe, 1989, JCPDS-2 database # 79-2205)		Commercial ZnO powder	ZnO powder synthesized from ZnCl ₂	ZnO powder synthesized from Zn(NO ₃) ₂ .6H ₂ O
	2θ	% Int.			
(100)	31.77	56.45	31.76	31.69	31.69
(002)	34.42	41.54	34.45	34.31	34.45
(101)	36.25	100	36.25	36.18	36.32
(102)	47.54	21.12	47.51	47.3	47.51
(110)	56.59	30.53	56.63	56.63	56.56
(103)	62.85	26.83	62.85	62.64	62.78
(200)	66.37	4.00	66.44	66.44	66.37
(112)	67.94	21.72	67.96	67.96	67.89
(201)	69.08	10.61	69.06	69.07	69.14

XRD spectra of commercial ZnO powder and ZnO powder synthesized from both ZnCl₂ and Zn(NO₃)₂.6H₂O are presented in Figure 4.7. Using X'Pert software, the existence of only ZnO in synthesized powders was confirmed. No peaks related to Zn(OH)₂ were observed. As seen in Figure 4.7, the commercial ZnO powder has greater crystallinity compared to synthesized ZnO powders. It should be that the conditions of XRD spectra analysis were kept a constant throughout this study, that is, data were collected in 2θ range of $5-80^\circ$ with ω scanning speed of 0.3360/sec.

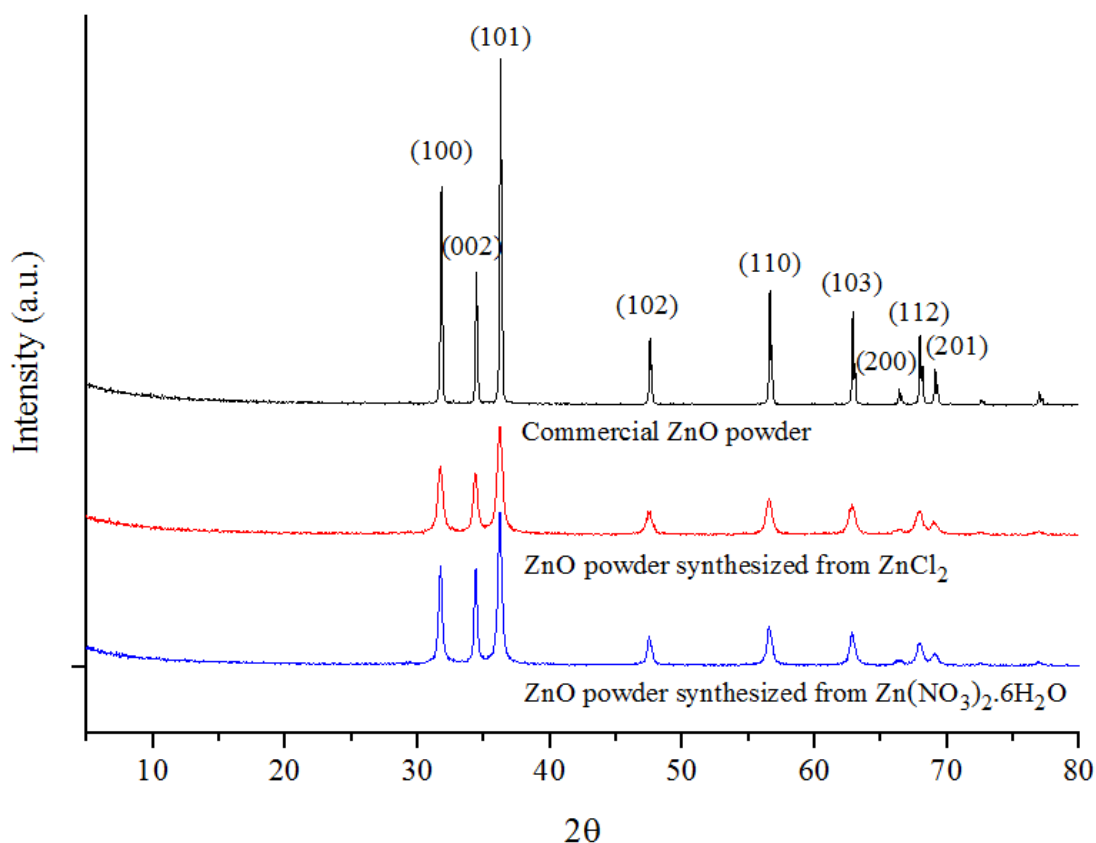


Figure 4.7. XRD spectra of commercial ZnO, ZnO powder from ZnCl_2 and ZnO powder from $\text{Zn}(\text{NO}_3)_2 \cdot 6\text{H}_2\text{O}$.

The specific surface area plays a key role for the geometrical shape and porosity of the ZnO particles. Table 4.2 presents the BET surface area (S_{BET}), micropore area (S_{μ}), total pore volume (V_p) and average pore diameter (calculated by Horvarth-Kawazoe method) of ZnO powders synthesized from both ZnCl_2 (at 50°C) and $\text{Zn}(\text{NO}_3)_2 \cdot 6\text{H}_2\text{O}$ (for 30 minutes aging time) and commercial ZnO powder. All ZnO samples show significant differences ($2.16\text{-}24.88 \text{ m}^2 \cdot \text{g}^{-1}$) in BET surface areas.

Table 4.2. The BET surface area, micropore area, total pore volume and average pore diameter of commercial ZnO powder, ZnO powder (from ZnCl_2) and ZnO powder (from $\text{Zn}(\text{NO}_3)_2 \cdot 6 \text{H}_2\text{O}$)

Types of ZnO powders	BET Surface Area, m^2/g (S_{BET})	Micropore Area, m^2/g (S_{μ})	Total pore volume, cm^3/g (V_p)	Average pore diameter * (median pore diameter), nm (d_{average})
ZnO powder synthesized from ZnCl_2	24.87	0.24	0.0077	1.3
ZnO powder synthesized from $\text{Zn}(\text{NO}_3)_2 \cdot 6\text{H}_2\text{O}$	16.79	3.48	0.0053	1.1
Commercial ZnO	2.16	3.17	0.0011	1.2

Based on the results of SEM, EDX, XRD and BET analysis mentioned above it can be stated that ZnO powder synthesized from ZnCl₂ and Zn(NO₃)₂·6H₂O yield much better control of the morphology in terms of particle size and shape compared to commercial ZnO powder. However, the role of initial ZnO powder morphology on the electrochemical performance of the zinc electrode is still a topic of debate.

4.1.4. Effect of Initial Morphology of Zinc Electrodes

4.1.4.1. Zinc Electrodes As Prepared (Before First Charge)

Zinc electrodes (Zn electrodes) that are used in NiZn batteries are usually prepared by mechanically mixing ZnO powder with desired additives, binders and wicking agents (if necessary) to form a paste to be coated as a thick layer on current collector. It is therefore necessary to charge the battery before its first discharge to convert ZnO into metallic zinc.

In literature there has been a debate about the effect of the initial morphology and microstructure of Zn electrode as prepared (before its first charge) on the electrochemical performance of the battery (Yuan et al., 2006b; Yang et al., 2010; Ma et al., 2008).

The initial microstructure of the Zn electrode before its first charge is determined by the morphology of ZnO powder and type and amount of binder, wicking agent and additives used during preparation. Detailed description of the Zn electrode preparation process is given in Chapter 3. Zinc electrodes prepared in this study contained calcium hydroxide (Ca(OH)₂), lead (II) oxide (PbO), polyethylene glycol (PEG), potassium hydroxide (KOH) in various amounts in addition to zinc oxide as the main ingredient.

The microstructure and surface morphology of the paste used for Zn electrode prepared using zinc oxide powder synthesized from ZnCl₂, is shown in Figure 4.8.

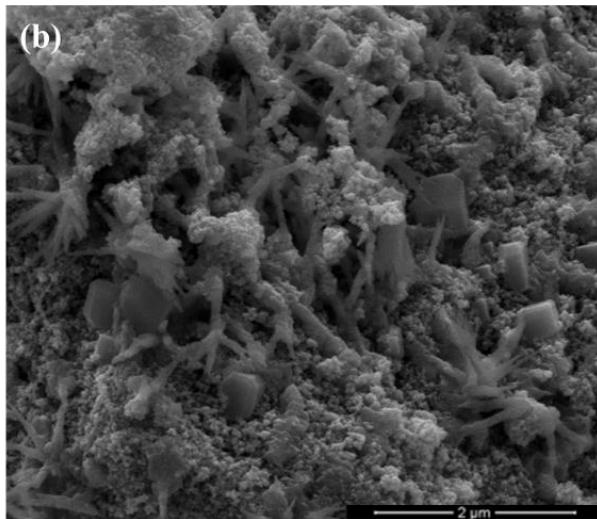
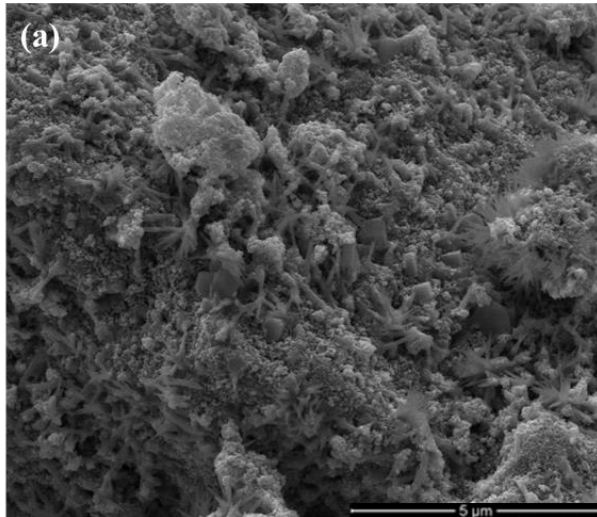


Figure 4.8. SEM images of the paste of Zn electrode as-prepared by ZnO powder synthesized from ZnCl_2 scale bars (a) 5 μm (b) 2 μm .

Similarly, the microstructure and surface morphology of the paste used for Zn electrode preparation using zinc oxide powder synthesized from $\text{Zn}(\text{NO}_3)_2 \cdot 6\text{H}_2\text{O}$ is shown in Figure 4.9.

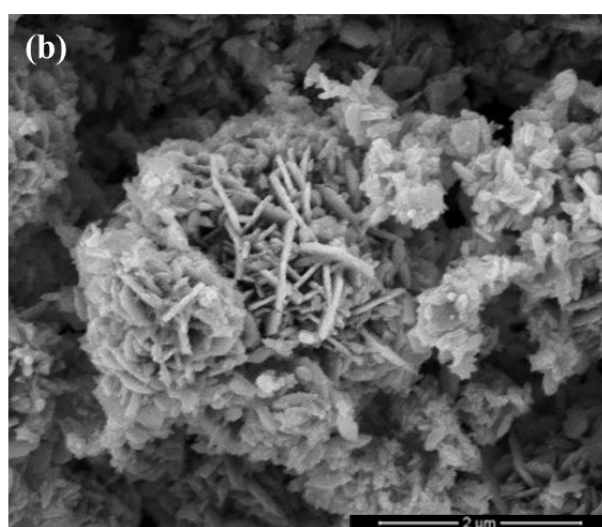
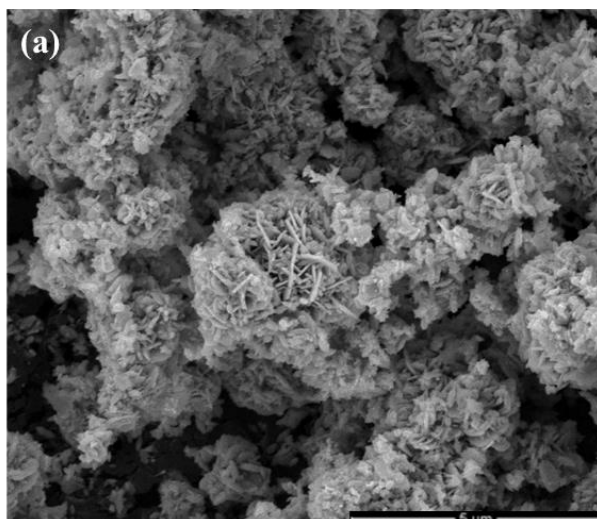


Figure 4.9. SEM images of the paste of Zn electrode as-prepared by ZnO powder synthesized from Zn(NO₃)₂·6H₂O commercial ZnO powder scale bars (a) 5 μm (b) 2 μm.

SEM analysis was also performed for the paste used for Zn electrode preparation using commercial zinc oxide powder to investigate the initial morphology of the electrode as seen in Figure 4.10.

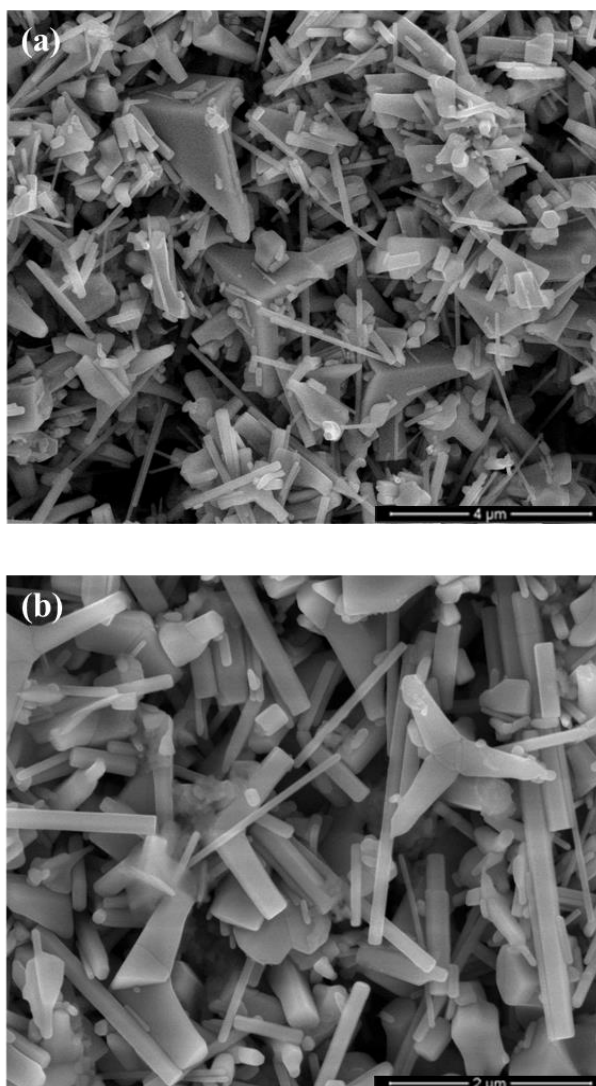


Figure 4.10. SEM images of the paste of Zn electrode as-prepared by commercial ZnO powder scale bars (a) 4 μm (b) 2 μm .

As expected SEM images of the paste exhibited a similar morphology with commercial ZnO powder with needle-like, tripods, and rod shaped particles with various sizes. Since the amount of additives compared to ZnO is very small, it can be stated that the initial morphology of Zn electrodes before their first charge is determined by the type of ZnO powder used. Based only on SEM images the effect of binders and wicking agents seems to be minimal.

In order to confirm initial findings related to morphology of the electrode before its first charge, XRD analysis was performed on each paste containing different ZnO powder. XRD spectra of Zn electrodes as-prepared (before their first charge) using commercial ZnO powder and ZnO powder synthesized from both ZnCl_2 and $\text{Zn}(\text{NO}_3)_2 \cdot 6\text{H}_2\text{O}$ are presented in Figure 4.11.

As seen in Figure 4.11, the XRD patterns showed that the content of zinc oxide was dominant for each paste of Zn electrode. In addition to this, there is no difference between XRD peak's for commercial ZnO powder and the paste Zn electrode as-prepared by commercial ZnO powder since high content, 93 % (w/w), of ZnO powder was used throughout this experiment. Compared all the XRD patterns, the course of the baseline indicated that no-impurity phase was observed.

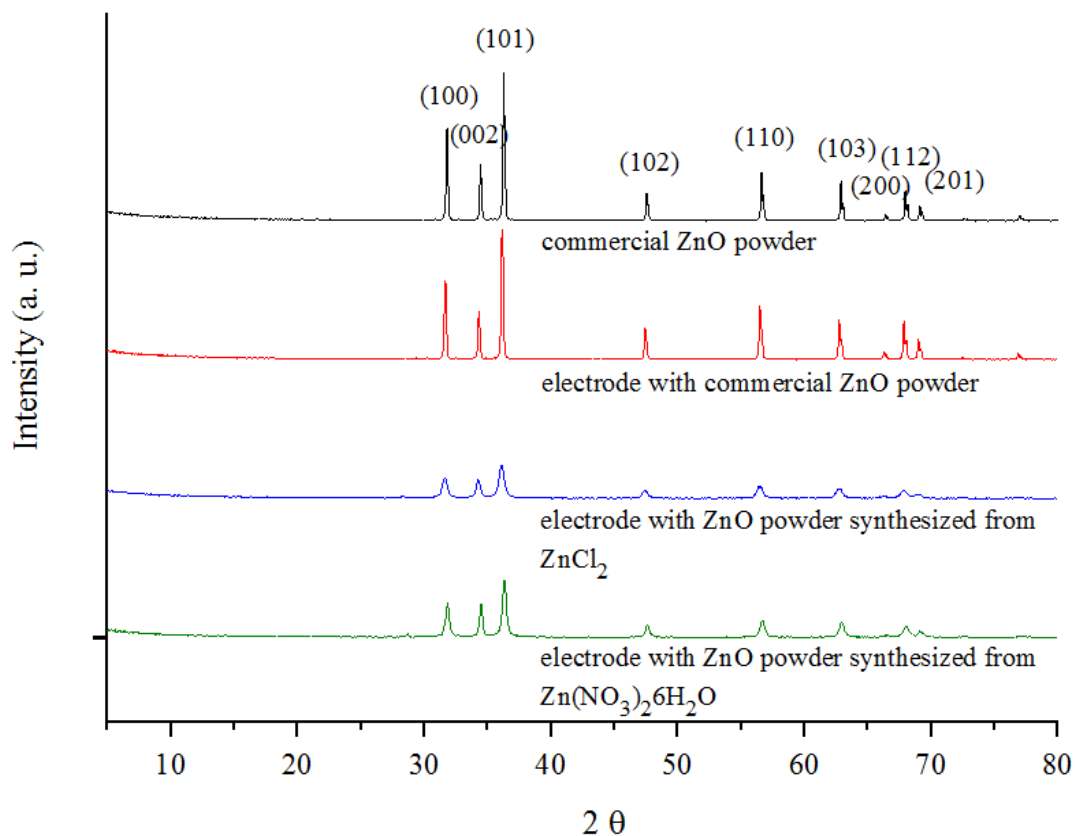


Figure 4.11. XRD spectra of the paste Zn electrode as-prepared from commercial ZnO powder, ZnO powder synthesized from ZnCl₂, and ZnO powder synthesized from Zn(NO₃)₂·6H₂O.

Table 4.3 shows all XRD peak's for ZnO powder in literature (same data listed in Table 4.1 for ZnO reference), commercial ZnO powder, ZnO powder (from ZnCl₂) and ZnO powder (from Zn(NO₃)₂·6H₂O). As expected, XRD spectra of ZnO powder and electrode paste before first charge are identical confirming no change in crystalline nature of the material after paste preparation and before first charge of the battery.

Table 4.3. XRD test results for the paste of Zn electrodes from commercial ZnO powder, ZnO powder (from ZnCl₂) and ZnO powder (from Zn(NO₃)₂·6H₂O).

Crystal plane	2 Theta values			
	Commercial ZnO powder	Zn electrode paste as prepared (commercial ZnO powder)	Zn electrode paste as prepared (ZnO powder synthesized from ZnCl ₂)	Zn electrode paste as prepared (ZnO powder synthesized from Zn(NO ₃) ₂ ·6H ₂ O)
(100)	31.76	31.73	31.61	31.9
(002)	34.45	34.36	34.3	34.47
(101)	36.25	36.17	36.17	36.28
(102)	47.51	47.48	47.48	47.6
(110)	56.63	56.52	56.41	56.76
(103)	62.85	62.83	62.65	62.88
(200)	66.44	66.33	66.33	66.5
(112)	67.96	67.96	67.9	68.08
(201)	69.06	69.07	69.13	69.13

Porosity also plays a role in electrode performance since large electrode surface area generally leads a minimal energy loss and increased electrode efficiency. In literature, there are several studies focusing on the issue over porosity of electrodes (Hitz & Lasia, 2001; Łosiewicz et al., 2003). The rate of hydrogen evolution reaction might vary location of the pores of electrodes in NiZn batteries. The structure (such as tortuosity, pore sizes), the conductivity of the solid matrix and the electrolyte influence the distribution of current density within the porous electrode. In this regard, pore geometry of electrode affects the shape of the impedance curves.

4.1.4.2. Zinc Electrodes (After First Charge and Discharge)

The effect of initial morphology of zinc oxide powder on the electrochemical performance of Zn electrode was investigated. The detailed description of Zn electrode preparation method and the details charge/discharge test setup were given in Chapter 3. The amount of zinc oxide powder (in-house synthesized and commercial zinc oxide powder) used in Zn electrode was 1 gram for all experiments.

Initial morphology of ZnO is a controversial issue with respect to its effect on the electrochemical performance of Zn electrode. Ma and co-workers compared Zn electrodes prepared from both the plate-like ZnO and conventional ZnO powders in terms of their electrochemical properties (Ma et al., 2008). They found that the effect of the plate-like ZnO powder on electrochemical performance of Zn electrode was better compared to the conventional ZnO powder (Ma et al., 2008). Similar to this study, Yuan et al. claimed that the initial morphology of ZnO might affect the electrochemical performance of Zn electrode during charge/discharge cycles (Yuan et al., 2005). Compared to the morphology of conventional ZnO, nanosized ZnO with prismatic form showed better electrochemical performance (Yuan et al., 2005). In this study, contrary to above-mentioned studies, it was observed that the initial morphology of ZnO powder on the electrochemical performance of Zn electrode was insignificant (Yuan et al., 2005).

The performance of each Zn electrode was investigated with discharge tests by using a 10-Ohm resistance as a load and by logging the battery voltage vs. time. Voltage vs. Capacity (first discharge) curve of each Zn electrodes with all additives in NiZn batteries is given in Figure 4.12.

Although not included here, the first few charging curves showed unpredictable behavior as observed in the literature. However, discharge testing provided more stable behavior. As seen in Figure 4.12, the first discharge capacity of Zn battery prepared from commercial ZnO powder is clearly much more than those prepared from ZnO powders synthesized from both ZnCl_2 and $\text{Zn}(\text{NO}_3)_2 \cdot 6\text{H}_2\text{O}$. In addition, compared to the theoretical value, the average utilization ratio of commercial ZnO is 37.53 %, whereas ZnO synthesized from ZnCl_2 and $\text{Zn}(\text{NO}_3)_2 \cdot 6\text{H}_2\text{O}$ show the average utilization ratio of 28.22 % and 29.44 %, respectively.

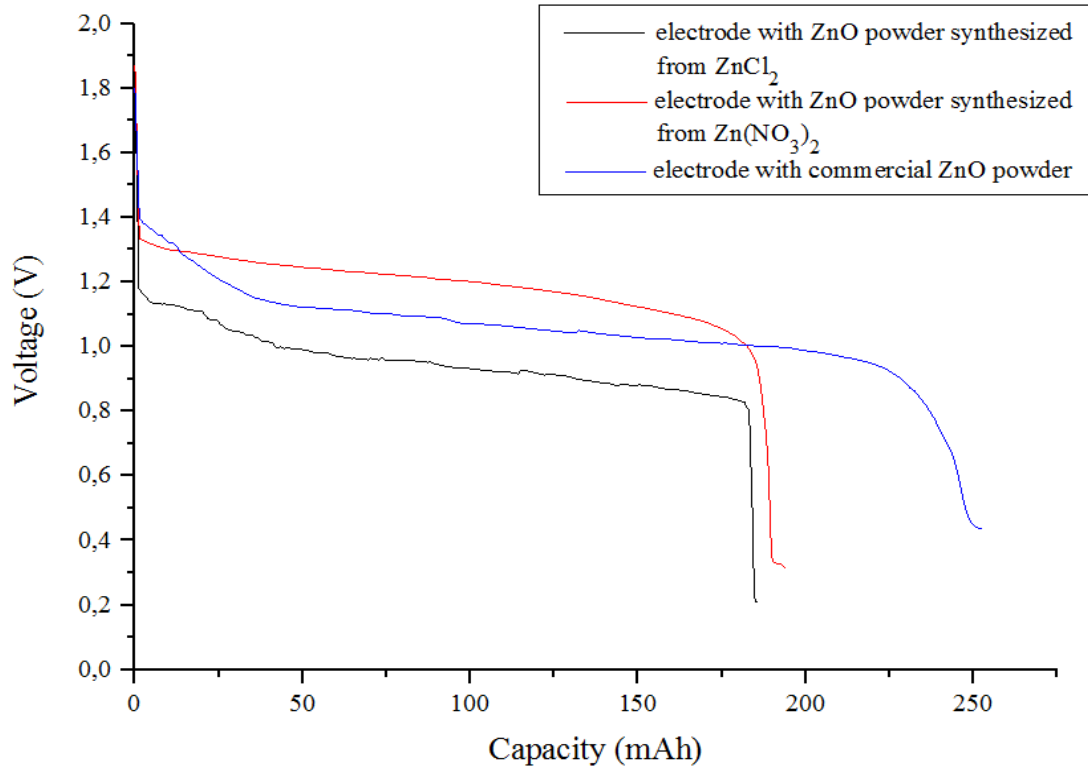


Figure 4.12. The first discharge curves (voltage vs. capacity) for Zn electrodes with all additives.

The microstructure evolution process of each Zn electrode with all additives after first charge is shown in Figure 4.13. Compared to Figure 4.8, Figure 4.9 and Figure 4.10 (the initial morphology of Zn electrode), the morphology of Zn electrode showed spindle-like structures, and most of the ZnO crystals were converted into zinc. However, detailed SEM analysis at different locations of the sample also revealed that first charging of these Zn batteries was not performed fully and there were some ZnO particles which were not converted into metallic zinc.

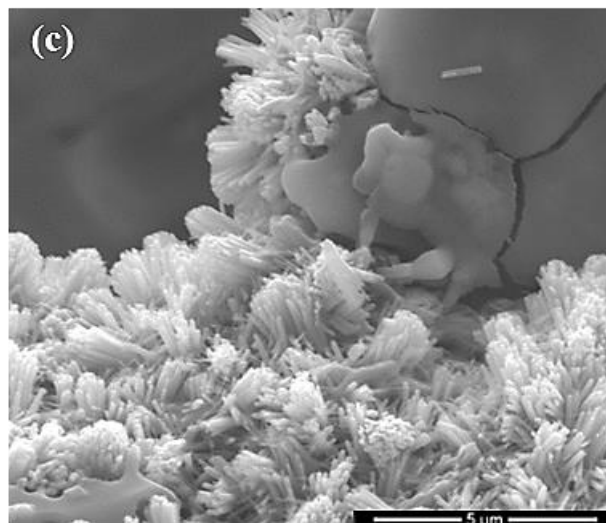
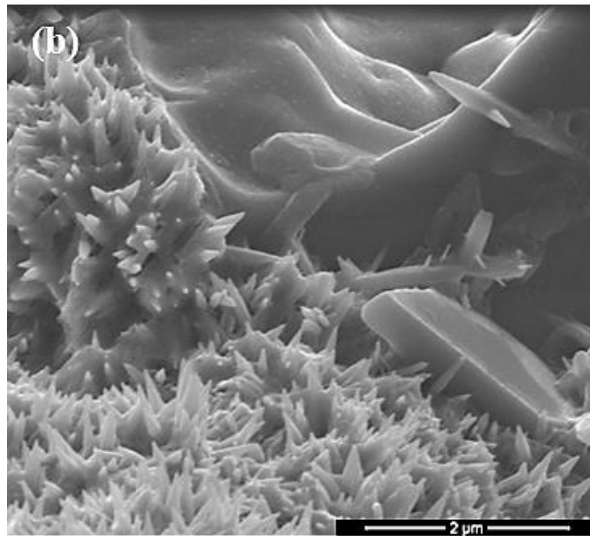
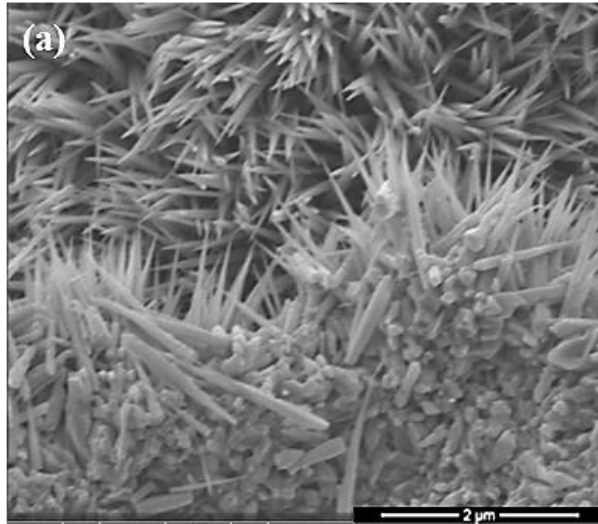


Figure 4.13. SEM images of Zn electrode prepared from (a) ZnO synthesized from ZnCl_2 (b) ZnO synthesized from $\text{Zn}(\text{NO}_3)_2 \cdot 6\text{H}_2\text{O}$ (c) commercial ZnO after first charge

Figure 4.14 shows the morphology evolution process of each Zn electrode with all additives after first discharge. Only Zn electrode prepared with commercial ZnO powder showed slightly different morphology. It was observed that regardless of the initial morphology, the electrodes showed similar morphologies almost completely erasing the memory of initial structure even after the first charging procedure.

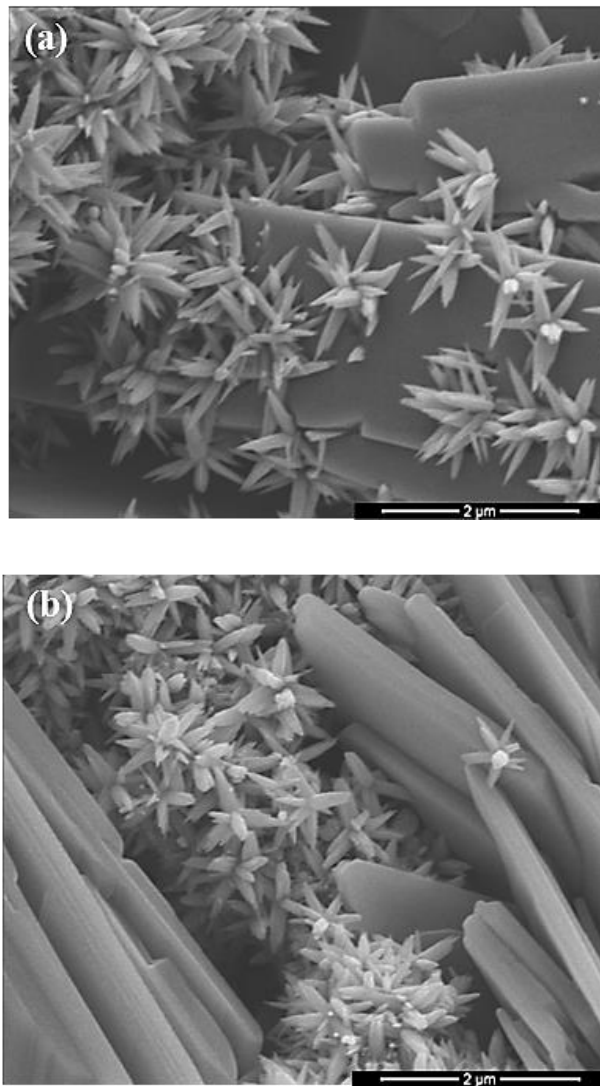


Figure 4.14. SEM images of Zn electrode prepared with (a) ZnO synthesized from ZnCl_2 (b) ZnO synthesized from $\text{Zn}(\text{NO}_3)_2 \cdot 6\text{H}_2\text{O}$ (c) commercial ZnO after first discharge

(Cont. on next page)

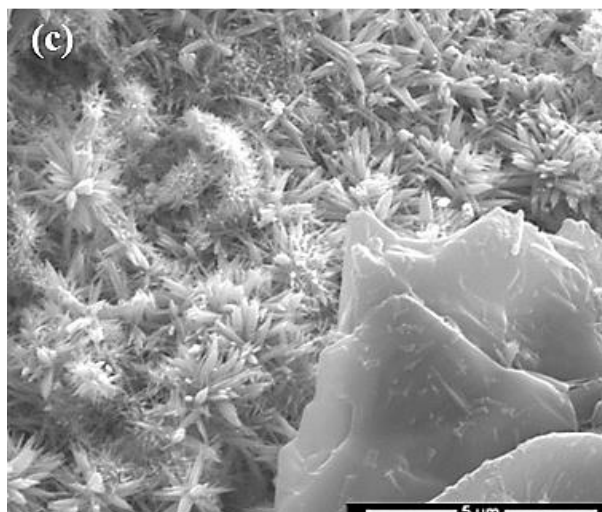


Figure 4.14. (Cont.) SEM images of Zn electrode prepared from (a) ZnO synthesized from ZnCl_2 (b) ZnO synthesized from $\text{Zn}(\text{NO}_3)_2 \cdot 6\text{H}_2\text{O}$ (c) commercial ZnO after first discharge

4.2. Morphology of Nickel Electrodes

Commercial nickel electrodes were obtained from two different sources. Due to restrictions imposed by the manufacturers, nickel electrodes used in this study will be named as commercial Ni-1 and commercial Ni-2 throughout the thesis.

Ni-based electrodes that are used in nickel-metal hydride and nickel-zinc batteries usually consist of nickel foam current collector and nickel positive plate with NiO_2 and/or NiOOH as active material and additives. A minimum amount of aqueous electrolyte made of a mixture of sodium hydroxide, lithium hydroxide and potassium hydroxide salts is generally absorbed in separator and electrode. In addition Ni electrodes may also contain trace amount of V-, Ti-, Zr-, Ni-, Cr-, Co-, Mn- and Fe-containing oxide and hydroxide species. Ti, Zr and V are capable of absorbing hydrogen, whereas Co and Mn provide surface activity. Cr and Fe were found to decrease corrosion resistance, and also, improve catalytic activity for reactions (Linden & Reddy, 2001; Shuklaa et al., 2001; Ayeb & Notten, 2008; Al-Thyabat et al., 2013).

Table 4.4 and Table 4.5 list the XRF analysis results for commercial Ni-1 electrode and Ni-2 electrode, respectively.

Table 4.4. The results of XRF analysis of commercial Ni-1 electrode.

Element	Amount (%)	Oxide	Amount (%)
Mg	1.39 %	MgO	2.31 %
K	6.52 %	K ₂ CO ₃ /KOH	7.85 %
Co	4.32 %	CoO	5.5 %
Ni	56.51 %	NiO	71.91 %
Zn	6.31 %	ZnO	7.85 %

Table 4.5. The results of XRF analysis of commercial Ni-2 electrode.

Element	Amount (%)	Oxide	Amount (%)
Mg	1.55 %	MgO	2.56 %
K	3.35 %	K ₂ CO ₃ /KOH	4.03 %
Co	4.28 %	CoO	5.45%
Ni	63.37 %	NiO	80.65 %
Zn	4.53 %	ZnO	5.63 %

As shown in tables above, two Ni electrodes used in this study showed slight differences in terms of the relative quantities of the materials used.

XRD analysis of commercial Nickel electrodes showed similar crystalline spectra as expected since the chemical contents were similar, as seen in Figure 4.15. In literature, XRD peaks of Ni(OH)₂ and Ni are given at 2θ values 19.15°, 33.01°, 38.45°, 51.9°, 58.97°, 62.61° and 44.5°, 51.85°, 76.38°, respectively (Szytula et al., 1971, JCPDS-2 database number 74-2075; Swanson at al., 1953, JCPDS-2 database number 87-0712). Peak positions and corresponding crystal planes are listed in Table 4.6.

Table 4.6. XRD test results for both commercial Ni electrodes.

Crystal plane		2 Theta values	
		Ni-1 electrode	Ni-2 electrode
(001)	Ni(OH) ₂	18.98	19.05
(100)	Ni(OH) ₂	33.02	32.95
(101)	Ni(OH) ₂	38.25	38.35
(111)	Ni	44.57	44.57
(200)	Ni(OH) ₂ , Ni	51.84	51.84
(110)	Ni(OH) ₂	58.68	59.16
(111)	Ni(OH) ₂	62.63	62.83
(220)	Ni		76.46

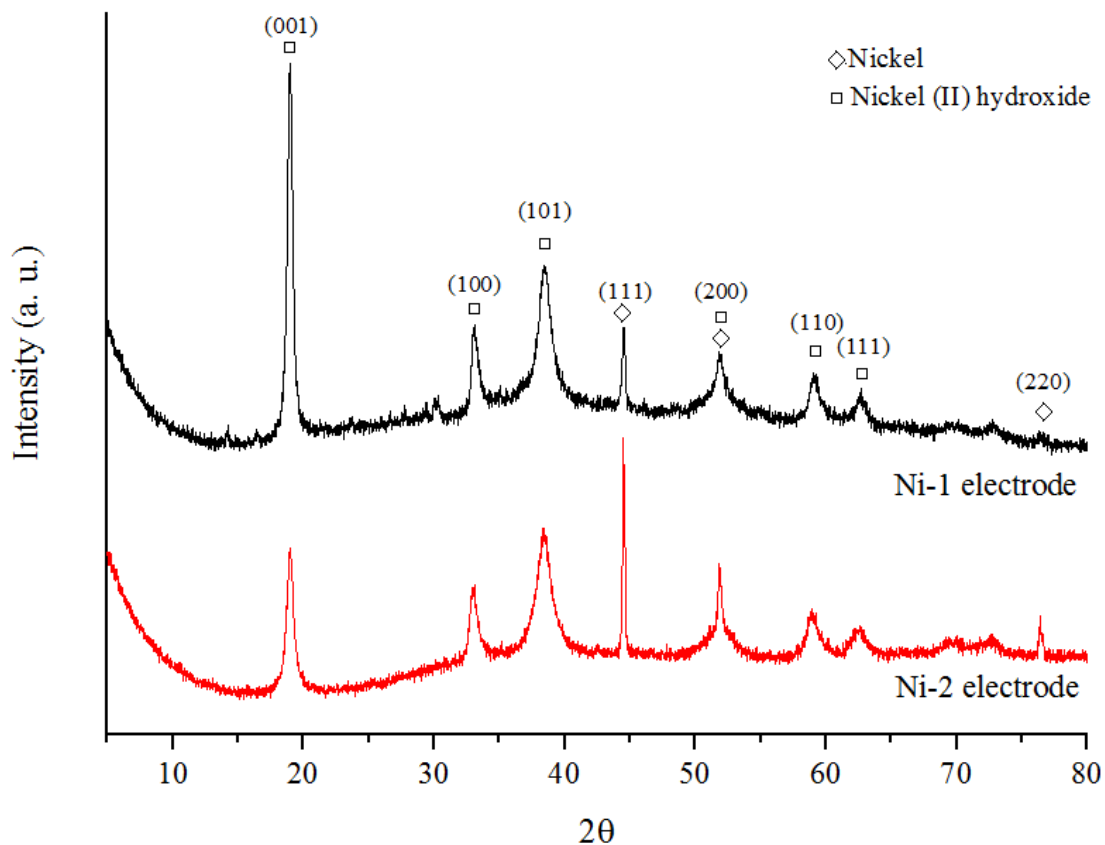


Figure 4.15. XRD analysis for commercial Ni electrodes.

Despite slight differences, reported electrochemical performances of these two electrodes are quite similar. Since the focus of this study was on the Zn electrode, these two Ni electrodes were used interchangeably.

4.3. Effect of Binder/Separator Material on Zinc Growth

A main problem of Zn electrodes is the limited capacity and lifetime when it is subjected to charge/discharge cycling. This problem is due to repeated zinc dissolution into alkaline solution and the formation of unwanted Zn electrode morphology during recharge. In this regard, the diffusion between Zn electrode and alkaline solution plays a key role in the cathode process owing to the concentration polarization resulting from low concentration of ions in the electrolyte near the surface of Zn electrode during charging. The zincate anions as a by-product of overall reaction diffuse on the protruding surface of Zn electrode, and therefore, these anions tend to combine and form zinc dendrites.

Organic materials that are used in separator and as binders in Zn electrode might affect the zinc growth mechanism during charge/discharge cycle. In literature, studies focused on the prevention of dendritic zinc growth was explained in Chapter 2 (Ein-Eli et al., 2003; Mohamad et al., 2003; Wu et al., 2008; Zhou et al., 2011; Ballesteros et al., 2007; Yang & Lin, 2002).

In the present work, the effects of only PVA and PEG were investigated as binders in electrolyte. The detailed description of this process is given in Chapter 3. In commercial NiZn batteries other organic binders are also used both in electrode structure and as additives to electrolyte.

4.3.1. Zinc Growth without Binders/Separator Material

Zinc morphology without any binder was analyzed by SEM to determine the effect of current flux (25 mA/cm^2 and 75 mA/cm^2) on Zn electrode microstructure as seen in Figure 4.18 and Figure 4.19.

As seen in Figure 4.16(a), SEM image showed a mixture of different shape and size of zinc crystals after the electrodeposition at 25 mA/cm^2 . However, some large cubic and pyramidal zinc crystals aggregated on the zinc metal surface as can be seen in Figure 4.17(b). Although there is not a clear explanation for this, it might be related to the surface morphology of the zinc sheet used in the experiment or impurities present on its surface.

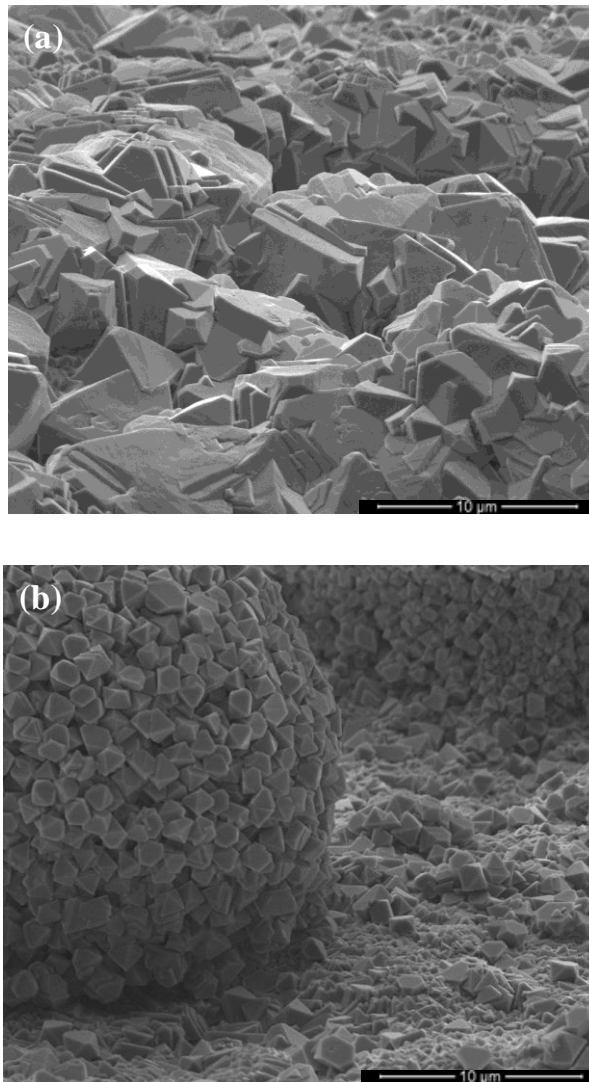


Figure 4.16. SEM images of Zn electrode without binders/seperator material after deposition at 25 mA/cm² scale bars (a) 10 μm (b) 10 μm.

SEM images of the Zn electrode deposited at 75 mA/cm² exhibited a different morphology compared to Zn electrode deposited at 25 mA/cm². No prismatic, nanorod, or nanofiber were observed as seen in Figure 4.17(a). In addition similar to the zinc crystals observed at 25 mA/cm² current flux, much smaller spherical zinc crystals were observed. Based only on SEM images, the effect of current flux seems to be important and somehow responsible for zinc morphology.

It can be said that some crystals might be ZnO because of excess ZnO used in these experiments.

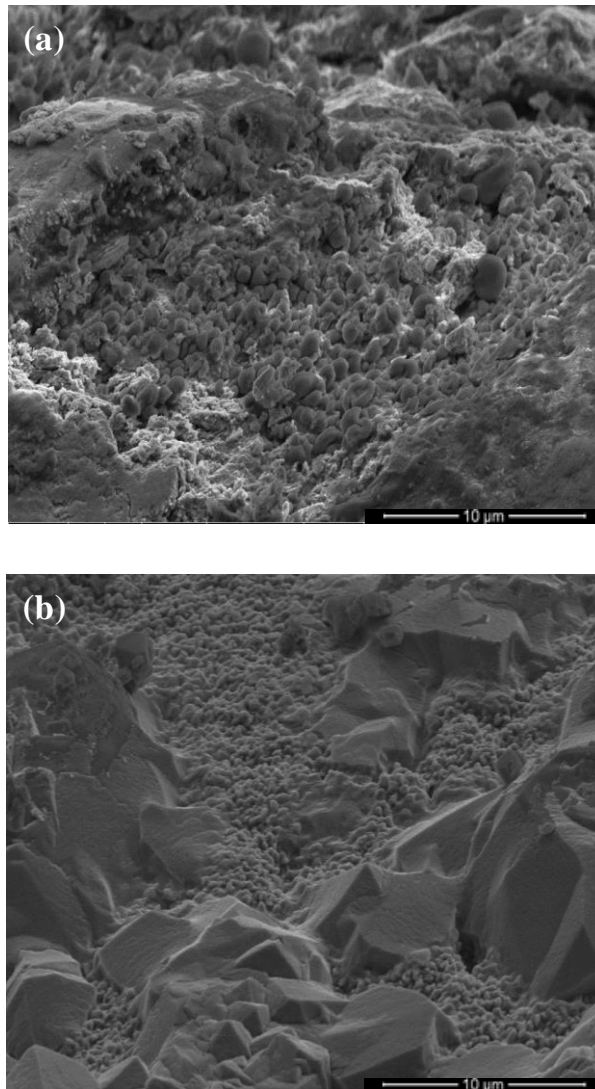


Figure 4.17. SEM images of Zn electrode without binders/separator material after deposit at 75 mA/cm^2 scale bars (a) $10 \text{ }\mu\text{m}$ (b) $10 \text{ }\mu\text{m}$ at different locations on the substrate.

4.3.2. The Effect of PVA on Zinc Growth

As seen in Figure 4.18, the morphology also depends on the presence of PVA. In contrast to the morphology observed in the absence of binders, Zn electrode deposited at 25 mA/cm^2 with PVA addition showed variety of particle size distribution with some of the particles having small spherical shapes and some of them having perfect crystals similar to ones deposited without binders. Based on SEM images, the impact of PVA led to flower-like shaped zinc crystals on binder surface. Also one might speculate that nonuniform distribution of PVA on the surface might lead to very different zinc morphologies.

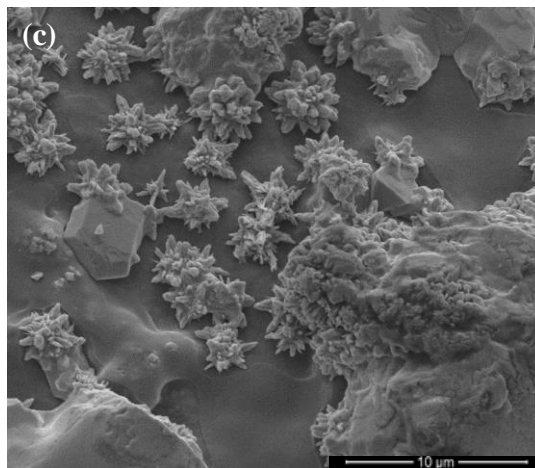
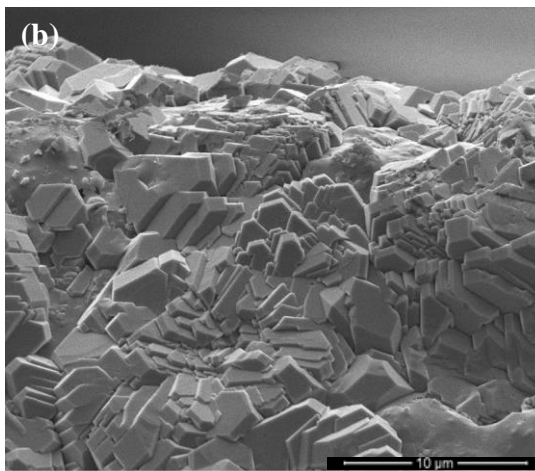
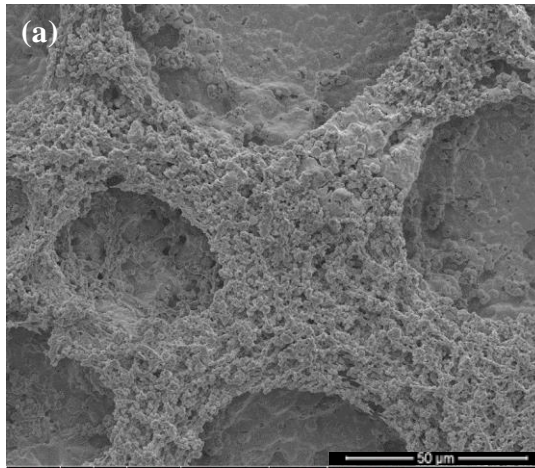


Figure 4.18. SEM images of Zn electrode with PVA as a binder after deposit at 25 mA/cm² scale bars (a) 50 μm (b) 10 μm (c) 10 μm at different locations on the substrate.

SEM images of the zinc deposited at high current flux exhibited a different morphology from zinc deposited at low current flux. As seen in Figure 19(a), the morphology of Zn electrode deposited at 75 mA/cm² was smaller flower-like shape than

that at 25 mA/cm^2 . Thus, the morphology is also dependent on the current flux in presence of PVA. In addition to this, the crystals aggregated on the zinc surface as can be seen in Figure 4.19(b) and (c). Figure (a) and Figure (b) show different locations on the same substrate. The columnar structures were observed on cross-section area of zinc metal. Based only on SEM images, the effect of current flux seems to be great.

It can be said that some crystals might be ZnO because of excess ZnO used in these experiments.

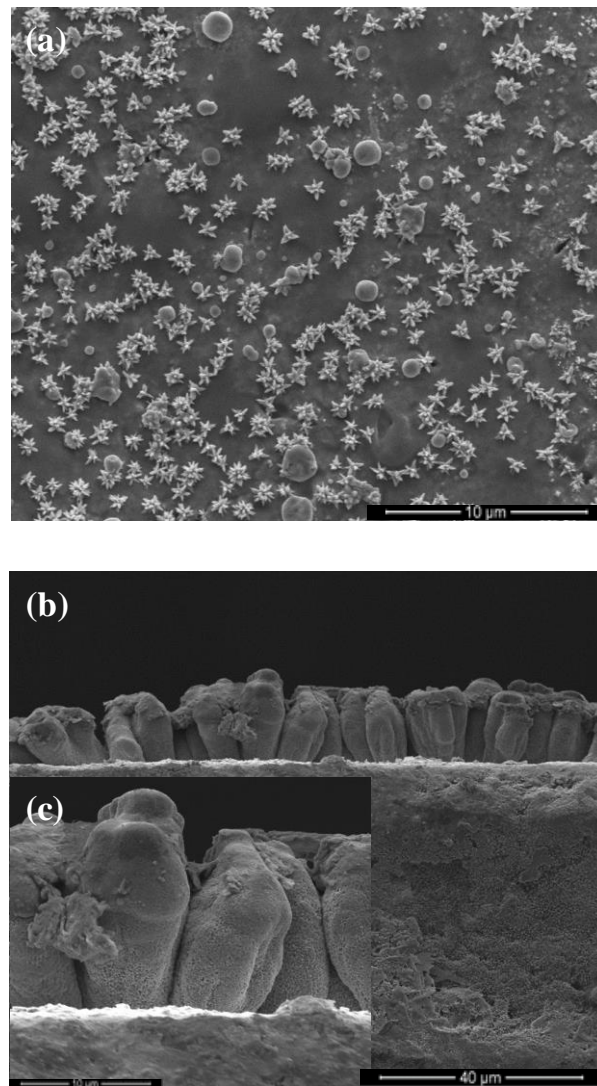


Figure 4.19. SEM images of Zn electrode with PVA as a binder after deposit at 75 mA/cm^2 scale bars (a) $10 \text{ }\mu\text{m}$ (b) $40 \text{ }\mu\text{m}$ (c) $10 \text{ }\mu\text{m}$ at different locations on the substrate.

4.3.3. The Effect of PEG on Zinc Growth

As expected zinc morphology depends also on the presence of PEG. As seen in Figure 4.20, SEM images of zinc deposited in the presence of PEG showed clearly different phases with particles having different sizes and shapes. Interestingly, some agglomerates with needle shape particles were observed, namely, dendrites were formed. There were some particles with larger crystals on the surface of Zn electrode after slow current deposition.

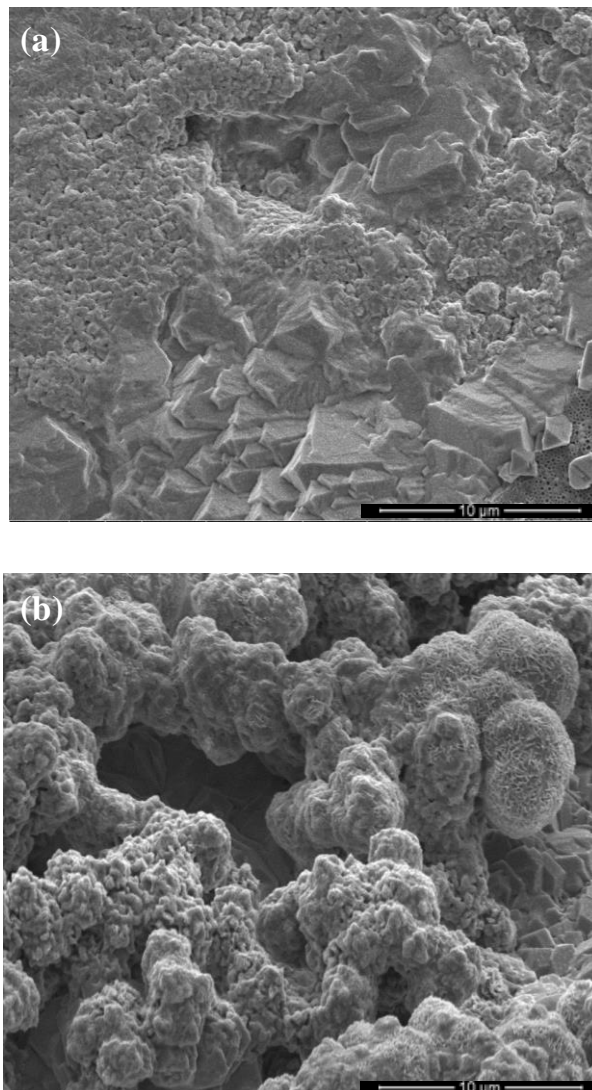


Figure 4.20. SEM images of Zn electrode with PEG as a binder after deposit at 25 mA/cm² scale bars (a) 10 μm (b) 10 μm at different locations on the substrate.

In presence of PEG, the SEM images of the zinc deposited at high current flux exhibited a different morphology compared to low current flux deposition. Compared to slow deposition, high deposition led smaller particles having needle-like shapes. As seen in Figure 4.21(b) and (c), it can be pointed out that the agglomerates with small prismatic crystals were observed after the electrodeposition at high current. Some of the perfect prismatic crystals aggregated on this surface.

It can be said that some crystals might be ZnO because of excess ZnO used in these experiments.

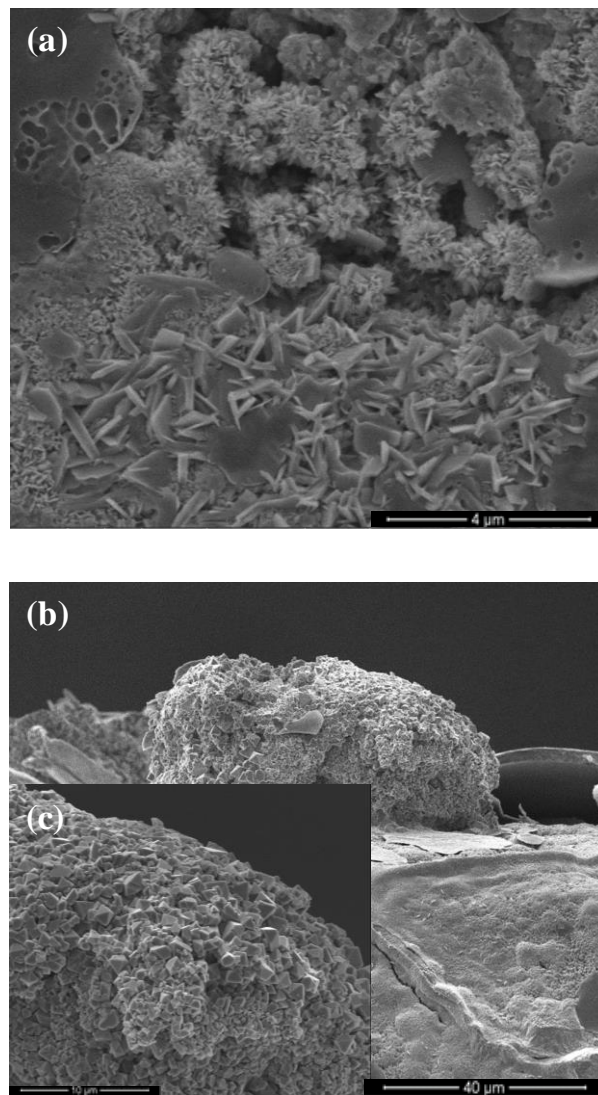


Figure 4.21. SEM images of Zn electrode with PEG as a binder after deposit at 75 mA/cm² scale bars (a) 4 μm (b) 40 μm (c) 10 μm at different locations on the substrate.

The shape of crystals can be related to the presence of binders. It was seen that the change of shape depends on both the presence of binders and the type of binders. In addition, the crystals of particles turn out to be smaller in case of fast current flux compared to slow current flux.

The brief experimental work presented here generated additional questions related to Zn electrode problems described in literature. It should be noted that in order to evaluate the effect of the binder used in Zn electrode and electrolyte, more research is needed. The effects of binder type (PEG, PVA etc.), concentration of binder, and discharge/charge current density on the morphology of the Zn electrode as battery ages must be investigated separately and in detail.

4.4. Effect of Additives on Electrochemical Performance of Zinc Electrode

The effect of selected Zn electrode additives on the electrochemical performance of Zn electrode was also investigated. The detailed description of Zn electrode preparation process is given in Chapter 3. In this study, the weight of zinc oxide powder used in Zn electrodes also was 1 gram for all experiments. This amount of ZnO used in all experiments has a theoretical capacity of 659 mAh. Zinc electrode contents for electrochemical testing are listed in Table 4.7.

Table 4.7. Zinc electrode additives.

Types of Zinc Electrode	Ratios of gradients (wt.%)			
	Commercial ZnO powder (1 gram)	Ca(OH) ₂	PbO	PEG
Zn electrode with all additives	93	3	1	3
Zn electrode without Ca(OH) ₂	96	-	1	3
Zn electrode without PbO	94	3	-	3
Zn electrode without PEG	96	3	1	-

The details of charge/discharge test setup were given in detail in Chapter 3. It should be noted there is a difference in electrochemical performance and charge/discharge testing protocol between all dry NiZn cells (almost all commercial NiZn batteries) and wet-cells (employing pouch electrodes) that are used in this study. Much

higher internal resistivity due to liquid electrolyte of wet cells is responsible for electrochemical performance of studied batteries. One advantage of using wet cells (pouch electrodes) in battery research is that the effect of counter electrode can be minimized since the physical distance between electrodes is larger compared to dry electrodes. In addition, due to larger electrolyte volume, chemical reactions or phase transformations that might arise due to limited solubility can be avoided. In general, isolation of electrodes from each other and reduction of unwanted chemical reactions can be exploited in wet cell setup to study electrochemical behavior of a single electrode in detail.

4.4.1. Electrochemical Performance of Zinc Electrodes with PEG, PbO and Ca(OH)₂

Discharge tests of batteries were performed using a 10-Ohm resistance as load and by logging the battery voltage vs. time. Voltage vs. Time (discharge) and Voltage vs. Capacity (discharge) curves of Zn batteries with all additives (Ca(OH)₂, PbO and PEG) are given in Figures 4.22 and 4.23, respectively. Even with all additives present in Zn electrode, ZnO content of electrode is 93 % (w/w). As explained in the previous section, while the initial morphology of the electrode is determined primarily by ZnO morphology, after first several cycles the morphology changes according to charge/discharge conditions.

Although there is no mention about the charging curves of Zn batteries prepared in this study, similar to NiZn dry batteries, first several charging curves of Zn batteries prepared in this study showed unpredictable behavior. However, discharge testing provided more stable behavior yielding a capacity range of 250-300 mAh. As seen in all discharge capacities, the maximum utilization ratio of ZnO with all additives is calculated to be 48.86 %. In the beginning of discharge procedure, the first discharge curve showed a sharp decline, while the decline for other curves was smoother. Battery voltage showed slight fall by the next dramatic drop.

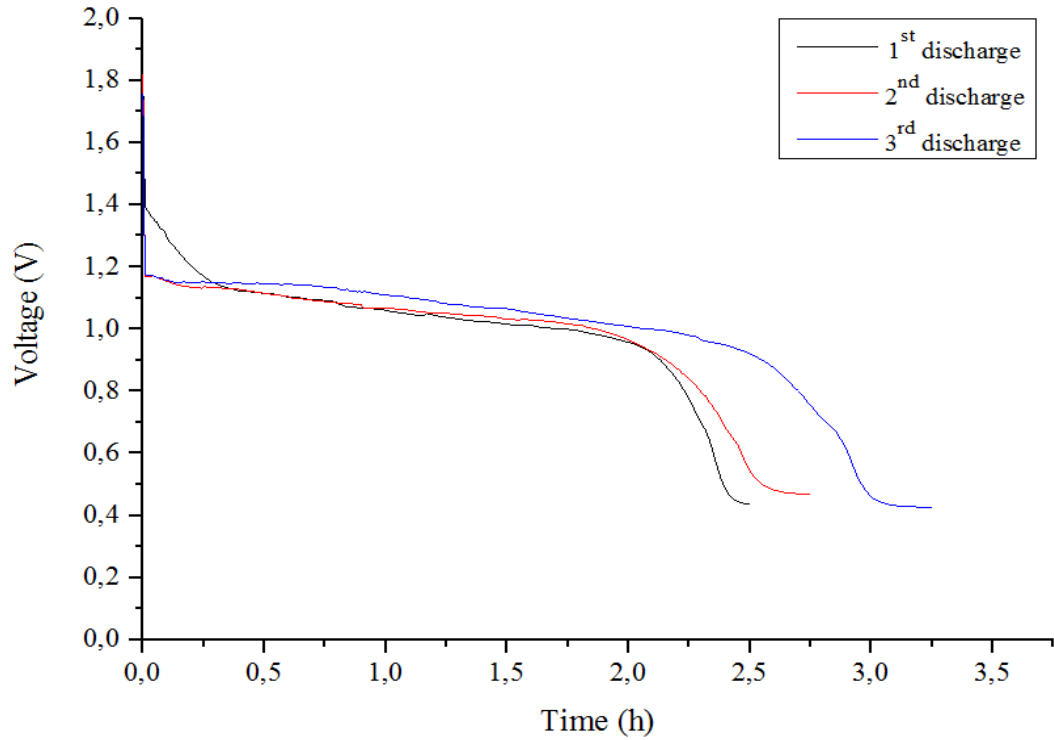


Figure 4.22. The discharge curves (voltage vs. time) for Zn electrode with all additives.

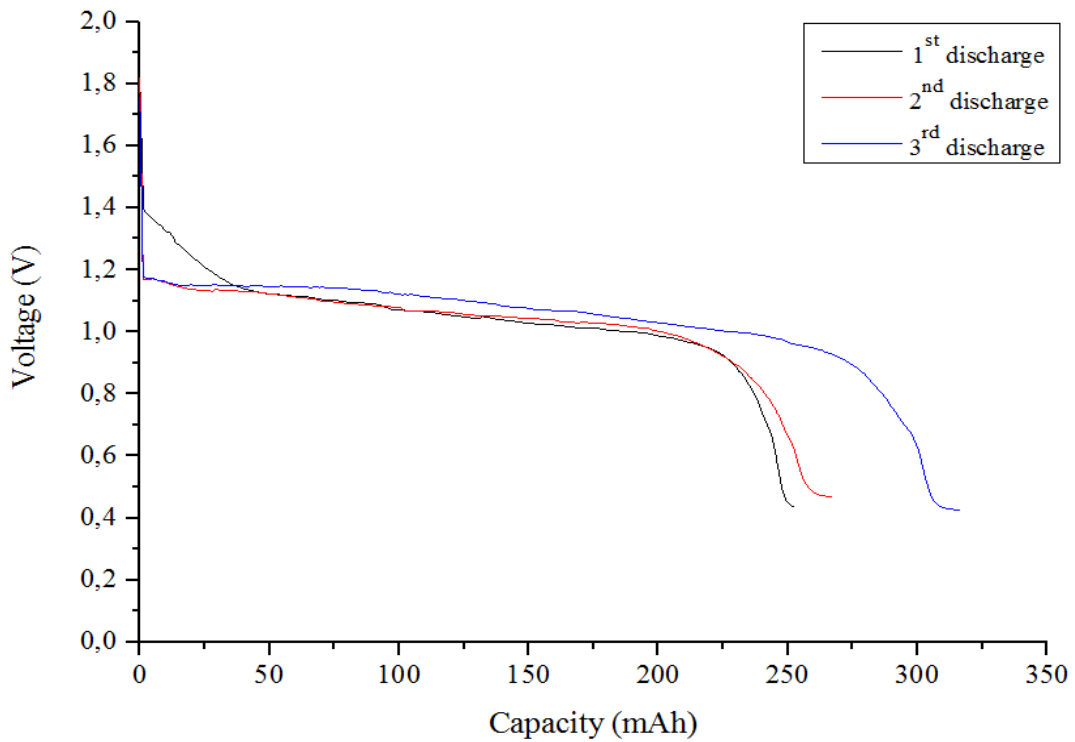


Figure 4.23. The discharge curves (voltage vs. capacity) for Zn electrode with all additives.

The detailed procedure for the preparation of Zn electrode and discharge tests are given in Chapter 3. SEM images of Zn electrode prepared using all additives ($\text{Ca}(\text{OH})_2$,

PbO and PEG) after 3rd discharge is shown in Figure 4.24. Compared to Figure 4.9 (the initial morphology of Zn electrode), the morphology of ZnO changed, with zinc particles in acicular form, namely the dendritic zinc. However, it was also observed that 100 % zinc oxide to zinc transformation was not achieved since mixed morphologies were observed in different locations of the sample. In this regard, it can be said that the initial charging of this Zn battery was not properly performed.

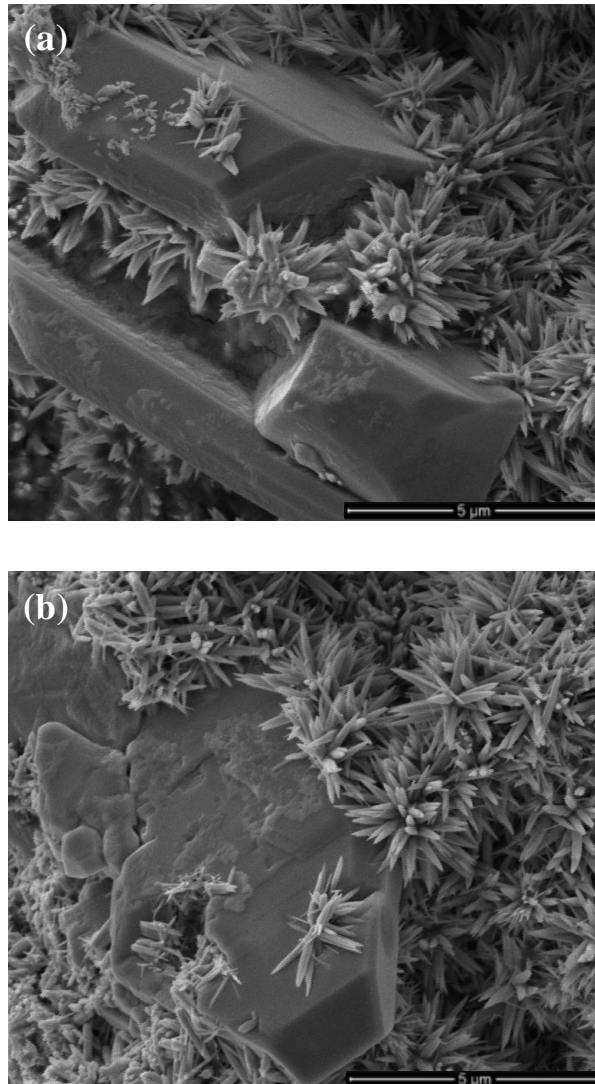


Figure 4.24. SEM images of Zn electrode with all additives after 3rd discharge scale bars (a) 5 μm (b) 5 μm at different locations on the substrate.

4.4.2. Electrochemical Performance of Zinc Electrodes with PEG and PbO

In the absence of Ca(OH)_2 , the performance of Zn electrode was investigated with discharge tests using a 10-Ohm resistance as load and by logging the battery voltage vs. time. Voltage vs. Time (discharge) and Voltage vs. Capacity (discharge) curves of Zn batteries without Ca(OH)_2 (only PbO and PEG) are shown in Figure 4.25 and Figure 4.26, respectively. In the absence of Ca(OH)_2 , ZnO content of electrode is 96 % (w/w). Taking into account the initial morphology of ZnO, the morphology changes of Zn electrode were observed after several discharge tests.

Although there is no mention about the charging curves of Zn batteries prepared in this study, it should be emphasized that it also showed unpredictable behavior. However, discharge testing provided more stable behavior. In comparison to Zn battery containing all additives (Ca(OH)_2 , PbO and PEG), the discharge capacity declined more gradually over discharge testing. It was observed that the initial discharge capacity was about 65 mAh whereas the discharge capacity unexpectedly increased to nearly 130 mAh after the third discharge. There is no explanation for this behavior for the initial discharge cycle at this point. However, the capacity is clearly much less compared to Zn batteries with all additives. In addition to this, the maximum utilization ratio of ZnO without calcium hydroxide is found to be 19.73 %, while the ZnO with all additives presents the maximum utilization ratio of 48.86 %. Therefore Ca(OH)_2 addition seems to be causing a much higher battery capacity.

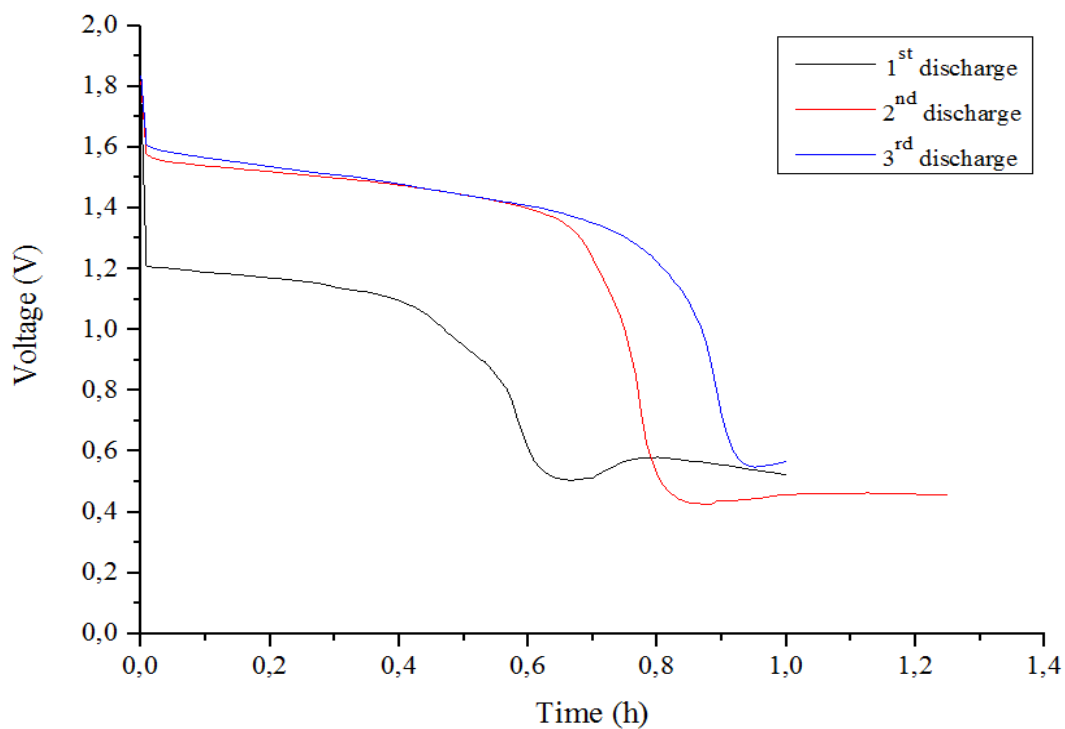


Figure 4.25. The discharge curves (voltage vs. time) for Zn electrode without $\text{Ca}(\text{OH})_2$.

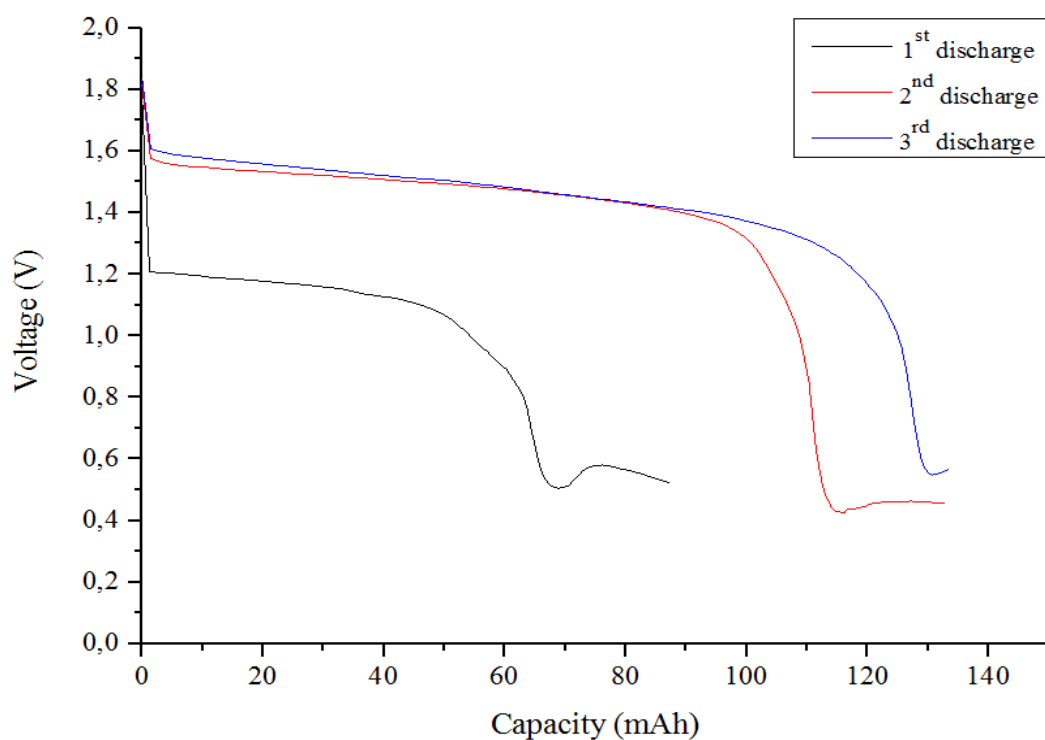


Figure 4.26. The discharge curves (voltage vs. capacity) for Zn electrode without $\text{Ca}(\text{OH})_2$.

The microstructure evolution process of Zn electrode prepared using all additives (PbO and PEG) after 3rd discharge is shown in Figure 4.27. As seen in Figure 4.27, the

morphology of ZnO seemed to be spindle-like structure. In comparison with different locations of the substrate, the growth of zinc dendrite was not completed properly, and thus, this asserted that the initial charging of this Zn battery was also not performed fully.

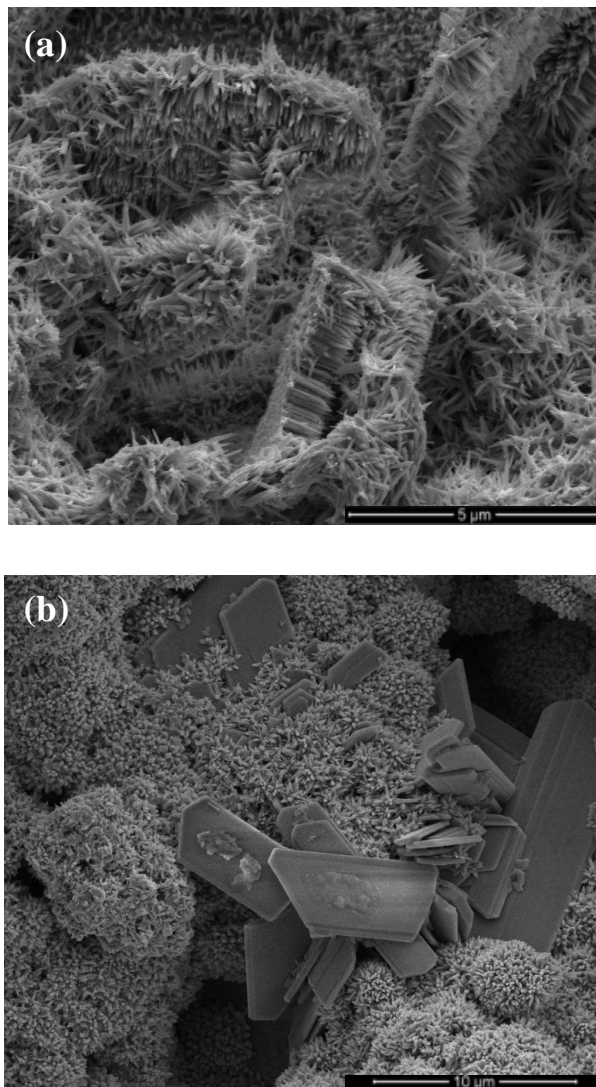


Figure 4.27. SEM images of Zn electrode without $\text{Ca}(\text{OH})_2$ after 3rd discharge scale bars (a) 5 μm (b) 10 μm at different locations on the substrate.

4.4.3. Electrochemical Performance of Zinc Electrodes with PEG and $\text{Ca}(\text{OH})_2$

The electrochemical study in the absence of lead (II) oxide was carried out using a 10-Ohm resistance load and by logging the battery voltage vs. time, similar to previous experiments. Figure 4.28 and Figure 4.29 illustrate the Voltage vs. Time (discharge) and

Voltage vs. Capacity (discharge) curves of Zn batteries without PbO (only Ca(OH)₂ and PEG), respectively. The ratio of zinc oxide used in the electrode is 94 % (w/w).

Although there is no mention about the charging curves of Zn batteries prepared in this study, it should be emphasized that it also showed unpredictable behavior. The behavior of discharging curves was more consistent in shape but showed very different capacities between 145 and 220 mAh. It can be said that the maximum utilization ratio of ZnO without lead (II) oxide is 33.38 %. It was obvious that the curves remained relatively stable until the next sharp decline. This is followed by a sharp final decline to the lowest limit of approximately 0.2 V.

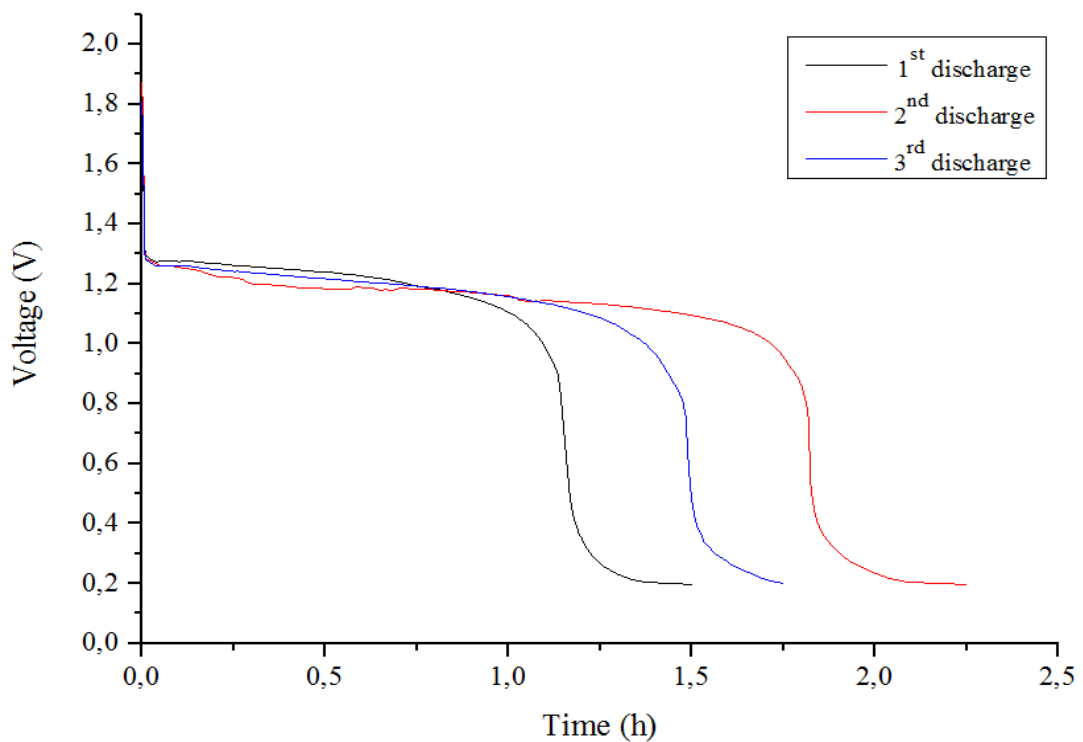


Figure 4.28. The discharge curves (voltage vs. time) for Zn electrode without PbO.

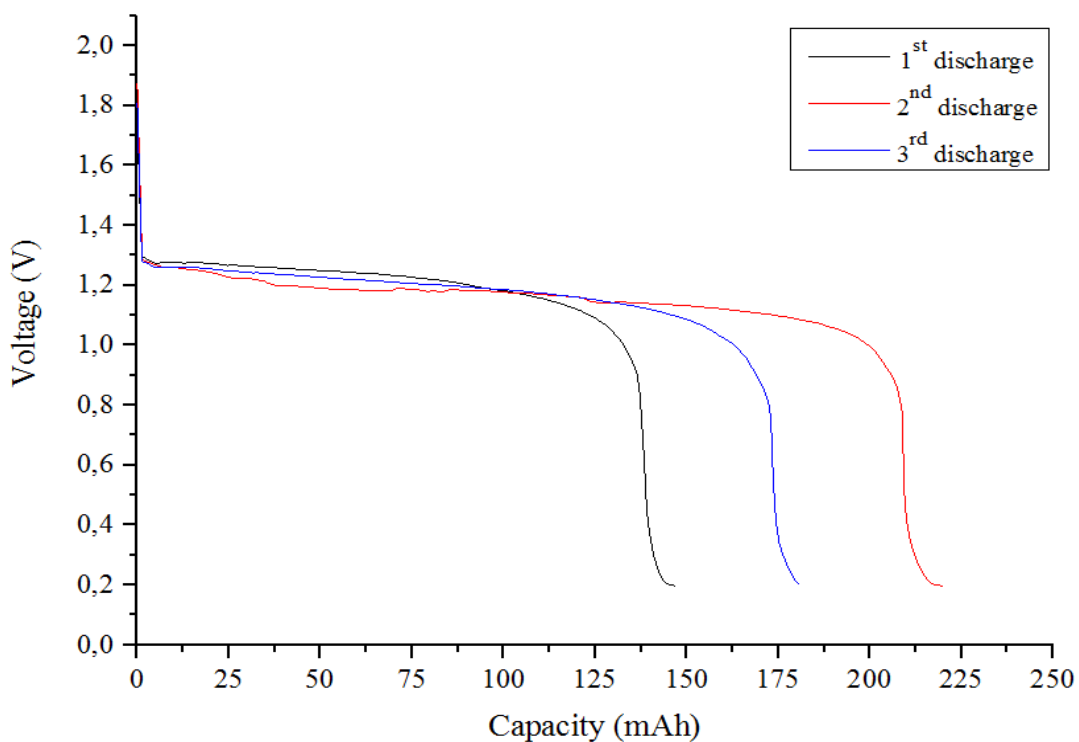


Figure 4.29. The discharge curves (voltage vs. capacity) for Zn electrode without PbO.

Figure 4.30 shows the morphology evolution process of Zn electrode prepared using additives $\text{Ca}(\text{OH})_2$ and PEG after 3rd discharge. In some locations large zinc crystals (flower like growth) with high aspect ratios were observed. However, these large crystals were also accompanied by smaller dendritic structures. As with all other samples, mixed morphology observed at different locations of the sample proved that the initial charging of this Zn battery was not performed fully.

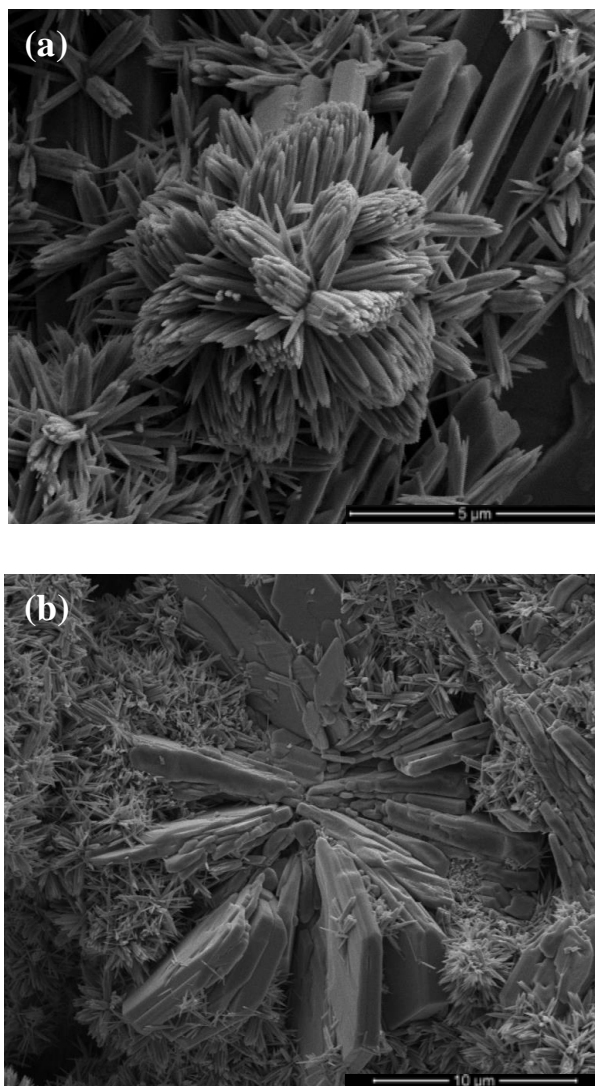


Figure 4.30. SEM images of Zn electrode without PbO after 3rd discharge scale bars (a) 5 μm (b) 10 μm at different locations on the substrate.

4.4.4. Electrochemical Performance of Zinc Electrodes with PbO and Ca(OH)₂

In this study, the Zn battery was prepared without binder, and thus, the effect of binder, polyethylene glycol, on the performance of Zn batteries was investigated. Discharge tests of batteries were conducted by attaching a 10-Ohm resistance load. Figure 4.31 and Figure 4.32 present Voltage vs. Time (discharge) and Voltage vs. Capacity (discharge) curves of Zn batteries without PEG binder (only Ca(OH)₂ and PbO), respectively. Even without binder present in Zn electrode, ZnO content of electrode is 96 % (w/w).

As observed with all other samples, initial charging curves displayed unpredictable behavior. However, discharge testing provided more stable behavior with between 250 and 275 mAh in capacity. It can be said that the maximum utilization ratio of ZnO without polyethylene glycol is 41.73 %. However, the shapes of discharge curves were not similar. This behavior might be explained by the lack PEG as binder thus resulting a nonuniform morphology in zinc electrode.

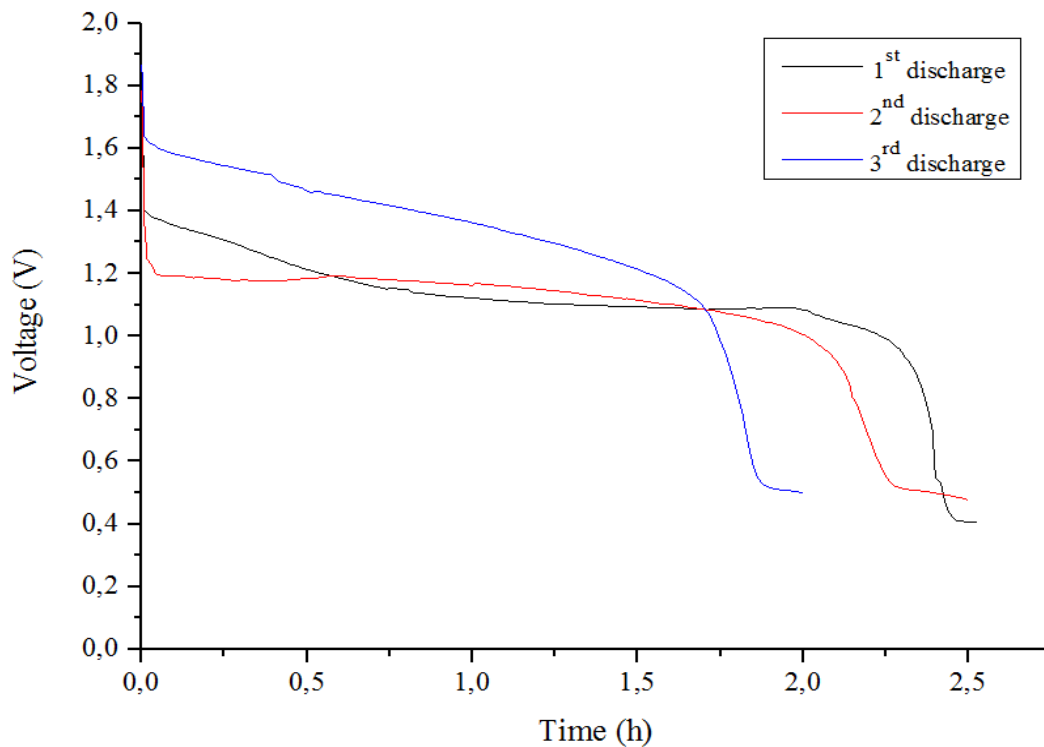


Figure 4.31. The discharge curves (voltage vs. time) for Zn electrode without PEG.

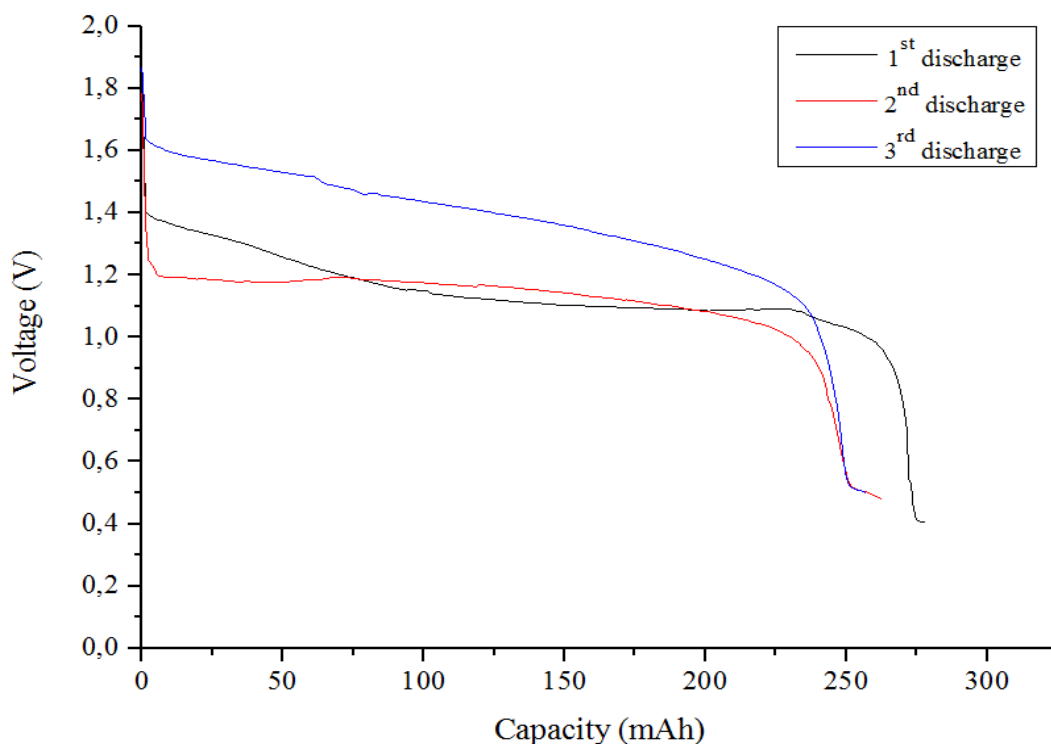


Figure 4.32. The discharge curves (voltage vs. capacity) for Zn electrode without PEG.

SEM images of Zn electrode prepared using additives without binder ($\text{Ca}(\text{OH})_2$ and PbO) after 3rd discharge is shown in Figure 4.33. As expected the particles of ZnO were elongated and it became a spindle-like form, but the zinc dendrite was not completely formed on all substrate locations.

Based on these observations, it is very difficult to explain the effect of each additive both on the morphology and electrochemical response of Zn electrode. The uniform distribution of each additive in the microstructure and the amount of additives are extremely important parameters. These parameters will definitely have an impact on the charging/discharging behavior of the electrode, however the current flux used in charge/discharge tests is also have a huge impact on the morphology, thus effecting the behavior of the battery in the next cycle.

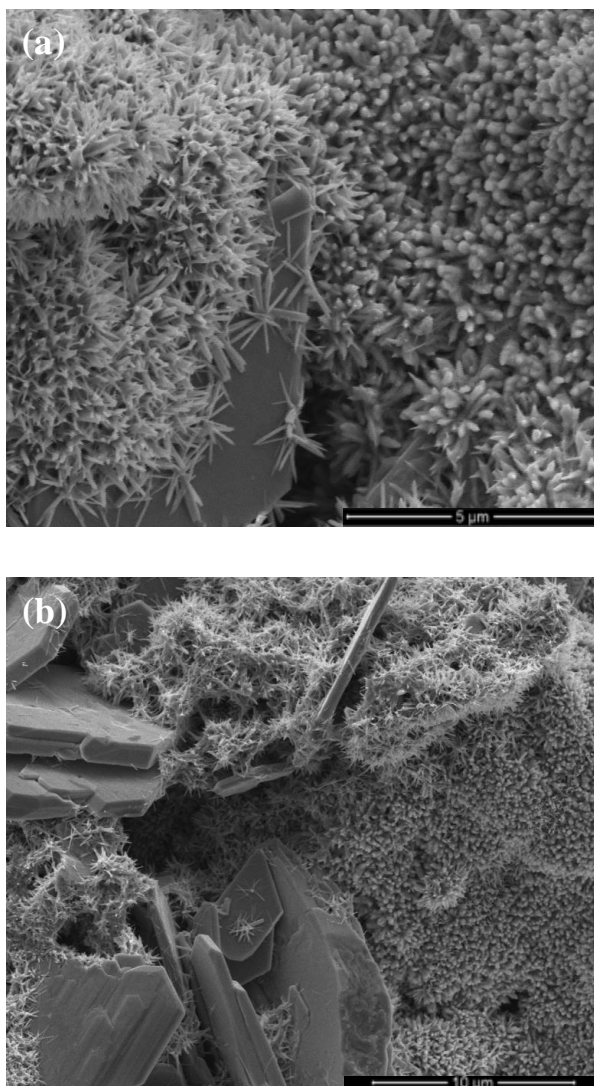


Figure 4.33. SEM images of Zn electrode without PEG after 3rd discharge scale bars (a) 5 μm (b) 10 μm at different locations on the substrate.

XRD spectra of all Zn electrodes with various additives are presented in Figure 4.34. As seen Figure 4.34, the XRD patterns showed that zinc oxide was dominant phase for each Zn electrode after three charge/discharge cycles. Based on XRD spectra for each zinc electrode excluding zinc electrode with PEG and PbO, there were some weak peaks of calcium zincate (CaZn). Therefore, it could be concluded that the dominant phase determining the microstructure in each electrode was zinc oxide.

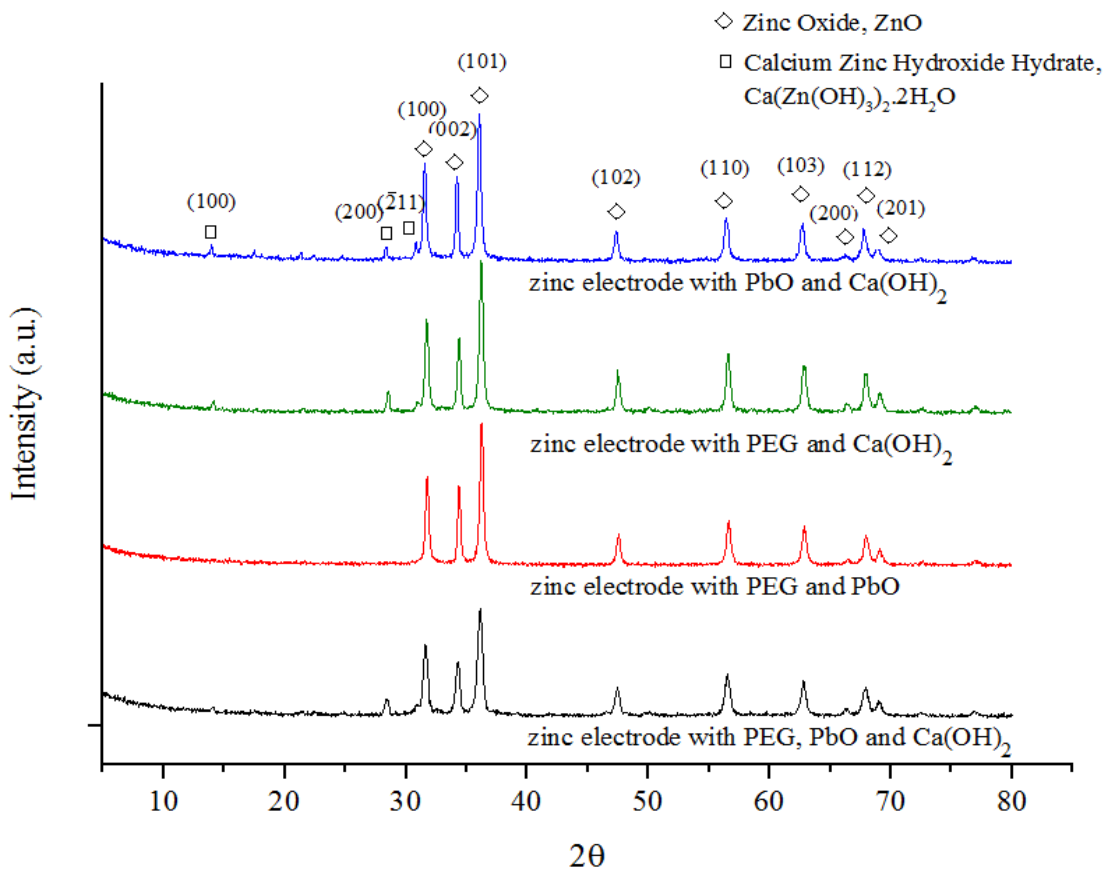


Figure 4.34. XRD spectra of Zn electrode with PEG, PbO and $\text{Ca}(\text{OH})_2$, Zn electrode with PEG and $\text{Ca}(\text{OH})_2$, Zn electrode with PEG and PbO, Zn electrode with PbO and $\text{Ca}(\text{OH})_2$ after third discharge.

Table 4.8 shows all XRD peak's for all Zn electrodes with various additives after third discharge. As expected, there is no difference between all Zn electrodes after third discharge and electrode paste before first charge related to XRD results Kisi & Elcombe, 1989, JCPDS-2 database number 79-2205; Schwick, JCPDS-2 database number 24-0222).

Table 4.8. XRD test results for Zn electrode with PEG, PbO and Ca(OH)₂, Zn electrode with PEG and Ca(OH)₂, Zn electrode with PEG and PbO, Zn electrode with PbO and Ca(OH)₂ after third discharge.

Crystal plane		2 Theta values			
		Zn electrode with PEG, PbO and Ca(OH) ₂	Zn electrode with PEG and Ca(OH) ₂	Zn electrode with PEG and PbO	Zn electrode with PbO and Ca(OH) ₂
(100)	CaZn	14.05	14.22	-	13.93
(200)	CaZn	28.56	28.56	-	28.33
($\bar{2}$ 11)	CaZn	30.89	31.01	-	30.84
(100)	ZnO	31.59	31.77	31.83	31.54
(002)	ZnO	34.33	34.45	34.39	34.28
(101)	ZnO	36.14	36.26	36.2	36.08
(102)	ZnO	47.45	47.57	47.57	47.33
(110)	ZnO	56.54	56.06	56.6	56.31
(103)	ZnO	62.9	62.72	62.84	62.66
(200)	ZnO	66.34	66.34	66.51	66.28
(112)	ZnO	67.68	67.91	67.97	67.79
(201)	ZnO	69.02	69.08	69.08	68.9

CHAPTER 5

CONCLUSIONS

In this study, the electrochemical behavior of zinc electrodes for battery applications was investigated using different zinc oxide powders with various morphologies and additives.

In order to examine the effect of initial zinc oxide morphology on the performance of zinc electrode in nickel-zinc battery, ZnO powders with different morphologies were synthesized using ZnCl_2 and $\text{Zn}(\text{NO}_3)_2 \cdot 6\text{H}_2\text{O}$ as precursors. In addition to the synthesized ZnO powders, commercial ZnO powder produced by thermal vaporization was used. The microstructure of each ZnO powder was investigated with SEM and XRD. ZnO powder was synthesized using ZnCl_2 under ultrasonic treatment at different temperatures, 35°C and 50°C. ZnO particles were spherical in shape with particle diameters from 48 to 78 nm, and from 20 to 40 nm, respectively. The particles of ZnO powders synthesized using $\text{Zn}(\text{NO}_3)_2 \cdot 6\text{H}_2\text{O}$ with different aging times, 15 minutes and 30 minutes, were found to have nonuniform shape and size distribution. Particles were mostly plate-like in shape. Commercial ZnO powder had a wide particle size distribution with most of the particles having needle-like shape as well as having tripod and nanorod in smaller fractions. Based on these findings the following conclusions can be made:

- The morphology of ZnO can be controlled to a certain extent by changing process parameters during synthesis. However, commercially available ZnO powders are usually produced via thermal vaporization leading to a wide range of particle shape and size distribution.
- Based on the limited studies, it was concluded the initial morphology of ZnO powder was not crucial for the electrochemical performance of zinc electrode for this study since after a few charge/discharge cycle the initial morphology is completely lost.
- The average capacity (using pouch cells and commercial Ni electrodes) was determined to be around 247 mAhg^{-1} based on several charge/discharge cycles.

One of the main problems of zinc electrode is dendritic growth of zinc that causes short circuit in the battery. In a quick study using only SEM analysis, the effects of a few

selected additives and current density on zinc morphology have been briefly studied. Based on this study the following statements can be made:

- It was observed that zinc morphology was greatly affected by additives (PVA and PEG) and current flux (25 mA/cm^2 and 75 mA/cm^2), respectively. However, due to limited number of samples, a definite conclusion cannot be made at this point.
- Based on very limited initial results, a detailed new research should be performed to investigate the effects of additives on the zinc growth process and zinc morphology.

Electrochemical performance of zinc electrodes prepared in this in study was evaluated with a limited number of charge/discharge cycles. The test setup was based on pouch cells and liquid KOH electrolyte. This setup is far from the ideal battery configuration (AA size or prismatic almost dry cell) however; it still provides valuable information regarding to zinc electrode behavior. Due to high internal resistivity of the cells used this study, voltage and current values measured during testing are far from commercial NiZn batteries. On the other hand, isolation of zinc electrode from Ni electrode in this setup by a large amount of KOH solution prevented passivation of zinc electrode at high discharge rates. It also prevented possible side reactions of nickel electrode interfering with the zinc electrode reactions, providing a good opportunity to focus solely on zinc electrode kinetics. In this study, the effect of some selected electrode additives (Ca(OH)_2 , PbO and PEG) on battery performance was also investigated. The following conclusions can be made based on the findings of these studies:

- Compared to zinc electrodes in the absence of each of additives, the zinc electrode with all additives showed improved electrochemical properties, such as higher discharge capacity and utilization ratio. The discharge capacity of its electrode was found to reach 322 mAhg^{-1} and the maximum utilization ratio was 48.86 % of the theoretical maximum.
- There are literally hundreds of additives for zinc electrodes and alkaline electrolytes that can be used to improve capacity, to minimize unwanted reactions, to reduce passivation and zinc electrode shape change and overall to improve battery performance and service-life. However, it is very difficult to determine the effect of each individual additive experimentally. That said, the findings of this study are in agreement with the results of previous studies involving Ca(OH)_2 , PbO and PEG as battery additives.

REFERENCES

- Acton, Q. A. (2013). *Sulfur Acids-Advances in Research and Application: 2013 Edition*. Atlanta, Georgia: Scholarly Editions.
- Adler, T. C., McLarnon, F. R., & Cairns, E. J. (1993). Low-zinc-solubility electrolytes for use in zinc/nickel oxide cells. *The Electrochemical Society*, 140, 289-294.
- Al-Thyabat, S., Nakamura, T., Shibata, E., & Iizuka, A. (2013). Adaptation of minerals processing operations for lithium-ion (LiBs) and nickel metal hydride (NiMH) batteries recycling: Critical review. *Minerals Engineering*, 45, 4-17.
- Avcı, Ö. (2009). *Türkiye-Avrupa Birliği Enerji Üretim ve Tüketiminin Karşılaştırmalı Olarak Değerlendirilmesi*. (The Degree of Master of Science), The University of Çukurova, Adana.
- Ayeb, A., & Notten, P. H. L. (2008). The oxygen evolution kinetics in sealed rechargeable NiMH batteries. *Electrochimica Acta*, 53(19), 5836-5847.
- Baes, C. J. & Mesmer, B. E. (1986). *The Hydrolysis Cations*, Robert E. Krieger Publishing Company, Inc., Newyork.
- Ballesteros, J. C., Díaz-Arista, P., Meas, Y., Ortega, R., & Trejo, G. (2007). Zinc electrodeposition in the presence of polyethylene glycol 20000. *Electrochimica Acta*, 52(11), 3686-3696.
- Braam, K. T., Volkman, S. K., & Subramanian, V. (2012). Characterization and optimization of a printed, primary silver–zinc battery. *Journal of Power Sources*, 199, 367-372.
- Chang, P. C., Fan, C., Wang, D., Tseng, W. Y., Chiou, W. A., Hong, J., & Lu, J. G. (2004). ZnO nanowires synthesized by vapor trapping CVD method. *Chemistry of Materials*, 16, 5133-5137.
- Cheng, J., Zhang, L., Yang, Y. S., Wen, Y. H., Cao, G. P., & Wang, X. D. (2007). Preliminary study of single flow zinc–nickel battery. *Electrochemistry Communications*, 9(11), 2639-2642.
- Cheng, Y., Zhang, H., Lai, Q., Li, X., Shi, D., & Zhang, L. (2013). A high power density single flow zinc-nickel battery with three-dimensional porous negative electrode. *Journal of Power Sources*.
- Chris, K. D., Patrick, T. M., Zempachi, O., David, A. J. R., & Bruno, S. (2009). Encyclopedia of Electrochemical Power Sources *Electrochemical Power Sources*.
- Christiansen, D., Alexander, C. K., & Jurgen, R. K. (2005). *Standard Handbook of Electronic Engineering* (5th ed.). New York: McGRAW-HILL.

- Coates, D., Ferreira, E., & Charkey, A. (1997). An improved nickel-zinc battery for ventricular assist systems. *Journal of Power Sources*, 65, 109-115.
- Crompton, T. R. (2000). *Battery Reference Book* (3rd ed.). London, UK.
- Dell, R. M. (2000). Batteries fifty years of materials development. *Solid State Ionics*, 134, 139-158.
- Edison, T. A. (1903). Reversible galvanic battery. Patent no: 727,117.
- Ein-Eli, Y., Auinat, M., & Starosvetsky, D. (2003). Electrochemical and surface studies of zinc in alkaline solutions containing organic corrosion inhibitors. *Journal of Power Sources*, 114(2).
- Fan, X. M., Zhou, Z.W., Wang, J., & Tian, K. (2011). Morphology and optical properties of tetrapod-like zinc oxide whiskers synthesized via equilibrium gas expanding method. *Transactions of Nonferrous Metals Society of China*, 21(9), 2056-2060.
- Fan, X., Yang, Z., Long, W., Yang, B., Jing, J., & Wang, R. (2013). The preparation and electrochemical performances of the composite materials of CeO₂ and ZnO as anode material for Ni-Zn secondary batteries. *Electrochimica Acta*, 108, 741-748.
- Fan, Z., & Lu, J. G. (2005). Zinc oxide nanostructures: Synthesis and properties. *Journal of Nanoscience and Nanotechnology*, 5, 1561-1573.
- Fauvarque, J. F., Guinot, S., Bouzir, N., Salmon, E., & Penneau, J. F. (1995). Alkaline poly(ethylene oxide) solid polymer electrolytes. Application to nickel secondary batteries. *Electrochimica Acta*, 40, 2449-2453.
- Geng, M. (2003). Development of advanced rechargeable Ni/MH and Ni/Zn batteries. *International Journal of Hydrogen Energy*, 28(6), 633-636.
- Hitz, C. and Lasia, A. (2001). Experimental study and modeling of impedance of the her on porous Ni electrodes, *Journal of Electroanalytical Chemistry*, 500, 213-222.
- Huang, H., Zhang, L., Zhang, W. K., Gan, Y. P., & Shao, H. (2008). Preparation and electrochemical properties of ZnO/conductive-ceramic nanocomposite as anode material for Ni/Zn rechargeable battery. *Journal of Power Sources*, 184(2), 663-667.
- Huang, Y. J., Lin, Y. L., & Li, W. S. (2013). Controllable syntheses of alpha- and delta-MnO₂ as cathode catalysts for zinc-air battery. *Electrochimica Acta*, 99, 161-165.
- Huggins, R. A. (2009). *Advanced Batteries*. New York: Springer.
- IEA. (2012). 2012 Key World Energy Statistics. France.
- IEA. (2013). International Energy Outlook 2013. U.S.

- Ito, Y., Nyce, M., Plivelich, R., Klein, M., Steingart, D., & Banerjee, S. (2011). Zinc morphology in zinc–nickel flow assisted batteries and impact on performance. *Journal of Power Sources*, *196*(4), 2340-2345.
- Iwakura, C., Murakami, H., Nohara, S., Furukawa, N., & Inoue, H. (2005). Charge–discharge characteristics of nickel/zinc battery with polymer hydrogel electrolyte. *Journal of Power Sources*, *152*, 291-294.
- Jindra, J. (1997). Progress in sealed Ni-Zn cells, 1991–1995. *Journal of Power Sources*, *66* 15-25.
- Kazeminezhadn, I., Sadollahkhani, A., & Farbod, M. (2013). Synthesis of ZnO nanoparticles and flower-like nanostructures using nonsono- and sono-electrooxidation methods. *Materials Letters*, *92*, 29-32.
- Kiehne, H. A. (2003). *Battery Technology Handbook* (2. ed.): CRC Press.
- Kisi, E. H., & Elcombe, M. M. (1989). u Parameters for the wurtzite structure of ZnS and ZnO using powder neutron diffraction. *Acta Crystallographica Section C*, *45*, 1867-1870.
- Lee, C. W., Sathiyarayanan, K., Eom, S. W., & Yun, M. S. (2006a). Novel alloys to improve the electrochemical behavior of zinc anodes for zinc/air battery. *Journal of Power Sources*, *160*(2), 1436-1441.
- Lee, C. W., Sathiyarayanan, K., Eom, S. W., Kim, H. S., & Yun, M. S. (2006b). Effect of additives on the electrochemical behaviour of zinc anodes for zinc/air fuel cells. *Journal of Power Sources*, *160*(1), 161-164.
- Lee, C. W., Eom, S. W., Sathiyarayanan, K., & Yun, M. S. (2006c). Preliminary comparative studies of zinc and zinc oxide electrodes on corrosion reaction and reversible reaction for zinc/air fuel cells. *Electrochimica Acta*, *52*(4), 1588-1591.
- Lee, C. W., Sathiyarayanan, K., Eom, S. W., Kim, H. S., & Yun, M. S. (2006d). Novel electrochemical behavior of zinc anodes in zinc/air batteries in the presence of additives. *Journal of Power Sources*, *159*(2), 1474-1477.
- Lee, J. S., Tai Kim, S., Cao, R., Choi, N. S., Liu, M., Lee, K. T., & Cho, J. (2011a). Metal-Air Batteries with High Energy Density: Li-Air versus Zn-Air. *Advanced Energy Materials*, *1*(1), 34-50.
- Lee, S. H., Yi, C. W., & Kim, K. (2011b). Characteristics and Electrochemical Performance of the TiO₂-Coated ZnO Anode for Ni/Zn Secondary Batteries. *The Journal of Physical Chemistry C*, *115*(5), 2572-2577.
- Liang, S., Zhu, L., Gai, G., Yao, Y., Huang, J., Ji, X., Zhang, P. (2014). Synthesis of morphology-controlled ZnO microstructures via a microwave-assisted hydrothermal method and their gas-sensing property. *Ultrason Sonochem*, *21*(4), 1335-1342.

- Linden, D., & Reddy, T. B. (2001). *Handbook of Batteries* (David Linden & T. B. Reddy Eds. 3rd ed.).
- Loh, K. P., & Chua, S. J. (2007). Zinc Oxide Nanorod Arrays: Properties and Hydrothermal Synthesis. In G. A. Mansoori, T. F. George, L. Assoufid & G. Zhang (Eds.), *Molecular Building Blocks for Nanotechnology* (109). Berlin: Springer.
- Łosiewiczza, B., Budniok, A., Rówiński, E., Łągiewka, E. and Lasia, A. (2004). The structure, morphology and electrochemical impedance study of the hydrogen evolution reaction on the modified nickel electrodes, *International Journal of Hydrogen Energy*, 29, 145 – 157.
- Luo, Z., Sang, S., Wu, Q., & Liu, S. (2012). A conductive additive for Zn electrodes in secondary Ni/Zn batteries: The magneli phase Titanium Sub-Oxides conductive ceramic Ti_nO_{2n-1} . *ECS Electrochemistry Letters*, 2(2), A21-A24.
- Ma, M., Tu, J. P., Yuan, Y. F., Wang, X. L., Li, K. F., Mao, F., & Zeng, Z. Y. (2008). Electrochemical performance of ZnO nanoplates as anode materials for Ni/Zn secondary batteries. *Journal of Power Sources*, 179(1), 395-400.
- Markov, I. V. (1996). *Crystal Growth for Beginners: Fundamentals of Nucleation, Crystal Growth and Epitaxy*. USA: World Scientific Publishing Co Pte Ltd.
- Masri, M. N., & Mohamad, A. A. (2009). Effect of adding potassium hydroxide to an agar binder for use as the anode in Zn–air batteries. *Corrosion Science*, 51(12), 3025-3029.
- McBreen, J., & Gannon, E. (1981). The electrochemistry of metal oxide additives in pasted zinc electrodes. *Electrochimica Acta*, 26 1439-1446.
- Mirmohseni, A., & Solhjo, R. (2003). Preparation and characterization of aqueous polyaniline battery using a modified polyaniline electrode. *European Polymer Journal*, 39, 219-223.
- Mohamad, A. A. (2006). Zn/gelled 6M KOH/O₂ zinc–air battery. *Journal of Power Sources*, 159(1), 752-757.
- Mohamad, A. A., Mohamed, N. S., Yahya, M. Z. A., Othman, R., Ramesh, S., Alias, Y., & Arof, A. K. (2003). Ionic conductivity studies of poly(vinyl alcohol) alkaline solid polymer electrolyte and its use in nickel–zinc cells. *Solid State Ionics*, 156, 171- 177.
- Musić, S., Dragčević, Đ., & Popović, S. (2007). Influence of synthesis route on the formation of ZnO particles and their morphologies. *Journal of Alloys and Compounds*, 429(1-2), 242-249.
- Müeller, S., Holzer, F., & Haas, O. (1998). Optimized zinc electrode for the rechargeable zinc-air battery. *Journal of Applied Electrochemistry*, 28, 895-898.

- Othman, R., Basirun, W. J., Yahaya, A. H., & Arof, A. K. (2001). Hydroponics gel as a new electrolyte gelling agent for alkaline zinc–air cells. *Journal of Power Sources*, *103*, 34-41.
- Ömürlü, Ö. F. (2009). *Enhancement of thermal, electrical and optical properties of zinc oxide filled polymer matrix nano composites*. (Doctor of Philosophy), Izmir Institute of Technology, İzmir.
- Pavlov, D. (2011). Fundamentals of Lead-Acid Batteries *Lead-Acid Batteries - Science and Technology - A Handbook of Lead-Acid Battery Technology and its Influence on the Product* (pp. 3-28): Elsevier.
- Pei, P., Wang, K., & Ma, Z. (2014). Technologies for extending zinc–air battery’s cyclelife: A review. *Applied Energy*, *128*, 315-324.
- Pérez-Lombard, L., Ortiz, J., & Pout, C. (2008). A review on buildings energy consumption information. *Energy and Buildings*, *40*(3), 394-398.
- Perez, M. G., O’Keefe, M. J., O’Keefe, T., & Ludlow, D. (2006). Chemical and morphological analyses of zinc powders for alkaline batteries. *Journal of Applied Electrochemistry*, *37*(2), 225-231.
- Pistoia, G. (2005). *Batteries for Portable Devices*. National Research Council, Rome, Italy: Elsevier.
- Saleem, M., Sayyad, M. H., Karimov, K. H. S., & Ahmad, Z. (2009). Fabrication of investigation of the charge-discharge characterization of Zinc-PVA-KOH-Carbon Cell. *Acta Physica Polonica A*, *116*, 1021-1024.
- Schwick, Instit. fur Baustoffkunde and Stahlbetonbau, Private Communication.
- Shen, G., Bando, Y., & Lee, C. J. (2005). Synthesis and evolution of novel hollow ZnO urchins by a simple thermal evaporation process. *The Journal of Physical Chemistry B*, *109*, 10578-10583.
- Shivkumar, R., Kalaignan, G. P., & Vasudevan, T. (1995). Effect of additives on zinc electrodes in alkaline battery systems. *Journal of Power Sources*, *55*, 53-62.
- Shivkumar, R., Paruthimal Kalaignan, G., & Vasudevan, T. (1998). Studies with porous zinc electrodes with additives for secondary alkaline batteries. *Journal of Power Sources*, *75*, 90-100.
- Shuklaa, A. K., Venugopalan, S., & Hariprakash, B. (2001). Nickel-based rechargeable batteries. *Journal of Power Sources*, *100*, 125-148.
- Swanson, H. E. and Tatge, E. (1953). NBS Circular 539, Vol 1, data for 54 inorganic substances.

- Sue, K., Kimura, K., Murata, K., & Arai, K. (2004). Effect of cations and anions on properties of zinc oxide particles synthesized in supercritical water. *The Journal of Supercritical Fluids*, 30(3), 325-331.
- Szytula, A., Murasik, A. and Balanda, M. (1971). Neutron Diffraction Study of Ni(OH)₂. *Physica Status Solidi B*, 43, 125-128.
- Tahvonen, O., & Salo, S. (2001). Economic growth and transitions between renewable and nonrenewable energy resources. *European Economic Review*, 45 1379-1398.
- Tan, Z., Yang, Z., Ni, X., Chen, H., & Wen, R. (2012). Effects of calcium lignosulfonate on the performance of zinc–nickel battery. *Electrochimica Acta*, 85, 554-559.
- Technical Marketing Staff of Gates Energy Products, I. (1998). *Rechargeable Batteries Applications Handbook*. United States of America: Elsevier.
- Tester, J. W., Drake, E. M., Driscoll, M. J., Golay, M. W., & Peters, W. A. (2005). *Sustainable Energy: Choosing Among Options*: the MIT press.
- Vincent, C. A., & Scrosati, B. (2003). *Modern Batteries: An Introduction to Electrochemical Power Sources* (2nd ed.). Butterworth-Heinemann.
- Wang, R., Yang, Z., Yang, B., Fan, X., & Wang, T. (2014). A novel alcohol-thermal synthesis method of calcium zincates negative electrode materials for Ni–Zn secondary batteries. *Journal of Power Sources*, 246, 313-321.
- Wang, Y., Ma, C., Sun, X., & Li, H. (2002). Preparation of nanocrystalline metal oxide powders with the surfactant-mediated method. *Inorganic Chemistry Communications*, 5, 751-755.
- web1, <http://depts.washington.edu/masteed/batteries/MSE/classification.html>. Classification of Cells or Batteries. Retrieved 22.04.2014, 2014
- web2, <http://www.powergenix.com/>. POWERGENIX. Retrieved 22.04.2014, 2014
- web3, <http://www.pkcell.net/>. PKCELL Professional Battery Manufacturer Retrieved 22.04.2014, 2014
- web4, <http://www.share4dev.info/telecentreskb/documents/4538.pdf>. ReVolt Portable Battery Technology Brief. Retrieved 22.04.2014, 2014
- web5, <http://media.wv2.duracell.com>. (2004). Zinc Air Tech Bulletin. Retrieved 22.04.2014, 2014
- Wei, Y. L., & Chang, P. C. (2008). Characteristics of nano zinc oxide synthesized under ultrasonic condition. *Journal of Physics and Chemistry of Solids*, 69(2-3), 688-692.
- Winckler, G. A. F., Reinhardt, M., & Reinhardt, O. K. (1953). United States.

- Wu, J. Z., Tu, J. P., Yuan, Y. F., Ma, M., Wang, X. L., Zhang, L., Zhang, J. (2009). Ag-modification improving the electrochemical performance of ZnO anode for Ni/Zn secondary batteries. *Journal of Alloys and Compounds*, 479(1-2), 624-628.
- Wu, Q., Zhang, J., & Sang, S. (2008). Preparation of alkaline solid polymer electrolyte based on PVA–TiO₂–KOH–H₂O and its performance in Zn–Ni battery. *Journal of Physics and Chemistry of Solids*, 69, 2691-2695.
- Yang, C. C., Chien, W. C., Wang, C. L., & Wu, C. Y. (2007). Study the effect of conductive fillers on a secondary Zn electrode based on ball-milled ZnO and Ca(OH)₂ mixture powders. *Journal of Power Sources*, 172(1), 435-445.
- Yang, C. C., & Lin, S. J. (2002). Alkaline composite PEO–PVA–glass-fibre-mat polymer electrolyte for Zn–air battery. *Journal of Power Sources*, 112 497-503.
- Yang, C. C., Yang, J. M., & Wu, C. Y. (2009). Poly(vinyl alcohol)/poly(vinyl chloride) composite polymer membranes for secondary zinc electrodes. *Journal of Power Sources*, 191(2), 669-677.
- Yang, J. L., Yuan, Y. F., Wu, H. M., Li, Y., Chen, Y. B., & Guo, S. Y. (2010). Preparation and electrochemical performances of ZnO nanowires as anode materials for Ni/Zn secondary battery. *Electrochimica Acta*, 55(23), 7050-7054.
- Yu, J., Yang, H., Ai, X., & Zhu, X. (2001). A study of calcium zincate as negative electrode materials for secondary batteries. *Journal of Power Sources*, 103, 93-97.
- Yuan, Y. F., Tu, J. P., Wu, H. M., Li, Y., & Shi, D. Q. (2005). Size and morphology effects of ZnO anode nanomaterials for Zn/Ni secondary batteries. *Nanotechnology*, 16(6), 803-808.
- Yuan, Y. F., Tu, J. P., Wu, H. M., Li, Y., Shi, D. Q., & Zhao, X. B. (2006a). Effect of ZnO nanomaterials associated with Ca(OH)₂ as anode material for Ni–Zn batteries. *Journal of Power Sources*, 159(1), 357-360.
- Yuan, Y. F., Tu, J. P., Wu, H. M., Yang, Y. Z., Shi, D. Q., & Zhao, X. B. (2006b). Electrochemical performance and morphology evolution of nanosized ZnO as anode material of Ni–Zn batteries. *Electrochimica Acta*, 51(18), 3632-3636.
- Yuan, Y. F., Tu, J. P., Wu, H. M., Zhang, C. Q., Wang, S. F., & Zhao, X. B. (2007). Influence of surface modification with Sn₆O₄(OH)₄ on electrochemical performance of ZnO in Zn/Ni secondary cells. *Journal of Power Sources*, 165(2), 905-910.
- Yuan, Y. F., Yu, L. Q., Wu, H. M., Yang, J. L., Chen, Y. B., Guo, S. Y., & Tu, J. P. (2011). Electrochemical performances of Bi based compound film-coated ZnO as anodic materials of Ni–Zn secondary batteries. *Electrochimica Acta*, 56(11),
- Zeray, C. (2010). *Renewable Energy Sources*. (The Degree of Master of Science Msc Thesis), University of Çukurova, Adana.

- Zhang, L., Huang, H., Zhang, W. K., Gan, Y. P., & Wang, C. T. (2008). Effects of conductive ceramic on the electrochemical performance of ZnO for Ni/Zn rechargeable battery. *Electrochimica Acta*, 53(16), 5386-5390.
- Zhang, X. G. (1996). *Corrosion and Electrochemistry of Zinc*. New York: Springer.
- Zhou, H., Huang, Q., Liang, M., Lv, D., Xu, M., Li, H., & Li, W. (2011). Investigation on synergism of composite additives for zinc corrosion inhibition in alkaline solution. *Materials Chemistry and Physics*, 128(1-2), 214-219.
- Zhu, X. M., Yang, H. X., Ai, X. P., Yu, J. X., & Cao, Y. L. (2003). Structural and electrochemical characterization of mechanochemically synthesized calcium zincate as rechargeable anodic materials. *Journal of Applied Electrochemistry*, 33, 607-612.
- Zito, R. (2010). *Energy Storage: A New Approach* (R. Zito Ed.): John Wiley & Sons.